Filter-feeding in common bream (*Abramis brama*), white bream (*Blicca bjoerkna*) and roach (*Rutilus rutilus*); structures, functions and ecological significance

Promotor:	Prof. Dr. J.W.M. Osse Hoogleraar Algemene Dierkunde
Co-promotor:	Dr. F.A. Sibbing Universitair Hoofddocent Functionele Diermorfologie

Coen van den Berg

Filter-feeding in common bream (*Abramis brama*), white bream (*Blicca bjoerkna*) and roach (*Rutilus rutilus*); structures, functions and ecological significance

Proefschrift
ter verkrijging van de graad van
doctor in de landbouw- en milieuwetenschappen
op gezag van de rector magnificus,
dr. H.C. van der Plas,
in het openbaar te verdedigen
op donderdag 17 juni 1993
des namiddags te vier uur in de aula
van de Landbouwuniversiteit te Wageningen

ISN 582073

Het onderzoek dat in dit proefschrift is beschreven is mogelijk gemaakt door een subsidie van NWO/Stichting BION (projectnummer 428-265) aan Prof. Dr. J.W.M. Osse van de sectie Functionele Diermorfologie van de vakgroep Experimentele Diermorfologie en Celbiologie van de Landbouwuniversiteit teWageningen

Stellingen

1 De effectiviteit van een kieuwzeef in het tegenhouden van prooideeltjes hangt af van de vorm van die deeltjes. Verschillen in retentie effectiviteit per prooisoort geven bovendien aanwijzingen over de vorm van de mazen van de kieuwzeef en daarmee tevens over het retentie mechanisme.
dit proefschrift

2 Microscopische anatomische details kunnen een groot effect hebben op de mogelijkheden van een individu om zijn omgeving te exploiteren. Morfologie en autoecologie zijn sterk verweven.
dit proefschrift

3 Bij het biomechanisch onderzoek van vissen is het gebruikelijk te proberen bewegingen loodrecht op de bewegingsrichting te filmen. Projectiefouten worden hierdoor echter verhuld zodat een tweedimensionale analyse van de bewegingen uit zulke films ongemerkt tot grote fouten kan leiden.
dit proefschrift

4 De bij 'suction feeding' onvermijdelijke kieuwboogbewegingen stellen een ondergrens aan de maaswijdte van de kieuwzeef wanneer het retentie mechanisme berust op interdigitatie van kieuwdoorns.
dit proefschrift

5 De energie kosten van het ophappen en verwerken van dierlijke prooi spelen geen noemenswaardige rol in vergelijking met de energie inhoud van zulke prooi. Beperkingen aan het spectrum van voedselorganismen worden in de eerste plaats opgelegd door de bouw van de voedselverwerkende structuren.

6 Niet zonder cynisme kan opgemerkt worden dat door de mens veroorzaakte oecologische rampen interessante evolutionaire experimenten zijn.

7 Tot een standaard lengte van 20-24 mm groeit een groot aantal lengteparameters van karperlarven sterk positief allometrisch ten opzichte van de standaardlengte. Een minder extreem groeibeeld kan verkregen worden door te stellen dat de standaardlengte zelf negatief allometrisch groeit tijdens deze periode.
Hoda & Tsukahara. J. Fac. Agricult., Kyushu Univ. 16: 387-509 (1971)

8 Wetenschappelijke kennis heeft tot doel de waarneembare werkelijkheid met een zo eenvoudig mogelijk stelsel van theoriën te ordenen en voorspelbaar te maken. Hoewel, gezien het onzekerheidsprincipe van Heisenberg, een puur deterministisch beeld van de werkelijkheid metafysisch (principieel onbewijsbaar) is, helpt dit beeld toch de werkelijkheid te ordenen en is dus zinvol.
A. Einstein:: 'God dobbelt niet'.

9 Het menselijk bewustzijn is de verschijningsvorm op een hoog abstractie nivo van de fysische principes die ten grondslag liggen aan de werking van de hersenen. Het is daarom niet logisch te veronderstellen dat bewustzijn beperkt is tot de mens of zelfs tot levende wezens.

10 Het huidige onderwijsbeleid leidt tot verlaging van de kwaliteit van het universitair onderwijs. Er zou op het *aantal* studenten bezuinigd moeten worden door de toelatingseisen van de universiteiten te verzwaren (toelatingsexamen) en het nivo van het onderwijs hoog te houden.

11 Intensieve centrale sturing en toetsing van onderzoek resulteert in vervlakking van onderzoeksprogramma's en bureaucratisering van onderzoeksinstanties. Wetenschap gedijt het beste in een licht anarchistisch klimaat.

12 Langdurige periodes van overwerk zijn contraproductief.

13 Selectieve economische boycot van een land is mogelijk een alternatief voor oorlog. Culturele en sport boycots zijn echter ongeschikte en hypocriete alternatieven.

14 Het aanvallen van de stellingen bij een proefschrift is veelal een teken van slechte voorbereiding van de opponent.

15 Voor mensen met zwakke enkels verdient het aanbeveling slechts open deuren in te trappen.

16 Een (vakgroepsbestuurs)vergadering is dikwijls een OH-Erlebnis.

bij het proefschrift:
"Filter-feeding in common bream (*Abramis brama*), white bream (*Blicca bjoerkna*) and roach (*Rutilus rutilus*); structures, functions and ecological significance." van Coen van den Berg.
17 juni 1993

Contents/Inhoud

General introduction

The majority of freshwater fishes in Europe belongs to the family *Cyprinidae* (carp-like fishes). Most cyprinid fishes are opportunistic feeders, although most species prefer a certain habitat and certain food types (Lammens and Hoogenboezem 1991, Sibbing 1991). The research in this thesis is part of a major research line of the section Functional Morphology (Department of Experimental Animal Morphology and Cell Biology). This research line studies the relations between the structural design of the feeding apparatus of cyprinids, their effectiveness of food-intake and -processing (functional morphology) and their ecological niche (ecomorphology). A fish design which is optimal for processing all available food types probably does not exist, since an optimal design for the exploitation of one food type is likely to impose limitations on the exploitation of other food types (functional demands are often incompatible). A detailed comparative study of relevant morphological and kinematical parameters may therefore reveal structural adaptations (or limitations) for the utilization of particular food types. In general, structural or mechanical models are used to study the adaptations of the feeding apparatus for a particular food type. These models reflect the ideas of the researcher about the function of (parts of) the feeding apparatus. Such models should have a limited set of morphological and kinematical parameters which determine the effectiveness of the utilization of specific food types. When the model parameters of a fish species are known, it should be possible to decide whether the model applies to that species. If it does, the model parameters of the fish can be used to predict its feeding effectiveness for the particular food type. Ideally, the optimal design and movement pattern of a fish for a specific food type can be determined by varying the value of the model parameters until an optimum in effectiveness is found.

An important question in ecomorphological studies is whether morphological adaptations are the cause or the result of the ecological niche of the fish under study. The answer to that question depends on the time scale: individual life span or geological time span. The former line of thought (adaptation as a cause) is useful to explain the structure of an existing ecosystem, whereas the latter is better suited to explain the evolution of species. Alexander (1988) stressed the importance of combining these two views. It is important to realize that morphology and ecology are strongly intertwined. The ecologist Schoener wrote (1982): "if morphological adaptations constitute a genetic memory of such competition, they will more accurately reflect its ecological importance".

Somewhat cynically, the drastic disturbance of the biotic and abiotic conditions of an ecosystem by human activity can be seen as a large scale ecomorphological experiment. The eutrophication of freshwater lakes is a good example of such an 'experiment'. In this thesis I try to explain changes in the fish fauna composition of eutrophic lakes from differences in the structure and functioning of the branchial sieves of three cyprinid species, only one of which appears to be successful in eutrophic lakes.

Obviously, the study of the effects of eutrophication is an important environmental issue, as well. It is one of many shocking examples of the destructive influence of man on its natural environment. A better understanding of the structure of, and the relations within ecosystems will help to predict the effects of human behaviour. Such knowledge is essential for designing meaningful environmental laws for long term protection of ecosystems and for restoration of eutrophic systems.

In this introduction I first present an outline of the effects of eutrophication on freshwater lakes and the importance of filter-feeding for survival in eutrophic lakes. I

proceed to compare the filter-feeding mechanisms of cyprinids with those of other filter-feeders and I briefly describe the previous research on this subject. Next I present my approach to the problem of cyprinid filter-feeding, the zooplankton retention mechanism of their branchial sieves and the ecological significance of filter-feeding in eutrophic lakes. The framework of this research is presented, followed by an outline of this thesis and some suggestions for further research. The closing paragraph of this introduction is a general discussion of the new insights.

Eutrophication

Freshwater can be classified according to the concentration of nutrients (e.g. nitrates and phosphates). An oligotrophic lake contains a very low concentration of nutrients and can therefore not sustain a large biomass. A eutrophic lake contains a very high concentration of nutrients. During the last decades, many freshwater lakes in the Netherlands have become eutrophic. The process of eutrophication is caused largely by human waste material like sewerage, manure and industrial waste. Eutrophication has led to a strong reduction of the biodiversity in freshwater lakes. Tjeukemeer is a well studied eutrophic lake in the north of the Netherlands (Limnologisch Instituut 1983, Lammens 1989, 1986, de Nie 1987). Due to the high concentration of nutrients algae are very abundant. The algae cause the characteristic green colour and high turbidity of eutrophic lakes. The light level in the water is strongly reduced and macrophytes and the associated fauna have almost disappeared. Since many zooplankters feed on algae, they have become abundant. Together with chironomid larvae, which are buried in the soft substrate, they are the major food source for the fishes in eutrophic lakes. The substrate has lost much of its firmness, possibly due to the absence of macrophyte roots. Therefore, the activity of fishes digging for chironomid larvae and the water turbulence caused by the wind suspends increased quantities of bottom particles, which further increases the turbidity and resuspends nutrients.

Common bream (*Abramis brama*), white bream (*Blicca bjoerkna*) and roach (*Rutilus rutilus*) are opportunistic cyprinids; their diets show a considerable degree of overlap (Lammens and Hoogenboezem 1991). It is assumed that a certain amount of niche segregation is required for species to coexist in an ecosystem, but it is unclear how this relation can be quantified. Common bream, white bream and roach do coexist in a mesotrophic, diverse habitat with both vegetation zones and open water. In eutrophic lakes however, common bream has become the dominant fish species, the other two cyprinid species are reduced in number and average size (Lammens 1986, 1989). Apparently, the possibility for coexistence is reduced in eutrophic lakes, presumably due to the reduced number of available niches. The shift in species composition in eutrophic lakes is well-suited to study potential relations between morphological specializations and competition for food.

Since zooplankton is a dominant food source in eutrophic lakes (Lammens 1984), we hypothesized that the effectiveness of filter-feeding may be of crucial importance for survival. Hence, this thesis concentrates on the comparison of cyprinid adaptations for filter-feeding. However, there are other factors which might play a role. One of them is the changed predation risk (Lammens 1986, 1989). An important aspect of the predation risk is the body depth of the prey fishes: fishes with a relatively high back are more difficult to ingest for a predator. The body shape of common bream and white bream is very similar in this respect (in fact, these species are hard to tell apart). Hence, it is unlike-

ly that a difference in predation risk can explain the difference in success of these species.

Fishes feeding on zooplankton exert a positive size selection on the zooplankton and will therefore change the size-frequency distribution of the zooplankton populations. The average size of each zooplankton species in Tjeukemeer is smaller than in non-eutrophic lakes (de Nie et al. 1980, Lammens 1985), presumably due to the high predation pressure in eutrophic lakes. In the summer the zooplankton size is reduced even stronger, mainly due to the growth of the new 0+ generation of fish larvae (Vijverberg and Richter 1982). Furthermore, all cyprinid species in Tjeukemeer, especially the large specimens, are often malnourished (Lammens 1984). Apparently, the interspecific competition for food, in particular zooplankton, is strong in eutrophic lakes. Therefore, the effectiveness of filter-feeding is expected to be of great significance for survival. Data of cyprinid gut contents from Tjeukemeer (Lammens et al. 1987) indicate that common bream retains small zooplankton species up to a much larger fish length than white bream and roach. This strengthens the hypothesis that the effectiveness of filter-feeding is the key factor in the dominance of common bream in eutrophic lakes.

Filter-feeding

In general, cyprinid fishes use two feeding modes to ingest small food particles: particulate intake (directed at individual particles) and filter-feeding (not directed at an individual prey, although it may be directed at patches of prey). In both feeding modes small food particles are sieved by the branchial sieve after having been taken up.

Cyprinid filter-feeding is classified as intermittent suction feeding (Sanderson & Wassersug in press) or pump filter-feeding (Lazzaro 1987) or gulping (Sibbing 1991). Water with small food particles is pumped through the branchial sieve by rhythmic expansion and compression of the buccal cavity and the opercular cavities. This method is contrasted by continuous ram-feeding, where the fish swims continuously with its mouth wide open and stationary. Water is forced through the branchial sieve by the forward thrust of the fish. This latter method is used by certain coregonid and clupeid filter-feeders (Sanderson and Wassersug in press, Lazzaro 1987). In both cases, particles larger than the local mesh size in the branchial sieve will be retained, whereas smaller particles and water pass through the meshes. Like most cyprinids, the species under study are facultative filter-feeders with a branchial sieve with a relatively large mesh size, retaining relatively large particles (typically >200 μm) (Lammens and Hoogenboezem 1991). Specialized cyprinid filter-feeders, which retain much smaller particles, do exist, e.g. silver carp and bighead carp (Sibbing 1991) and blackfish (Sanderson et al. 1991).

The three species under study do not have a 'sticky filter', their mechanism of particle entrapment is 'simple sieving' (Rubinstein and Koehl 1977). This is concluded from the fact that they retain no algae at all, although these small particles are very abundant in eutrophic lakes. Sticky filters are expected in filter-feeders, who retain very small particles, like algae, bacteria and detritus. A sticky filter retains all size classes of particles to some extent and is therefore not suited for filter-feeders who want to avoid capturing algae and detritus. In general, 'simple sieving' proves to be a very common mechanism of filter-feeding (Table 1). Drenner et al. (1984) and Mummert and Drenner (1986) showed that there is a direct correspondence between the inter raker distance and the retained particle size in the gizzard shad (*Dorosoma cepedianum*). This freshwater fish can retain particles as small as 20-75 μm. Smith (1989) similarly demonstrated that the branchial sieve of the silver carp (*Hypophthalmichthys molitrix* Val.) also works as a 'simple sieve'. The silver carp can retain particles as small as 10-70 μm.

Table 1

organism	mesh size	mechanism	author(s)
Tilapia galilaea	10 μm	sticky sieve	Drenner et al. 1987
Orthodon microlepidotus	10-25 μm	sticky sieve	Sanderson et al. 1991
Oikopleura (Tunicata)	0.2 μm	simple sieve	Flood et al. 1992
Daphnia spec.	0.5-1 μm	simple sieve	Gophen and Geller 1984
Hypophthalmichthys molitrix	10-70 μm	simple sieve	Smith 1989
Dorosoma cepedianum	20-75 μm	simple sieve	Drenner et al. 1984
Pomoxis annularis	0.1-0.2 mm	simple sieve?	Wright et al. 1983
Clupea harengus	0.2-0.5 mm	simple sieve?	Gibson 1988
Abramis brama	0.1-2 mm	simple sieve	Hoogenboezem et al. 1993
Blicca bjoerkna, Rutilus rutilus	0.1-1 mm	simple sieve	Van den Berg et al. 1993

Even some of the finest filter-feeders use simple sieving. Gophen and Geller (1984) demonstrated that four species of *Daphnia* use simple sieving. The mesh size of their sieve (0.5 -1 μm) corresponded to the minimum size of the retained particles. Flood et al. (1992) showed that tunicates of the genus *Oikopleura* filter suspended particles down to about 0.2 μm in diameter by means of simple sieving. This was concluded from the close correspondence between the pore diameter of their filter (0.2 μm) and the average size of ink particles in their faecal pellets (0.17 μm).

In some filter-feeding experiments with fishes, no correspondence between mesh size and retention ability (smallest particle that can be retained) was found. Gibson (1988) and Wright et al. (1983) found that herring (*Clupea harengus*) and white crappies (*Pomoxis annularis*) respectively, have a worse retention ability than predicted from their inter-raker distance. Such a mismatch probably indicates that the wrong size parameter of the food particles or of the mesh size of the branchial sieve was used (compare chapter 2 of this thesis) and/or that another size selective process conceals the selection by the branchial sieve. Drenner et al. (1987) showed that the removal of gill rakers and microbranchiospines did not influence the retention ability of the cichlid *Tilapia galilaea*. Even without gill rakers this species retains particles as small as 10 μm. Sanderson et al. (1991) showed that the particles ingested by the cyprinid *Orthodon microlepidotus* (blackfish) rarely pass the gill rakers at all. They flow along the gill arches and are collected in mucus, which covers the roof of the oral cavity. The blackfish can retain particles as small as 10-25 μm. Both the above experiments suggest a 'sticky filter'. As expected, both fish species in these experiments are able to retain very small particles (~10 μm).

A simple sieve is by no means simple. It is quite difficult to determine its actual mesh size. First of all, the morphological parameters of the branchial sieve often vary throughout the branchial sieve, hence the mesh size is not constant. Furthermore, the exact site of prey retention is not immediately obvious. The mesh size of the sieve may even be dynamic, changing in time. The most straight forward model for the retention mechanism of the branchial sieve is the comb model, in which the inter raker distance is the mesh size of the branchial sieve (Fig. 1a). The branchial sieves of certain coregonid and clupeid filter-feeders indeed are remarkably similar in appearance to a comb. The structure of the branchial sieve of cyprinids is quite different, with short rakers, raker cushions and channels on the surface of the gill arch. Sibbing (1991) postulated the saw-tooth model of filter-feeding. In this model particles are retained on the gill slits. The mesh size in this model is determined by the distance between the gill arches and by the shape and size of the gill rakers, which extend into the gill slits (Fig. 1b).

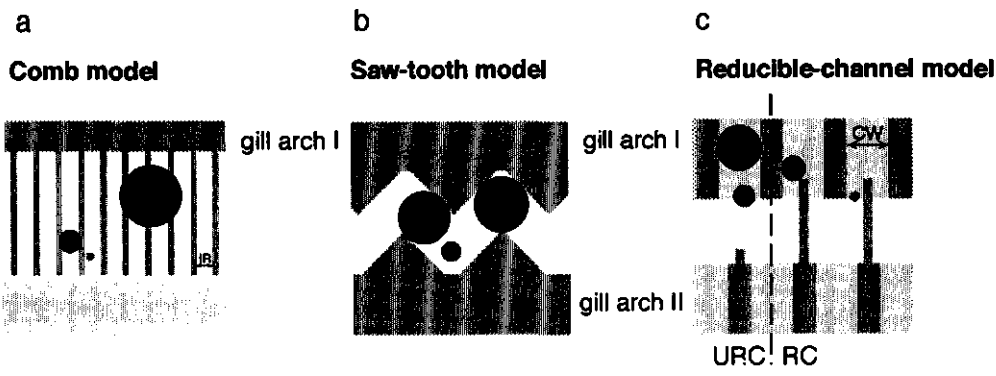

Figure 1 Three models of the retention mechanism of the branchial sieve.
IR = inter raker distance; CW = channel width; URC = unreduced channels;
RC = reduced channels

Hoogenboezem et al. (1991) introduced the reducible-channel model of filter-feeding for common bream. In this model particles are retained in the medial channels on the gill arch surface (Fig. 1c, see also Fig. 1 in chapter 3). Hence, the medial channel width is the mesh size of the branchial sieve. Furthermore, the mesh size of the branchial sieve can be reduced, according to this model, by rotating (abducting) the lateral gill rakers of one gill arch into the medial channels of the neighbouring gill arch (Fig. 1c). Zooplankton feeding experiments clearly showed that common bream indeed adjusts the mesh size of its branchial sieve (Hoogenboezem et al. in press b). In order to reduce the mesh size of the medial channels, the lateral gill rakers must have abductor muscles. Hoogenboezem et al. (1991) found that the lateral gill rakers of each gill arch of common bream have abductor muscles, whereas the medial gill rakers do not, which corroborates the reducible-channel model. X-ray analysis of the movements of the gill arches of common bream showed that during gulping the lateral rakers can always bridge the gap between the gill arches (Hoogenboezem et al. 1990), which is a further support of the reducible-channel model .

How are the particles which are trapped in the medial channels transported to the oesophagus? In freshly caught common bream multi-layered mucus boluses containing numerous zooplankters are found at the back of the pharynx. Hoogenboezem and Van den Boogaart (in press a) postulated that particles which are trapped in the medial channels stimulate the mucus cells in the channel walls, become encapsulated in mucus and are collected in such a multi-layered mucus bolus. When the bolus reaches a certain size, it is swallowed and a new one is built up.

In this thesis I expand on the research of filter-feeding in cyprinids by including white bream and roach. Furthermore, I quantified the morphology, the filter-feeding performance, the effect of zooplankton shape and the influence of gill arch movements of these species. In this way a detailed knowledge of their zooplankton retention mechanisms was obtained. Furthermore, the quantification allowed us to compare the effectiveness of filter-feeding of the three species, which shed light on the question why common bream has become the dominant species in eutrophic lakes rather than white bream or roach.

Framework of this study

Before presenting the major research lines in this thesis I present an overview of research topics related to filter-feeding, which serves as a framework for this study (Fig. 2a). Not all these topics were studied in this thesis. The numbers in figure 2a refer to the subsequent chapters, which are treated in separate paragraphs. It is important to have a continuous feedback between the functional morphological investigations and their implications for the level of ecosystems and populations (Fig. 2a). In figure 2b the research topics are classified in another way. The structures of the feeding apparatus of a fish serve to perform actions (functions), the interaction between structure and action determines the performance of the fish in its environment (fig. 2b).

The effectiveness of filter-feeding is mainly determined by two factors. 1) The 'retention ability' is defined as the range of particle sizes that can be retained, which is determined usually by the smallest particles that can still be retained. In other words, it is a measure of the fraction of particles that can be retained from a sieved volume of water. Formally, it can be defined as one divided by the minimal prey size. 2) The 'filtering rate' is defined as the volume of water that a fish can sieve per unit time. The product of retention ability and filtering rate gives the number of particles that can be retained per unit time, which is a measure of the effectiveness of filter-feeding. Both the retention ability and the filtering rate will be dependent on the fish size. A full understanding of the process of filter-feeding can only be achieved by studying a range of aspects (Fig. 2).

Different ideas about the retention mechanism of the branchial sieve are reflected in different retention models. The models that were tested in this thesis are the reducible-channel model and the saw-tooth model (Fig. 1b,c). The first input for such models is a quantitative study of relevant morphological parameters of the branchial sieve and the relation between these parameters and the size of the fish (chapter 1). For an experimental test of the retention models it is essential to know the influence of the shape of the zooplankton on its retention by the branchial sieve (chapter 2). Using the information of chapter 1 and 2 the retention models can be tested with filter-feeding experiments (chapter 3). Even when these tests are positive, unknown other retention models may well agree with the experimental results, as well. Therefore, we made a detailed study of the gill raker micro anatomy to see whether the anatomical prerequisites for the reducible-channel model were present (chapter 4). Furthermore, we studied the movements of the gill arches in great detail to see whether the kinematical prerequisites for the reducible-channel model were fulfilled and whether the saw-tooth model is a valid alternative (chapter 5 and 6). The flow pattern in the branchial sieve is another important factor to validate the postulated retention mechanisms. We performed a pilot study of flow visualization using Nuclear Magnetic Resonance imaging. Although it proved to be a promising technique, no relevant data have been obtained as yet. The influence of the palatal organ on the flow pattern is potentially large, but no detailed data about palatal organ movements are available.

The filtering rate was measured in the filter-feeding experiments (chapter 3). The retention ability and the filtering rate are not independent. The amplitude of the gill arch movements increases as the filtering rate increases, but gill arch movements disturb the retention function of the branchial sieve. Therefore, there is a conflict between increasing the retention ability and increasing the filtering rate (chapter 6).

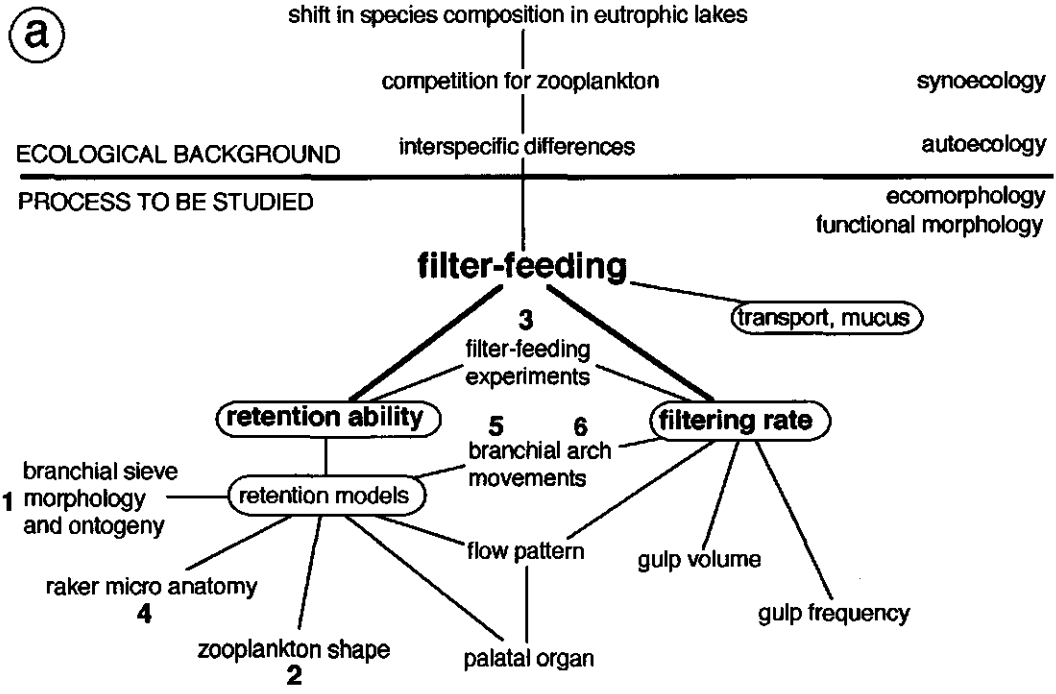

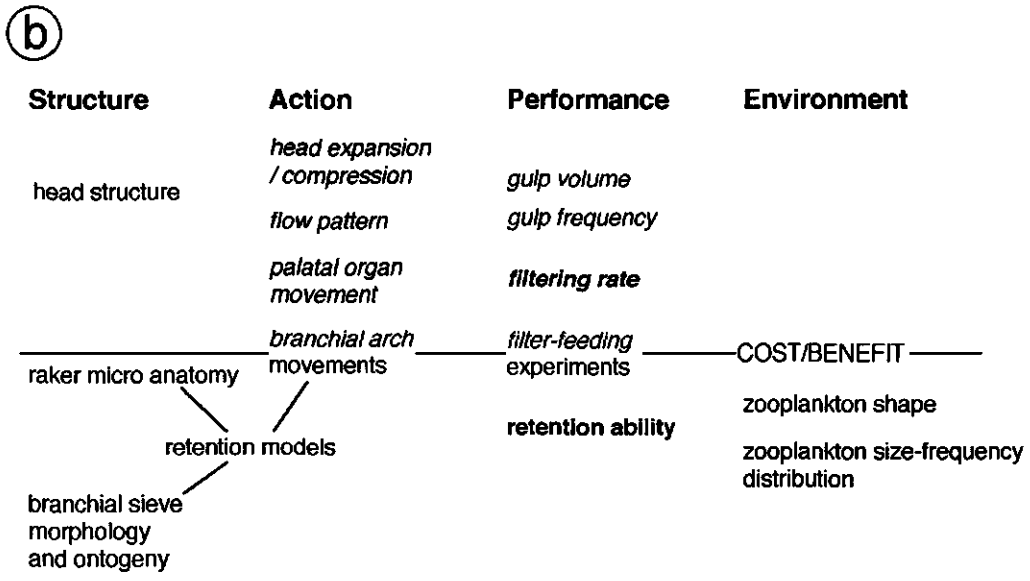

Figure 2
a) This diagram shows the relations between the topics that were studied in this thesis and the original ecological and functional morhological questions.
b) This diagram shows a classification of the research topics. The *italic topics* above the line are associated with the filtering rate, whereas the topics below the line are associated with the retention ability.

Chapter 1; morphological measurements of the branchial sieve

The primary input of models of the retention mechanism of the branchial sieve consists of accurate morphological measurements of the branchial sieve. For both the reducible-channel model and the saw-tooth model the width of the channels (CW) and the length of the rakers (LR) are essential parameters. These parameters (among others) were measured in a range of sizes of common bream, white bream and roach. The parameters grow approximately isometrical. At any standard length (SL) common bream has the widest channels. The relatively wide channels of common bream were a surprise, since we had evidence that common bream has the highest retention ability of the three species. In fact, the channel width of common bream was wider than the smallest particles it is known to retain (Lammens et al. 1987). Possibly, common bream is the only species that is able to reduce its channels. This result stressed the importance of a detailed comparison of the cyprinids under study to determine the retention mechanism of their branchial sieves.

At any standard length (SL) common bream has the longest rakers. The long and pointed lateral rakers of common bream are well-adapted for the reducible-channel model, whereas the shorter and blunt lateral rakers of white bream and roach are not.

We estimated the filtering rate of these species as the total area of the channels of the branchial sieve, assuming an equal flow velocity through the channels. This simple model indicated that common bream has the highest filtering rate of the three species and roach the lowest. The model also indicated that the increase of the filtering rate during growth cannot keep up with the increase of the metabolic demand, since the area increases roughly as SL^2 whereas the metabolic demand increases as $SL^{2.4}$.

Chapter 2; the relation between zooplankton shape and retention

In order to test the retention models the retention ability of the fishes was measured in filter-feeding experiments (chapter 3). However, a problem came up which needed to be solved before we could interpret the results of such experiments. What is the influence of the shape of zooplankters on retention by a sieve with a certain mesh size and mesh shape? Which size parameter of the zooplankters is critical for retention? We measured body length, width and depth of copepods and *Daphnias* which had been sieved in a stack of industrial sieves with diminishing mesh size from top to bottom. These sieves had square meshes. The cycloid copepods were retained according to their width, whereas *Daphnias* up to 40% wider than the meshes still passed through them. The ratio of depth to width ('flatness') of the zooplankton proved to be a critical parameter for retention by the sieves. *Daphnias* are flatter than copepods (depth width ratio of 0.6 versus 0.9), therefore they could pass the meshes diagonally ($\sqrt{2} \approx 1.41$).

Using a geometrical model of unreduced and reduced channels, it was predicted that this phenomenon has important consequences for the reducible-channel model. The geometrical model predicted that in unreduced channels both copepods and *Daphnias* are retained according to their width, whereas in reduced channels both are retained according to their depth. In the filter-feeding experiments retention percentage is plotted versus zooplankton width. Therefore, the geometrical model predicts that in reduced channels copepods are retained better than *Daphnias*, but not in unreduced channels. Preliminary results of filter-feeding experiments with common bream and white bream fully confirmed these expectations. Common bream was feeding with reduced channels

and white bream was not. As expected, common bream retained copepods better than *Daphnias*, whereas white bream did not.

In general, the retention ability of a filter-feeder for a particular prey species depends on the shape of the prey and on the shape of the meshes of its branchial sieve. Hence, a filter-feeder may be specialized in retaining a particular shape (species) of zooplankton.

Chapter 3; filter-feeding experiments

Experiments with filter-feeding fish were performed to test the retention models. These experiments are very important, because they link the morphological data to the actual filter-feeding performance of the living fishes. In the experiments a range of size classes of zooplankton was offered to the experimental fishes (of three size classes). The filtering rate and the retention ability were calculated from the decline in concentration of each size class of zooplankton in the experimental tanks.

With the information from chapter 1 and 2 the theoretical retention curves for unreduced channels and reduced channels could be determined. There are two retention curves for reduced channels, one for copepods and one for *Daphnias*. If the reducible-channel model applies, the retention data can correspond to both the reduced and the unreduced channel curves. No theoretical retention curves for the saw-tooth model could be determined, but two predictions could be made: 1) the mesh size of the branchial sieve is adjustable and 2) copepods will always be retained better than *Daphnias*.

The experimental data of common bream agreed with the predictions of the reducible-channel model, those of white bream with the predictions of the unreducible-channel model (retention in the channels, but no channel reduction) and those of roach with the predictions of the saw-tooth model. The maximal filtering rate of the three species was rather similar in these experiments (20-25 litres per hour at 17.5 cm standard length).

Three different retention models were needed to interpret the retention data of the three species under study. The relation between the morphology of the branchial sieve and the retention ability appears to be complex and diverse in cyprinid fishes. Hence, a detailed knowledge of the morphology and functioning of the branchial sieve is required to predict its retention ability.

At any particular length, common bream has the highest retention ability of the three species (when its channels are reduced) whereas the retention ability of roach is slightly higher than that of white bream, in particular for copepods. These differences in retention ability were quantified with an energy approach. The size-frequency distribution of zooplankton in eutrophic water was expressed in terms of energy. Next, the retention models were used to calculate which fraction of the available zooplankton energy each fish species can extract as a function of their standard length (SL). The advantage of this approach is that the retained amount of zooplankton energy is an ecologically relevant measure of the interspecific differences in retention ability.

In each species the retained amount of energy decreases sigmoidly with standard length. Common bream in the range of 10 to 50 cm SL can retain more zooplankton energy than white bream and roach. Therefore, the population of common bream has an advantage over the populations of white bream and roach in the competition for zooplankton. Since zooplankton is a major food source in eutrophic lakes, this advantage might well be the key factor explaining the dominance of common bream in eutrophic lakes.

Chapter 4; micro anatomy of the branchial sieve

In the reducible-channel model it is assumed that the lateral rakers can be lowered into the medial channels. An obvious prerequisite for this model is the presence of an abductor muscle for the lateral rakers. A study of the micro anatomy of the branchial sieves of common bream, white bream and roach was performed to study their gill raker musculature. 3D computer reconstructions were made of histological sections of the second gill arch of the above species. We also studied serial sections of carp (*Cyprinus carpio*), asp (*Aspius aspius*), grass carp (*Ctenopharyngodon idella*) and rudd (*Scardinius erythrophthalmus*).

The reconstructions provided a detailed view of the structures and their spatial organization. There were large interspecific differences in the presence of the raker abductor muscle, *musculus abductor branchiospinalis* (MAB). This muscle was never present on the medial side of the gill arches in the studied species. In all the examined species it was present at the lateral side of the first gill arch. These muscles can have no function for the reducible-channel model since there is no gill arch opposite the lateral rakers of the first gill arch. It was hypothesized that during gulping these muscles serve to extend the lateral rakers into the wide first gill slit, thus forming a sieve. Only in common bream and carp the gill rakers of the lateral side of gill arch 2, 3 and 4 had abductor muscles. Therefore, the reducible-channel model may be applied to common bream and carp, but not to the other five cyprinid species that were studied.

In the paper it is argued that fylogenetic restraints may have prevented the development of abductor muscles for the medial rakers.

Chapter 5; a 3D method of analysis of X-ray films

Up to now, only static parameters of the retention models were studied. However, the movements of the branchial sieve have important consequences for the functioning of the retention models. In the saw-tooth model the mesh size of the branchial sieve is largely determined by the distance between the gill arches. Furthermore, gill arch movements set limits to the functioning of the reducible-channel model (see chapter 6).

In order to study the movements of the branchial sieve dorsal X-ray films were made of filter-feeding white bream. The gill arches and other relevant structures in the fish were marked with radio-opaque platinum markers. The analysis of these films proved to be a problem, because a film is a 2D projection of a 3D movement. In earlier movement studies projection errors were usually avoided by careful experimental design. However, we required a detailed quantitative analysis of the gill arch movements, hence the 2D method of analysis was unacceptable. A method was developed to calculate the 3D movements of structures from single view films and to calculate rotational movements in a fish-bound frame. One prerequisite for these calculations is that each structure should have at least two markers. The method was illustrated with the gill arch movements of white bream. This example showed that the difference between the 2D and 3D method of analysis can be very large (up to 100%). In the example, the 2D method of analysis even resulted in qualitative errors. Hence, the 3D method of analysis is strongly recommended for movement analysis from single view movies.

Chapter 6; gill arch movements and retention mechanisms

The three cyprinids under study filter-feed by means of gulping. Water with potential prey particles is sucked in by volume increase of the buccal and opercular cavities. The expansion and compression movements of the head during this suction feeding inevitably result in movements of the branchial sieve. The retention mechanism of reduced channels depends on the proper position of the lateral rakers with respect to the medial channels. The relative position of the rakers on opposite sides of a gill slit changes due to the gill arch movements. Gill arch movements can be described as changes in the abduction angle between the gill arch and the *copula communis*. Stated simply, the width of the gill slit (SW) is determined by the sine of this angle and the position of the lateral rakers with respect to the centre of the medial channels (RP) by the cosine of this angle. In other words, when the gill arch angle decreases, the lateral rakers move deeper into the medial channels (SW decreases) and at the same time shift out of their centre (RP increases). If these movements are too large, the prey retention mechanism of the reduced channels will be disturbed.

The variation of the gill arch abduction angles was determined in X-ray films of filter-feeding white bream, using the 3D method of analysis (chapter 5). Platinum markers were inserted in the white bream, at the positions required for the 3D method. Furthermore, previously made X-ray films of common bream were re-analyzed. This re-analysis was imperfect because not all the essential markers were present. Unfortunately, we did not succeed in making X-ray films of roach.

In both white bream and common bream depressed lateral gill rakers can easily bridge the maximal slit width. Hence, they can be positioned in the medial channels. The disturbance of the centring of the lateral rakers, however, is considerable, more than half the medial channel width in common bream. Hence, a model of the dynamics of the reducible-channel model is required. Particles which are trapped in the medial channels become quickly encapsulated in mucus (Hoogenboezem and Van den Boogaart in press). Hence, they do not have to be retained mechanically during the entire gulp cycle. Furthermore, as the lateral rakers move into the medial channels their thickness at the outflow of the medial channels increases. Therefore, the centre of each medial channel remains blocked by the lateral raker even if it is not properly centred. In addition, the lateral rakers can rotate sidewards by asymmetric contraction of the raker abductor muscles. Such supposed sidewards movements should be in phase with the expansion and compression of the head of the fish, which is not inconceivable. A rotation over some 9-12° would be enough to keep the lateral raker tips exactly centred.

In conclusion, the influence of the variation of RP on the effective mesh size of reduced channels will be small. However, the gill arch movements of common bream only just allow the reduced channels to function. If common bream would increase its gill arch movements (to increase its filtering rate) or if it would reduce its medial channel width (to increase its retention ability) the reduced channels would not function anymore. Clearly, the optimization of the filtering rate and of the retention ability are in conflict. Common bream has found a compromise between these opposing demands.

Flow visualization pilot study

An important test for the reducible-channel model is to measure the water flow pattern in the branchial sieve of common bream during filter-feeding. Such a measurement will reveal whether the water flows through the medial channels, as predicted by

the model. The measurement of the water flow pattern in a living fish is technically very difficult. We performed some pilot experiments using Nuclear Magnetic Resonance imaging (NMRi) to visualize the flow pattern. NMRi is a very powerful technique with a wide variety of applications (Taylor et al. 1988, Mansfield and Hahn 1990). One application is to visualize the flow of water in intact biological objects (Van As and Schaafsma 1984). NMRi is very suitable for our problem because it is a non-invasive technique. The pilot study was performed in close cooperation with Henk van As, Dagmar van Dusschoten and Prof. Schaafsma of the department of Molecular Physics in Wageningen. The experiments were performed at the BION NMR centre in Utrecht and the Philips NMR centre in Best.

In the experiments we tried to visualize the flow pattern generated by a breathing carp. The imaging technique requires relatively motionless animals. Therefore, the carp always had to be heavily anaesthetized (MS222 or Nembutal) and immobilized in a clamp. We used carp rather than common bream, because common bream would probably not have survived the stress of these experiments. After various initial problems we obtained some preliminary results (in Best). The flow pattern integrated over the entire breathing cycle was visualized. Although this pattern has only limited biological meaning, the information is absolutely new. This research method is very promising, but probably a couple of years of further research are needed to improve both the animal technique side and the NMR technique side before 'the real thing' can be unveiled: a quantitative picture of the flow pattern at each phase of a breath and a gulp.

Suggestions for further research

I want to identify some loose ends of the research in this thesis and some new questions that have come up and that invite further research.

Gill raker musculature

Which cyprinid species have *m. abductor branchiospinalis* (MAB) on the lateral rakers of all gill arches and which ones do not? Can the reducible-channel model be applied to every cyprinid with MAB? Carp (*Cyprinus carpio*) is the second cyprinid we know of with MAB on the lateral rakers of all gill arches. Furthermore, it is a very cooperative fish in experiments, in contrast to common bream, white bream and roach. It would be extremely interesting to do filter-feeding experiments with carp and to measure its gill arch movements during filter-feeding. Indications of an adjustable mesh size in carp can be found in Uribe-Zamora (1975).

Can the results of a wider micro-anatomical study of cyprinid species be used to find parameters for eco-typing of facultative cyprinid filter-feeders? In other words, can the presence of (curved) channels and MAB be used to identify relatively specialized cyprinid filter-feeders?

Using very local electrical stimulation the effect of contraction of the raker muscles can be observed and their predicted functions can be checked. Preliminary experiments have shown that, although difficult, this type of micro-stimulation is possible; the lateral rakers of common bream can be depressed and they can rotate sidewards when they are stimulated. A more detailed micro-stimulation study is necessary.

X-ray analysis of branchial sieve movements

The gill arch movements of roach have not been studied yet and the existing X-ray films of common bream are suboptimal. Detailed information about the gill arch move-

ments of these species is badly needed. For common bream such data would provide another check of the reducible-channel model. If the saw-tooth model can be applied to roach, the width of its gill slits determines the mesh size of its branchial sieve. The X-ray studies should be complemented with a combined measurement of the levation and abduction of the branchial sieve, the hyoid arch and the suspensorium during filter-feeding as opposed to during the intake of other food items. In fact, there are hardly any quantitatively reliable data of head movements of fishes, since most authors in this field use a 2D method of analysis.

The palatal organ and water flow

The role of the palatal organ (typical for cyprinids) is probably of the utmost relevance for filter-feeding. Video recordings of the palatal organ of barbels of the *Barbus intermedius* species complex (lake Tana, Ethiopia) show its incredible flexibility of shape (F.A. Sibbing, pers. comm.). The palatal organ might well be involved in forming the roof of the medial channels during filter-feeding, in guiding the water flow into the medial channels and in blocking the wide first gill slit during gulping. The movements of the palatal organ can be studied with lateral X-ray films. Detailed NMRi studies of the water flow pattern during filter-feeding might reveal relations between flow and the design of the fish head (cf. Osse and Drost 1989).

Recommendations for filter-feeding experiments

In the design of filter-feeding experiments the statistical analysis of the data is often neglected. In cooperation with the department of Mathematics a statistical test for our experiments was set up (chapter 3). Some aspects of our data were suboptimal for statistical testing. Since the problem of statistical analysis of filter-feeding experiments is common and very important, I have the following recommendations for the design of future experiments:

1. Divide the zooplankton in as much size classes as possible. When the number of size classes is too low the statistical test does not work (<8 is bad news).

2. Measure more than 100 individuals of each zooplankton species in each (sub)sample; 500 is not exaggerated. For example, it is reasonable to divide 500 zooplankters in 20 size classes with on average 25 individuals per size class.

3. Measure all zooplankton in a (sub)sample. Choose the sample volume carefully to avoid excessively low or high numbers of zooplankters. Measuring a fixed number (e.g. 100) of individuals of each zooplankton species makes a statistical test comparing different zooplankton species very awkward.

General discussion

Our aquarium studies of the retention ability, the macro- and micro-anatomy of the gill arches and their movements provided evidence that the reducible-channel mechanism of filter-feeding can be applied to common bream, but not to white bream and roach. Why would a fish have such a complicated mechanism, with its demands of accurate interdigitation of all the rakers, its limitations of gill arch movements and with the need for special raker abductor muscles, which seem to be mostly absent in related cyprinids? A similar retention ability can be obtained much easier with channels of half the present width. However, a major advantage of the reducible-channel model is the ability to adjust the mesh size of the branchial sieve. Effectively, common bream has two sieves, a coarse one and a fine one.

Common bream is an opportunistic feeder, we should therefore not look at filter-feeding alone. Previous research showed that common bream is more effective in digging up chironomid larvae and in separating them from the substrate, than white bream and roach, in particular when the larvae are buried deep (Lammens et al. 1987). If the branchial sieve is too fine, separating food from substrate is ineffective because the sieve becomes clogged with substrate (Janssen 1978). Therefore, the reducible-channel mechanism might be a compromise for effective feeding on different size classes of food, e.g. cladocerans, copepods and chironomid larvae. Feeding with unreduced channels allows separation of chironomid larvae from substrate and feeding with reduced channels allows retention of small food particles. In Tjeukemeer chironomid larvae and zooplankton are, roughly speaking, equally important as food source (Lammens 1984). The branchial sieve of common bream seems to be better designed to exploit both these food sources than those of white bream and roach. The advantage of common bream over the sympatric cyprinids white bream and roach in the competition for chironomid larvae and zooplankton may well be a key factor in its dominance in eutrophic lakes.

How does the reducible-channel model (RC) compare with the unreducible-channel model (URC) and the (quite similar) comb model in an evolutionary scenario? Which model can achieve the largest retention ability? Figure 3 shows a simple model of the relation between retention ability and channel width (CW). The retention ability is defined as one divided by the mesh size. For simplicity, the mesh size of reduced channels is considered to be half the mesh size of unreduced channels[1]. As a result, at any CW the retention ability is always two times larger in the RC model than in the URC model. The stippled part of each curve indicates a 'forbidden zone'; the CWs in this zone are not allowed because this would strongly reduce the filtering rate (see below). The black dot indicates the maximum retention ability that can be reached with each retention model.

The 'forbidden zones' are estimated roughly using the present data and literature data[2]. In chapter 6 it was shown that common bream has reached the limits of what is 'allowed' by the RC model for pump filter-feeders. Its gill arch movements may not be larger and its CW may not be smaller. Therefore, for a fish of about 20 cm SL the lower limit of CW in the RC model will be in the order of 0.5 mm. In fishes who filter-feed according to the URC model or the comb model, CW (cq. the inter raker distance) may become much smaller. The lower limit in these retention models is reached when the flow resistance of the branchial sieve increases strongly due to the small size of the meshes. Silver carp (Smith 1989) of 32 gram, with a mesh size of 10-70 μm still have a filtering rate of 18.25 litres per hour (compare 20-30 litres per hour in common bream, white bream and roach of 17.5 cm SL ($\approx$ 120 gram); chapter 3). According to the formula in Drenner et al. (1984) ram-feeding gizzard shad of 17.5 cm SL, with a mesh size of 20-75 μm, even have a filtering rate of 75 litres per hour. Therefore, for a fish of about 20 cm SL the lower limit of CW in the URC model was estimated to be in the order of 50 μm.

The maximum retention ability of the URC model is much larger than that of the RC model, as a result of the above difference in lower limit of CW (Fig. 3). However, at a

---

[1]The differences in retention ability of the models could be refined, but for the present argument this approximation will do.

[2]The present model of the retention ability as a function of channel width can be refined when the exact relation between the filtering rate and the channel width is known. In that case the effectiveness of *filter-feeding* can be calculated as the product of filtering rate and retention ability.

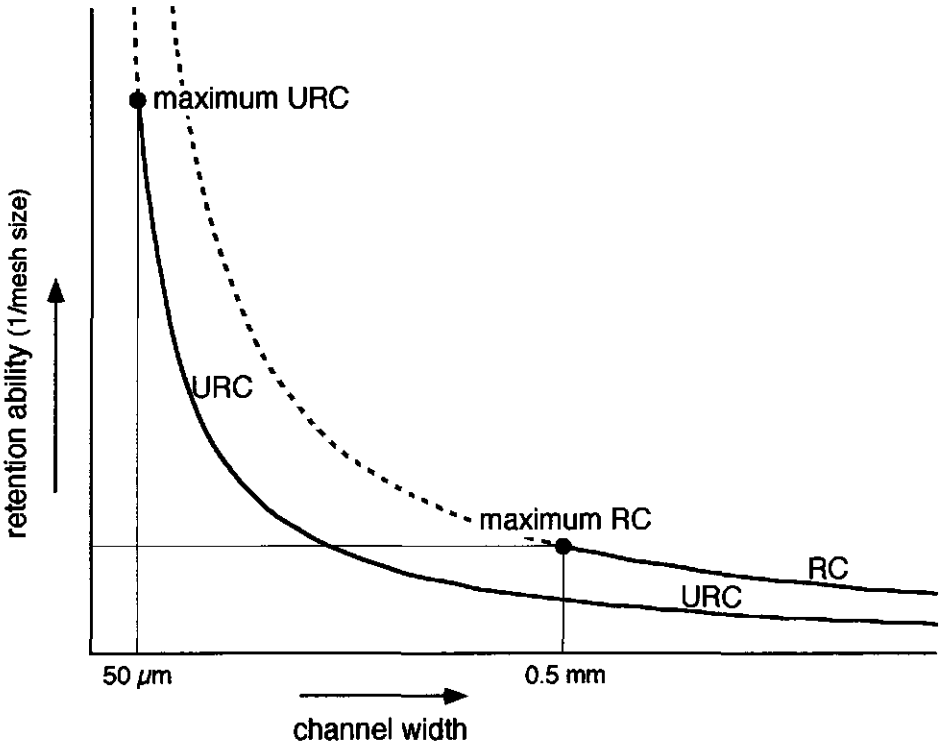

Figure 3 Model of the relation between the retention ability of the branchial sieve and its channel width. The stippled parts indicate 'forbidden zones', which are not allowed in the model, because the filtering rate would be strongly decreased at these values of the channel width. Notice that, although the RC curve is higher than the URC curve, the maximum of the URC curve is higher than the maximum of the RC curve.
RC = curve for the reducible channel model
URC = curve for the unreducible channel model

given, large CW the retention ability of the RC model is twice that of the URC model (Fig. 3). Suppose that an environmental pressure to increase the retention ability is exerted on several opportunistic cyprinid species with a relatively large CW, which live in the same ecosystem. Then the species which develops the RC model (common bream) will have an advantage over the other species (white bream and roach). However, once common bream *can* reduce its channels, a further increase of its retention ability is difficult to achieve. If common bream would decrease the mesh-size of its medial channels, its gill arch movements would impair the functioning of the reduced channels and the retention ability would fall back to the level of the URC curve (Fig. 3). Therefore, common bream is in an evolutionary dead-end, it cannot increase its retention ability by evolution unless with a large leap (of more than 50% reduction of CW, Fig. 3). In other

words, when CW is large, reduced channels are more effective than unreduced channels, but once a fish can reduce its channels it cannot reach the *higher* maximum retention ability of the URC model without reducing its retention ability in intermediate stages of evolution. Not unexpectedly, specialized filter-feeders never have a retention mechanism similar to that of the reducible-channel model, but usually have a comb-like sieve (Fig. 1a). The reducible-channel model is a typical compromise solution of an opportunistic species.

No evidence was found that the structural requirements of the reducible-channel model impair the use of other food sources. Requirements of the model are the presence of abductor muscles for the lateral rakers and a limited branchial sieve expansion *during filter-feeding*. When the channels are unreduced, the mesh size of the branchial sieve of common bream is larger than that of white bream and roach. Therefore, a reduced filtering rate in common bream was not expected (and not found). The fact that the reducible-channel model does *not* narrow down the food spectrum may well be an important factor in favour of this model for an opportunistic feeder. The very fine sieve of many obligate filter-feeders *does* tend to limit them to small food particles (hence the adjective 'obligate'). In general, in specialists the structural adaptations for their preferred food will more severely, and hence more clearly, limit the exploitation of other food sources than in opportunistic feeders.

It is unclear why the branchial sieves of white bream and roach do not operate according to the reducible-channel model, since it seems to increase the flexibility of food intake at a very low cost (i.e. the presence of lateral raker abductor muscles). Possibly, an evolutionary pressure was exerted on common bream, which was not present in white bream and roach.

There are interspecific morphological differences between the species under study which are related to differences in their effectiveness of exploiting certain food types, but these differences are not dictated by the reducible-channel model. Common bream has a narrower post lingual organ and smaller pharyngeal jaws than white bream and roach (Sibbing 1988, 1991), which possibly is the reason why common bream is less effective than white bream and roach in feeding on zebra mussels (*Dreissena polymorpha*) (Nagelkerke and Sibbing subm.). Common bream has a more protrusile mouth and a higher density of taste buds on its palatal organ than white bream and roach (Sibbing and Rauwerdink, unpubl. res.). These characteristics are probably associated with the higher effectiveness of common bream in digging up chironomid larvae and in separating them from the substrate.

The above interspecific differences indicate that none of the species under study is a pure generalist. This corroborates a basic ecological idea: a certain degree of niche segregation is required for species to coexist in an ecosystem.

Finally, the present thesis corroborates a basic assumption of ecomorphological research: there is a relation between niche segregation and interspecific differences in morphology.

Literature cited

Alexander, R.McN. 1988. The scope and aims of functional and ecological morphology. Neth. J. Zool. 38(1): 3-22.

As, H. van and T.J. Schaafsma. 1984. Noninvasive measurement of plant water flow by nuclear magnetic resonance. Biophys. J. 45: 469-472.

Drenner, R.W., J.R. Mummert, F.Jr. de Noyelles and D. Kettles. 1984. Selective particle ingestion by a filter-feeding fish and its impact on phytoplankton community structure. Limnol. Oceanogr. 29(5): 941-948.

Drenner, R.W., G.L. Vinyard, K.D. Hambright and M. Gophen. 1987. Particle ingestion by *Tilapia galilaea* is not affected by removal of gill rakers and microbranchiospines. Trans. Amer. Fish. Soc. 116: 272-276.

Flood, P.R., D. Deibel and C.C. Morris. 1992. Filtration of colloidal melanin from sea water by planktonic tunicates. Nature 355: 630-632.

Gibson, R.N. 1988. Development, morphometry and particle retention capability of the gill rakers in the herring, *Clupea harengus* L.. J. Fish Biol. 32: 949-962.

Gophen, M. and W. Geller. 1984. Filter mesh size and food particle uptake by *Daphnia*. Oecologia 64: 408-412.

Hoogenboezem, W., F.A. Sibbing, J.W.M. Osse, J.G.M. van den Boogaart, E.H.R.R. Lammens and A. Terlouw. 1990. X-ray measurements of gill-arch movements in filter-feeding bream, *Abramis brama* (Cyprinidae). J.Fish Biol. 36: 47-58.

Hoogenboezem, W., J.G.M. van den Boogaart, F.A. Sibbing, E.H.R.R. Lammens, A. Terlouw and J.W.M. Osse. 1991. A new model of particle retention and branchial sieve adjustment in filter-feeding bream (*Abramis brama* (L.), Cyprinidae). Can. J. Fish. Aquat. Sci. 48: 7-18.

Hoogenboezem, W. and J.G.M. van den Boogaart. in press a. The importance of oro-pharyngeal mucus in filter-feeding of bream (*Abramis brama*). Can. J. Fish. Aquat. Sci.

Hoogenboezem, W., E.H.R.R. Lammens, P.J. MacGillavry and F.A. Sibbing. in press b. Size selectivity and sieve adjustment in filter-feeding bream *Abramis brama* (L.), Cyprinidae. Can. J. Fish. Aquat. Sci.

Janssen, J. 1978. Feeding-behavior repertoire of the alewife, *Alosa pseudoharengus*, and the ciscoes *Coregonus hoyi* and *C. artedii*. J. Fish Res. Bd. Canada 35: 249-253.

Lammens, E.H.R.R. 1984. Growth, condition and gonad development of bream (*Abramis brama* L.) in relation to its feeding conditions in Tjeukemeer. Hydrobiologia 95: 311-320.

Lammens, E.H.R.R. 1985. A test of a model for planktivorous filter-feeding by bream *Abramis brama*. Env. Biol. Fish. 13: 288-296.

Lammens, E.H.R.R. 1986. Interactions between fishes and the structure of fish communities in Dutch shallow, eutrophic lakes. Ph.D. thesis Agricultural University Wageningen.

Lammens, E.H.R.R., J. Geursen and P.J. McGillavry. 1987. Diet shifts, feeding efficiency and coexistence of bream (*Abramis brama*), roach (*Rutilus rutilus*) and white bream (*Blicca björkna*) in eutrophicated lakes. Proc. V Congr. Europ. Ichtyol., Stockholm: 153-162.

Lammens, E.H.R.R. 1989. Causes and consequences of the success of bream in Dutch eutrophic lakes. Hydrobiol. Bull. 23: 11-18.

Lammens, E.H.R.R. and W. Hoogenboezem. 1991. Diets and feeding behaviour. p 353-376 in: Cyprinid fishes; systematics, biology and exploitation. Eds. I.J.Winfield and J.S.Nelson. 667 pp.

Lazzaro, X. 1987. A review of planktivorous fishes: their evolution, feeding behaviours, selectivities, and impacts. Hydrobiologia 146: 97-167.

Limnologisch instituut. 1983. Het oecosysteem Tjeukemeer. Vanellus 36(3).

Mansfield, P. and E.L. Hahn [Eds.]. 1990. NMR imaging. Proceedings of a royal society discussion meeting. Phil. Trans. R. Soc. Lond. A: 403-572.

Mummert, J.R. and R.W. Drenner 1986. Effects of fish size on the filtering efficiency and selective particle ingestion of a filter-feeding clupeid. Trans. Amer. Fish. Soc. 115: 522-528.

Nagelkerke, L.A.J. and F.A. Sibbing. subm. Efficiency of feeding on zebra mussel (*Dreissena polymorpha*) by bream (*Abramis brama*), white bream (*Blicca bjoerkna*) and roach (*Rutilus rutilus*).

Nie, H.W. de, H.J. Bromley and J. Vijverberg 1980. Distribution patterns of zooplankton in Tjeukemeer, the Netherlands. J. Plankton Res. 2(4): 317-334.

Nie, H.W. de 1987. The decrease in aquatic vegetation in Europe and its consequences for fish populations. EIFAC/CECPI Occasional paper 19: 52 p.

Osse, J.W.M. and M.R. Drost. 1989. Hydrodynamics and mechanics of fish larvae. Pol. Arch. Hydrobiol. 36(4): 455-465.

Rubenstein, D.I. and M.A.R. Koehl.1977. The mechanisms of filter feeding: some theoretical considerations. Amer. Natur. 111(981): 981-994.

Sanderson, S.L. and Wassersug R. in press. Convergent and alternative designs for vertebrate suspension feeding. In: The vertebrate skull, Vol. 3. Eds.: J. Hanken and B. Hall. The university of Chicago press.

Sanderson, S.L., J.J. Cech Jr. and M.R. Patterson. 1991. Fluid dynamics in suspension-feeding blackfish. Science 251: 1346-1348.

Schoener, Th.W., 1982. The controversy over interspecific competition. Am. Sc. 70: 586-595.

Sibbing, F.A. 1988. Specializations and limitations in the utilization of food resources by the carp, *Cyprinus carpio*: a study of oral food processing. Env. Biol. Fish. 22(3): 161-178.

Sibbing, F.A. 1991. Food capture and oral processing. p 377-412 in: Cyprinid fishes; systematics, biology and exploitation. Eds.: I.J. Winfield and J. Nelson. Chapman and Hall 667 p.

Sibbing, F.A. 1991. Food processing by mastication in cyprinid fish. Proceedings of SEB congress 1989.

Smith, D.W. 1989. The feeding selectivity of silver carp, *Hypophthalmichthys molitrix* Val.. J. Fish Biol. 34: 819-828.

Taylor, D.G., R. Inamdar and M-C. Bushell. 1988. NMR imaging in theory and in practice. Phys. Med. Biol. 33: 635-670.

Uribe-Zamora, M. 1975. Selection des proies par le filtre branchial de la carpe miroir (*Cyprinus carpio* L.). Thesis. University of Lyon.

Vijverberg, J. and A.F. Richter. 1982. Population dynamics and production of *Daphnia hyalina* (Leydig) and *Daphnia cucullata* (Sars) in Tjeukemeer. Hydrobiologia 95: 235-259.

Wright, D.I., W.J. O'Brien and C. Luecke. 1983. A new estimate of zooplankton retention by gill rakers and its ecological significance. Trans. Amer. Fish. Soc. 112: 638-646.

Chapter 1

Structure, development and function of the branchial sieve of bream (*Abramis brama*), white bream (*Blicca björkna*) and roach (*Rutilus rutilus*)

Coen van den Berg, Ferdinand A. Sibbing, Jan W.M. Osse, Wim Hoogenboezem
Appeared in 1992 in the Environmental Biology of Fishes 33: 105-124.

key words:
cyprinids, eutrophication, zooplankton, filter feeding, gill rakers, retention ability, capacity, comb model, channel model, energy ratio

Abstract

The filter feeding organ of cyprinid fishes is the branchial sieve, which consists of a mesh formed by gill rakers and tiny channels on the gill arches. In order to measure its possible role during growth we measured the following morphological gill raker parameters over a range of sizes in three cyprinid fishes, bream, white bream and roach: inter raker distance, bony raker length, raker width, cushion length and channel width. At any given standard length bream has the largest inter raker distance, roach the lowest and white bream is intermediate. In the "comb model" of filter feeding the inter raker distance is considered to be a direct measure of the mesh size and retention ability (= minimal size of prey that can be retained) of a filter. For the three species under study there is a conflict between the comb model and experimental data on particle retention. Lammens et al. (1987) found that bream has a large retention ability whereas roach and white bream have a much smaller one. A new model, the "channel model" (Hoogenboezem et al. 1990) has been developed for bream; in this model the lateral gill rakers can regulate the mesh size of the medial channels on the other side of the gill slit. The present data indicate that this model is not appropriate for white bream and roach. At any given standard length white bream and roach only reach 70% of the raker length of bream, which means that in this model the gill slits need to be very narrow during filter feeding. The gill rakers consist of a bony raker and a fleshy cushion. The bony rakers have a rather long needle-like part outside the cushion in bream, but not in white bream and roach which have blunt gill rakers. Blunt gill rakers are not suited to reduce the diameter of the medial channels. The comb model seems more appropriate for white bream and roach, but doubts about the validity of this simple model remain. The sum of the areas of the medial channels is an approximation of the area through which water flows in the filter. This channel area therefore gives an impression of the capacity or flow rate of the filter. With this capacity estimation and an estimation of energy consumption we calculated an energy ratio of filter feeding. The energy ratio decreases with increasing standard length with an exponent close to the expected exponent of -0.40. The energy ratio is highest in bream, intermediate in white bream and lowest in roach.

Introduction

In Tjeukemeer, a shallow, eutrophic fresh water lake in the Netherlands, the omnivorous bream (*Abramis brama*) and the piscivorous pike perch (*Stizostedion lucioperca*) are strongly dominant (Lammens 1986, Lammens 1989). The population sizes of white bream (*Blicca björkna*) and roach (*Rutilus rutilus*) are small (Lammens 1986, Lammens et al. 1987).

In this lake zooplankton and chironomid larvae are the major food source for fishes (de Nie et al. 1980, Vijverberg & Richter 1982a, 1982b, Lammens 1986, de Nie 1987). On an annual basis the diet of bream consists for one half of zooplankton and for one half on chironomid larvae (Vijverberg & Richter 1982a).

Small food, like zooplankton is retained by the branchial sieve, which is a filter formed by gill rakers on the branchial arches (Zander 1906, Hoogenboezem et al. 1990). The two main properties of a filter are its retention ability (the minimal size of particles that can be retained) and its capacity (the volume of water that can be filtered per unit time).There is evidence that bream has a better retention ability than white bream and roach; small food particles are still found in the intestines of freshly caught bream with a standard length at which these particles are absent in the other two species (Lammens et al. 1987; Fig. 11). Since zooplankton is a major food source in Tjeukemeer it is hypothesized that success in eutrophic water is coupled to a good retention ability and a large capacity of the branchial sieve.

The first hypothesis to be tested is whether differences in filter functioning (retention ability and capacity) between the three species can be related to differences in structure and growth of the branchial sieve. A second hypothesis is whether the functioning of the filter is related to success in zooplankton-rich environments. These relations have been investigated for bream by Hoogenboezem et al. (1989).

In this paper the relevance for the studied species of two filter feeding models, the comb model and the channel model, is evaluated with the present data. In the comb model of filter feeding the inter raker distance is considered to be a direct measure of the mesh size and retention ability (= minimal size of prey that can be retained) of a filter. The channel model has been proposed for bream by Hoogenboezem et al. (1990, Fig. 12b). In this model water and prey flow parallel to the arches and turn 90° into the medial channels where the prey is retained; the water flows into the gill slit towards the gills. The curvature of the channels in bream (Fig. 3a) could possibly help to guide the water current into the channels. Apart from this a mechanism to reduce the mesh size is introduced (Hoogenboezem et al. 1990). The gill rakers on the lateral side of an arch can be depressed into the medial channels on the opposite side of the gill slit. Evidence for this is provided by X-ray films of filter feeding bream, which show that during filter feeding the maximal inter arch distance is small enough to allow the gill rakers to reach the other side of the gill slit (Hoogenboezem et al. 1990). In this way the mesh size of the medial channels is reduced by at least 50 %. In other words, in this model the meshsize is adjustable using either the channel width or the reduced channel width.

The assumption is made that the branchial sieve acts as a mechanical sieve and does not have a sticky mucus layer so that the mechanism of prey retention is simple sieving (Rubinstein & Koehl 1977). This assumption is based on the observation that no small, free living algae are found in the mucus on the branchial sieve of bream in Tjeukemeer although such algae are the dominant particles in the lake (Hoogenboezem, pers. comm.). Simple sieving means that no particles smaller than the mesh size will be retained. This does not necessarily mean that retention curves must be perfect step functions because variations in mesh size within the filter may occur (see below, 'variations

within the branchial sieve'). A second assumption is that the only selection phase occurs in the branchial sieve.

For this paper Hoogenboezem measured a number of branchial sieve parameters in an ontogenetic series of bream; later van den Berg measured similar parameters for white bream and roach and some additional parameters for the three species and worked out the results.

Material and methods

The eleven white breams (SL 101-232 mm) and fifteen roaches (SL 48-281 mm) were collected from a number of Frysian lakes, but not from Tjeukemeer. The thirty-one breams (SL 30-430 mm) were captured in Tjeukemeer. All fish were captured with trawlnets and immediately killed and stored in Bouin's fluid (Romeis 1968). In order to estimate the effect of tissue deformation due to fixation we measured one fresh specimen of each species, stored it in Bouin's fluid and measured it again two weeks later. The inter raker distance and the raker length are almost unaltered (about 4% of change) in the three species. The cushions become lower and broader and due to this effect the channels become narrower. The trends of this change, but not the magnitude (up to 40% of change), are similar in the three species. We did not correct the measured values for the effect of tissue fixation.

We measured three groups of parameters: standard parameters, gill arch parameters and gill raker parameters. The first group (Fig. 1a) consists of standard length (SL), fork length (FL), anal length (AL), head length (SOL, snout operculum length), eye diameter (ED) and body weight (W). We measured these parameters with Vernier calipers (to the next 0.05 mm) or a spring rule (to the next 0.5 mm) depending on fish size. The orientation terms used below are defined in the section 'symbols'.

The gill arch parameters are : the number of gill rakers on the medial side of the ceratobranchials (NR); the length of each ceratobranchial (LCB), defined as the distance between the first and the last raker on the medial side of the ceratobranchial; the arch width from raker tip to raker tip (TAW) and the basal arch width of each arch (BAW), without the gill rakers (Fig. 1b); both widths were measured at the middle of the ceratobranchials. We measured at 30x magnification using an ocular micrometer (to the next 0.03 mm). The length of the ceratobranchials of the larger fish we measured with Vernier calipers (to the next 0.1 mm). We measured these parameters on the four gill arches of one side.

We measured the gill raker parameters (Fig. 1b) at 30x magnification with an ocular micrometer (to the next 0.03 mm). In a lateral view of the gill arch, perpendicular to the long axis of the bony rakers, the following parameters were measured : bony raker length (RL), inter raker distance (IR) and at half of the bony raker length the width of the raker cushion (RW) and the width of the channel (CW). We measured the same parameters in bream except for the inter raker distance, which we calculated however as the sum of cushion width and channel width. We measured the raker cushion length (RCL) in a top view of the gill arch. In bream we measured channel length instead of cushion length. We measured the gill rakers from the fifth to the ninth raker counting from anterior (which is approximately the middle of the ceratobranchial) and only on the medial side of the first arch, the lateral and medial side of the second arch and the lateral side of the third arch, in other words, the parameters of the second and third gill slit. In bream we measured the medial side of the first and the lateral side of the second arch, in other words the parameters of the second gill slit.

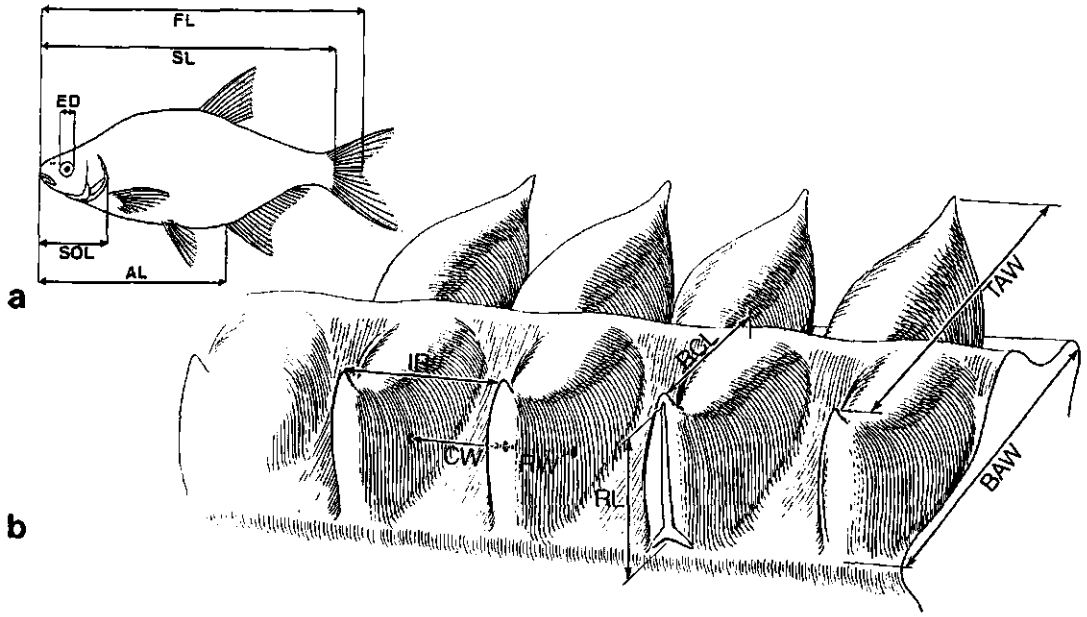

Figure 1

a) the definition of the standard parameters: standard length (SL), fork length (FL), eye diameter (ED), head length (SOL) and anal length (AL).

b) part of a gill arch of white bream; indicated are the definitions of the measurements of bony raker length (RL), inter raker distance (IR), channel width (CW), raker cushion width (RW), raker cushion length (RCL), tip arch width (TAW) and basal arch width (BAW). The position of measurement of CW and RW is indicated with large dots; this position is located at a height of 0.5 RL and about 0.25 RCL deep in the channel.

In order to quantify the variation of the gill raker parameters within a complete filter we measured all the rakers on all the ceratobranchials of one side of the branchial sieve for one specimen of each species. In this way we obtained information about variations within each arch and also about differences between the arches.

With the data of ceratobranchial lengths and widths we calculated the gill arch area (A_a), defined as the sum of the length width products of the first three arches multiplied by two to account for both sides:

$$A_a = 2 \sum_{i=1}^{3} LCB_i \times BAW_i$$

A more interesting area for capacity estimations is the filter area or the total cross sectional area where water passes the filter. Two different areas can be defined depending on the filter model that is used. The channel area (A_c, Fig. 2) is the sum of all the medial channel diameters of both sides, defined as raker length times channel width or, in other words, the diameter at the end of the channel; this area is based on the channel model (Hoogenboezem et al. 1990, Fig. 12b):

$$A_c = F \sum_{i=1}^{5} RL_i \times CW_i$$

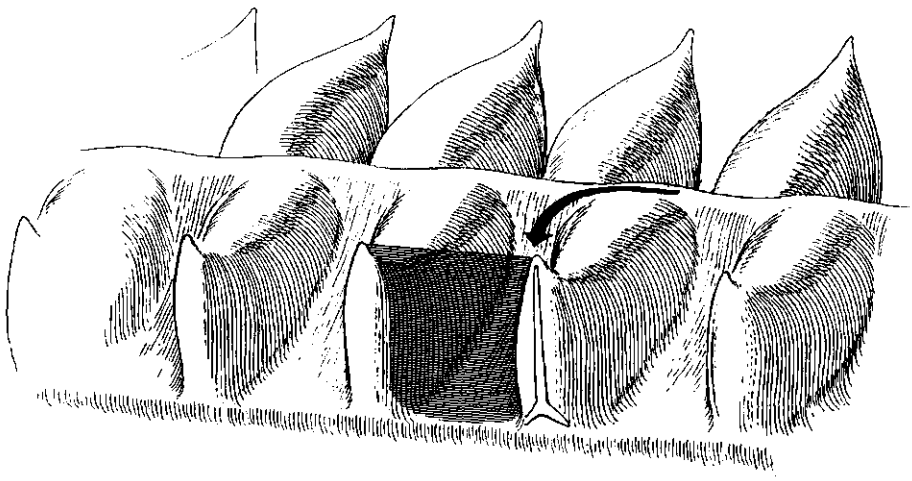

Figure 2

Part of a gill arch; the channel area is the sum of the areas of the medial channels (one of which is indicated by horizontal hatching). These areas are calculated as the product of bony raker length and channel width, as indicated here they are situated at the end of the channel, in the plane of the gill rakers. The expected water flow is indicated with an arrow, the areas of the medial channels are at right angles with the expected flow.

---

where F is a factor relating the sum of the five channel diameters of the standard measurements with the total medial channel area. We calculated this factor with the aid of the complete filter measurements (see above).The gill slit area, which depends on the distance between the arches, is based on the interdigitating model (Sibbing in press, Fig. 12a). There are no data of inter arch distances during filter feeding for white bream and roach so the gill slit area can not be calculated.

We analysed the data on a Macintosh II with a statistical program Statworks™. We calculated the relations between pairs of data sets with the model I type of linear regression rather than with model II assuming that the standard length was measured with a much higher degree of accuracy than the branchial sieve parameters(Sokal & Rohlf 1969). We tested the significance of differences between the species with the non-parametric Mann Whitney U-test, which assumes identical distributions of the three independent sets of data (Sokal & Rohlf 1969). The ratio of the y-value and the x-value (SL) is the test parameter (e.g. IR divided by SL); in the case of an area the test parameter is the ratio area/SL^2. The value of y/x has to be rather constant per species to be able to use the Mann Whitney U-test properly. If the relation between the parameters is linear and if the regression line tends to go through the origin, the value of y/x will be rather constant. In the present data the deviations from going through the origin are never very large and corrections were not necessary.

Anatomy of the branchial sieve

The filter feeding apparatus of cyprinids is the branchial sieve (Fig. 3). The cerato- and epibranchials bear gill rakers on the lateral and medial sides, pointing to the gill slits. The gill rakers filter the water current through the gill slits and retain particles larger than the local mesh size. Two possible functions of the branchial sieve are protection of the gills from damaging objects and retention of food particles (Zander 1906).

The fifth gill arches are the pharyngeal jaws (Sibbing 1982, 1988). They bear short rakers on the lateral side only. The ceratobranchials of the four gill bearing gill arches lie parallel in the floor of the pharynx and run latero caudally; they are slightly curved (Zander 1906). Rostrally they are connected in a complex of small hypobranchialia and basibranchialia, which is covered by the postlingual organ (Sibbing & Uribe 1985). Caudally they connect with the epibranchials which contribute to the roof of the pharyngeal cavity. The epibranchials are much shorter than the ceratobranchials and have smaller gill rakers. The palatal organ covers most of the roof of the pharyngeal cavity (Sibbing & Uribe 1985, Sibbing et al.1986); it plays an important role in food processing. The pharyngeal cavity in cross section has the shape of a horizontal slit; the palatal organ is right above the branchial sieve and probably plays an important role in the functioning of the branchial sieve (Hoogenboezem et al. 1990).

The gill rakers consist of a bony raker (branchiospine) from which a fleshy cushion runs to the middle of the arch surface, which in bream is elevated to a distinct central ridge (Fig. 3a-c). In bream the rakers have a clear needle-like point, whereas in white bream and roach they are blunt (Zander 1906); in bream the top 1/3 of the bony raker is covered only by a thin layer of tissue, whereas in white bream and roach the bony rakers are almost completely embedded in thick cushion tissue (Fig. 3a-c). Between two adjacent gill rakers a channel is present. In bream the channels start at the central ridge, first run almost parallel to the arch axis and then turn 90° towards the rim of the arch (fig 3a); this curvature becomes less distinct from anterior to posterior on the arches. In white bream and roach all the channels are straight and run perpendicular to the arch axis (Fig. 3b,c).

Gill rakers on opposite sides of a gill slit interdigitate so that a slit might form a functional sieving unit ; for bream evidence for this was provided by Hoogenboezem et al. (1990).

Figure 3 (see overleaf)

Photos of branchial sieves of fresh fish; the bars represent 1 mm.

a) bream with SL 230 mm; the second, third and part of the fourth gill arch are visible and in the right bottom corner a part of the postlingual organ is visible. The bony raker tips protrude quite far from under the raker cushion. Notice the curvature of the cushions and channels and the distinct medial ridge.

b) white bream with SL 204 mm; same orientation as bream in a). The bony raker tips hardly protrude from the fleshy cushion. The channels are straight and a clear medial ridge is absent.

c) roach with SL 254 mm; same orientation as bream in a). The bony raker tips do not protrude far from the fleshy cushion. The channels are straight and a clear medial ridge is absent.

d) bream with SL 55 mm. The raker cushions are small and straight, the bony rakers are already developed.

e) roach with SL 35 mm; the second gill arch in a top view. The bony rakers are present but the raker cushions have not yet developed.

f) roach with SL 70 mm. The bony rakers and raker cushions are developed now and a medial ridge has appeared. Notice the resemblance with the adult form (Fig. 3c).

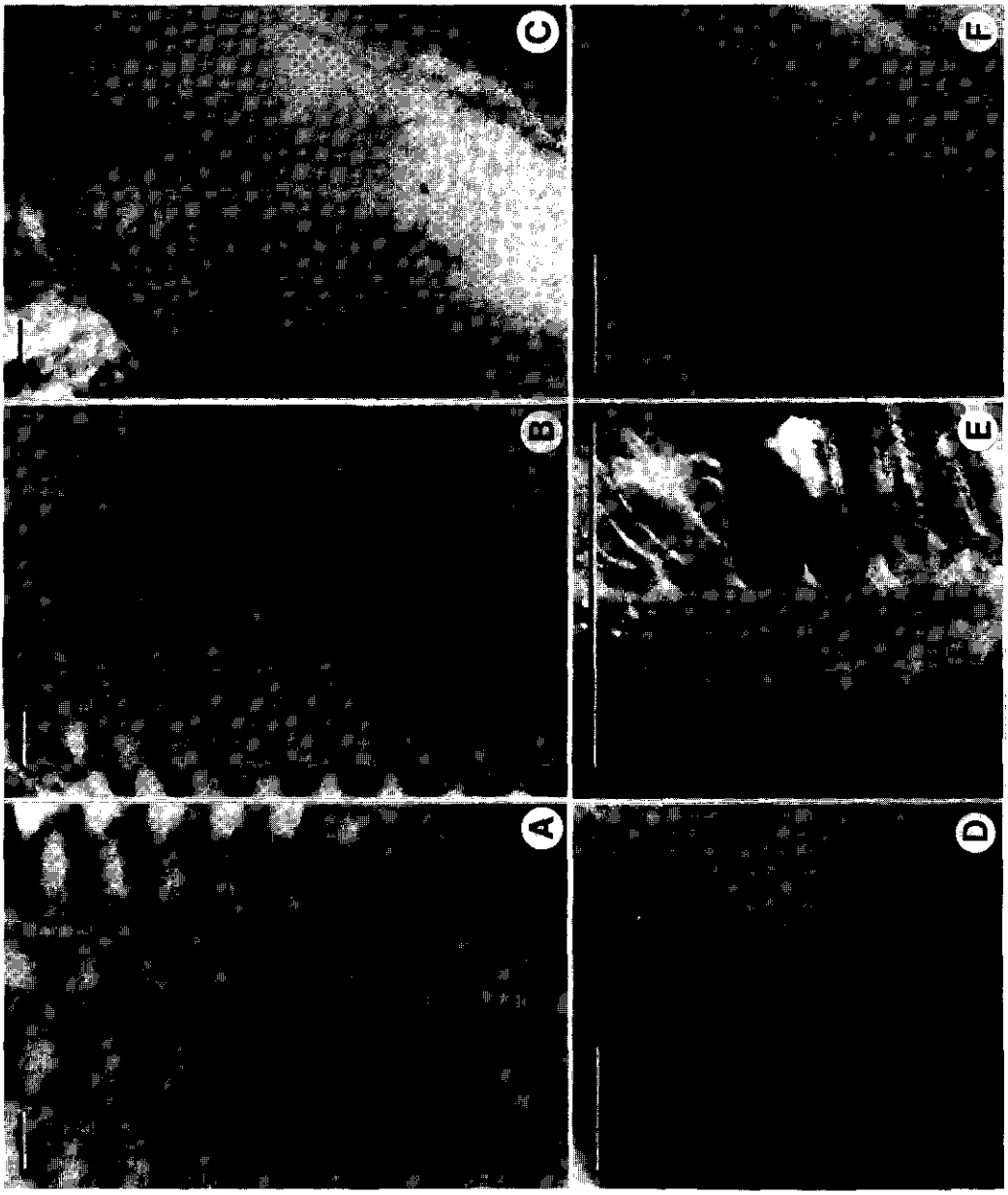
A
B
C
D
E
F

Results

Variations within the branchial sieve

We measured the gill raker parameters of all the rakers of one half of the branchial sieve of one bream (SL 310 mm), one white bream (SL 232 mm) and one roach (SL 141 mm). In figure 4 the hemibranchs are indicated on the x-axis from rostral (first arch, lateral side) to caudal (fifth arch, lateral side). The gill raker parameters are each indicated with a symbol. For each hemibranch the average parameter values of all the rakers on that hemibranch are indicated as well as the extreme parameter values (maximum and minimum). The heavy lines connect the average values of the hemibranchs and the bands indicate the range of values between the extremes.

The lateral side of the first arch has rather strongly deviating gill rakers. Especially in bream, where these rakers are about two times longer than the other rakers and have a flattened blade-like shape. Hoogenboezem et al. (1990) suggest that in bream these gill rakers are modified to be able to seal off the large first gill slit in cooperation with the palatal organ.This seems less likely for white bream and roach because the gill rakers on the lateral side of their first arch do not have such a strongly deviating length as those of bream.

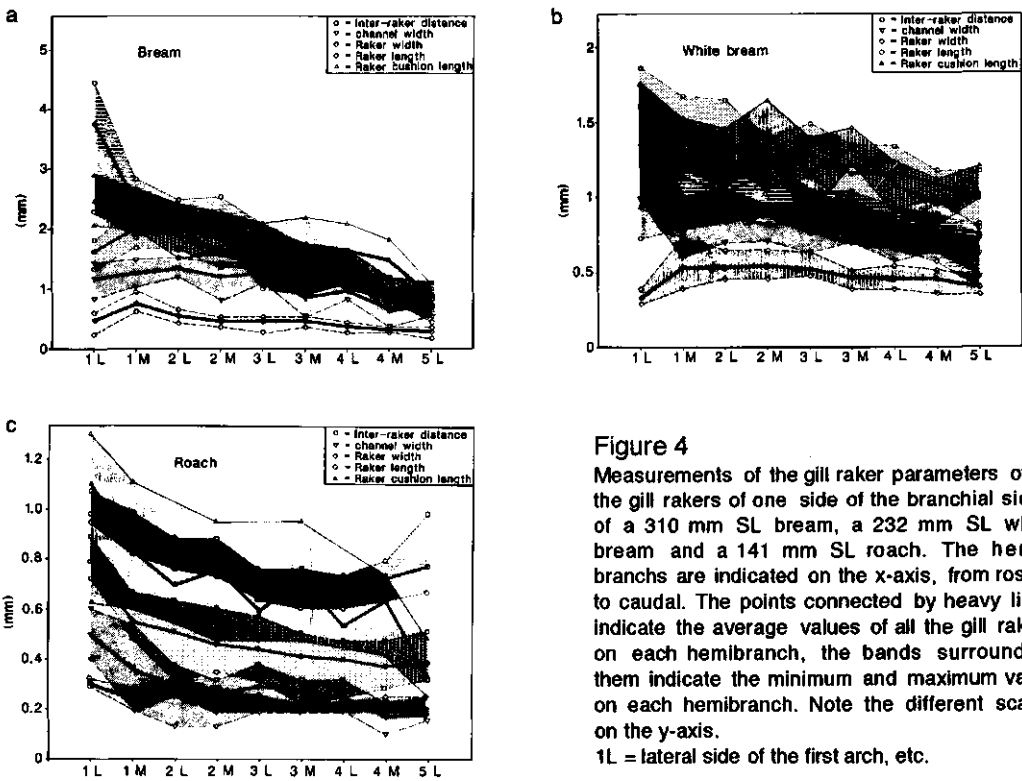

Figure 4

Measurements of the gill raker parameters of all the gill rakers of one side of the branchial sieve of a 310 mm SL bream, a 232 mm SL white bream and a 141 mm SL roach. The hemibranchs are indicated on the x-axis, from rostral to caudal. The points connected by heavy lines indicate the average values of all the gill rakers on each hemibranch, the bands surrounding them indicate the minimum and maximum value on each hemibranch. Note the different scales on the y-axis.

1L = lateral side of the first arch, etc.

Roughly speaking, the parameters tend to become smaller posteriorly. The raker cushion length of white bream and roach clearly shows an asymmetry of the gill arch surface; the medial cushions are longer than the lateral cushions (Fig. 4b,c).

A general conclusion is that these branchial sieves are not entirely homogeneous, both within the arches and between the arches there are differences in gill raker parameters. The standard measurements were done at the middle of the arches. The parameter values are about maximal there, in other words the measurement area represents the maximal branchial sieve values. It can be expected therefore that smaller particles than predicted from the standard measurements will be retained to a certain degree.

Another aspect of the complete filter measurements is the number of gill rakers of the species. We measured this parameter in five white breams and roaches and in seven breams. The number of gill rakers of bream is larger than that of white bream and roach (table 1). The number of gill rakers is constant above a standard length of about 60 mm. There is some literature evidence of intraspecific variation in these species. Zander (1906) found slightly higher gill raker numbers for roach and much higher ones for bream (table 1). Goldschmid et al. (1990) found intraspecific differences in the gill raker number of bream and roach populations from different mountain lakes in Austria and relates high gill raker numbers to abundance of planktonic food in certain lakes. Lindsey (1981) found intraspecific variation in gill raker numbers in *Coregonus* sp. and gives a review of literature on the subject. He found indications that the availability of food niches has an influence on the number of gill rakers of a population after several generations. The relatively low number of gill rakers in bream and roach from the Frysian lakes

Table 1

The number of rakers as measured by Zander (1906) (between brackets) and by us. The data by us are the averages of seven breams, five white breams and five roaches.

species	arch 1	arch 2	arch 3	arch 4
bream	16.1 (22)	15.5 (21)	14.2 (20)	13.3 (14)
white bream	12.8	12.8	12.0	9.0
roach	12.8 (13)	12.8 (14)	11.8 (14)	9.2 (8)

Table 2

The difference of typical parameters between the third and the second gill slit is expressed as the ratio of the parameter in the second slit and that in the third slit. In this way the measurements of the complete filters can be verified partly with data of more specimens per species. 1M = medial side of the first arch, etc.

parameter	roach		white bream	
IR 1M/2M	1.11 ±0.13[a]	p<0.005[b]	1.11 ±0.17	p<0.005
IR 2L/3L	1.12 ±0.12	p<0.005	1.08 ±0.14	p<0.005
CW 1M/2M	1.15 ±0.26	p<0.005	1.17 ±0.25	p<0.005
RL 2L/3L	1.12 ±0.11	p<0.005	1.13 ±0.12	p<0.005
LCB 1/2	1.08 ±0.08	p=0.05	1.05 ±0.05	p=0.025
NR 1/2	0.98 ±0.06	n.s.	0.98 ±0.06	n.s.

a = mean ± standard deviation

b = difference from 1 tested with sign-test; n.s. = not significant (p>0.05)

might be explained by the fact that the eutrophication of these lakes and the resulting dominance of plankton only started in the sixties (Lammens 1986, page 68) and that these populations have not adapted yet to the new food circumstances.

The differences between second and third gill slit can be treated in more detail for white bream and roach because the second and third slit of these species were measured in the developmental series. In table 2 the ratio of parameters from the first and the second arch is given; it is evident that the parameters are some 10% smaller in the third than in the second gill slit in both species. This is a support of the complete filter measurements of one specimen (Fig. 4 b,c) where we already noted the decrease of the parameters from the first to the fifth arch. The branchial sieves are not homogeneous.

Comparative structure and development of the branchial sieve

The parameters of the second slit are used throughout in order to make comparison with bream possible; the raker lengths on the lateral side of the second arch are used and for the other parameters the medial side of the first arch. This was done to be able to apply the channel model (Hoogenboezem 1990). All results are plotted versus the standard length (SL) allowing comparison within and between the species.

Head length (SOL) and weight (W)

The differences between the species in head length are small though significant ($p=0.05$, except white bream/bream).

Since weight and standard length are expected to have a cubic relation log W is plotted versus log SL. The exponent of the increase of weight of the three species is slightly higher than the isometric value 3; the exponent is 3.11, 3.03 and 3.13 for bream, white bream and roach; in bream and roach the difference from 3 is significant ($p=0.01$, $p=0.05$). The differences between the species are very small, despite the apparent clear difference in body shape between white bream & bream and roach (in particular, the height of the back). Roach and bream are not significantly different ($p=0.05$) but each is significantly different from white bream ($p=0.005$). The effect of fixation is probably large here, the fresh weight is higher than the presently found values.

The results below, which are always plotted versus standard length, would not become really different if they were plotted versus head length or weight.

Inter raker distance (IR, Fig. 5)

The inter raker distances increase isometrical in all the species and the regression lines almost go through the origin, which means that the isometry can possibly be extrapolated back to standard length zero. The value for bream at a given length is larger than that for white bream, which in turn is larger than the roach value. The ratio bream, white bream, roach is about 1 : 0.85 : 0.60. The differences between the species are significant ($p<<0.001$).

Channel width (CW, Fig. 6) and raker cushion width (RW)

The sum of CW and RW is the inter raker distance. These parameters show a different pattern of growth than the inter raker distance. The extrapolated regression lines of white bream and roach pass the origin closely, but the one of bream not at all. The explanation for this may be an allometric growth in the early stages of development. Extrapolating a line from the smallest measured SL to the origin gives an idea of early growth. Judging from this approximation in bream the growth of CW accelerates after the early stages whereas the growth of RW decelerates. A consequence of this bend in the curve is that at SL 120 mm the channel widths of bream and white bream are about

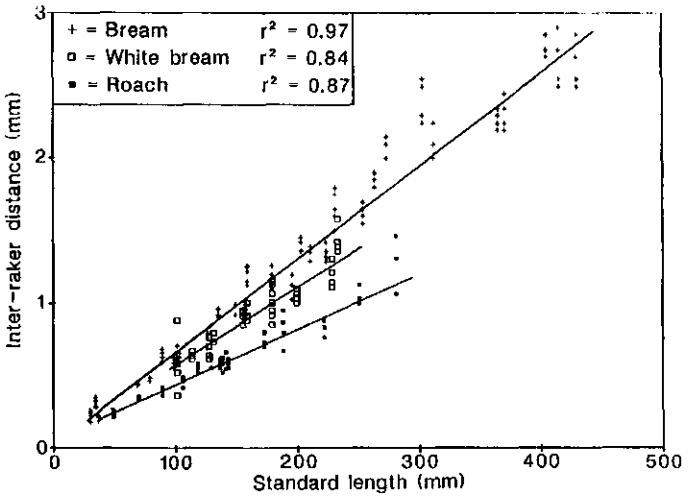

Figure 5
Inter raker distance versus standard length; notice that bream reaches larger lengths than the other two species

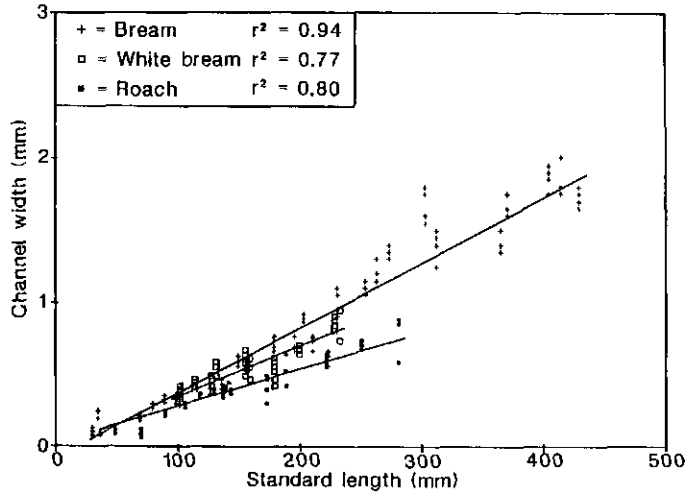

Figure 6
Channel width versus standard length

the same whereas at SL 250 mm the ratio bream, white bream, roach is about 1 : 0.85 : 0.60, which is the same ratio as for the inter raker distance. Apparently the early development differs in the three species under study.

Allometric growth in the early stages of fish development is very common and is well described in literature, e.g. for carp (*Cyprinus carpio*) (Hoda & Tsukahara 1971;

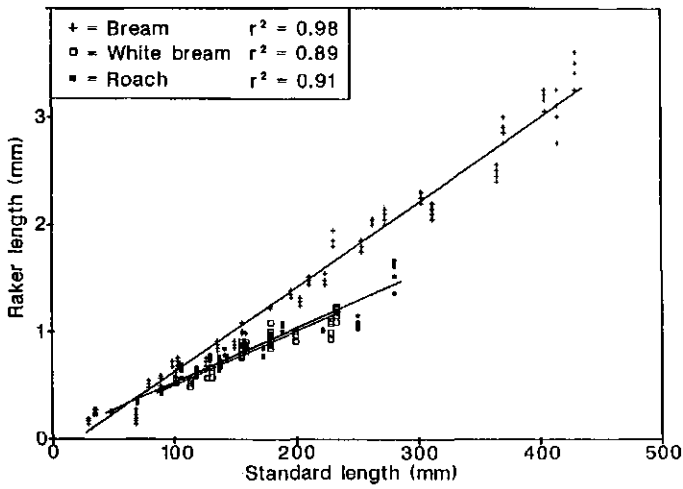

Figure 7
Raker length versus standard length

Osse et al. 1986). Roughly, growth of the carp can be described in two quite discreet phases, an allometric one up to about 20 mm SL and an isometric one above 20 mm. We only have indirect information about the first phase since all measurements were done with fishes above about 50 mm SL.

The differences in channel width between the species are significant (p=0.001 and p=0.02 for white bream/bream).

Raker length (RL, Fig. 7)

The extrapolated linear regression lines do not go through the origin, for neither of the three species. The same approximation as described above is used here. Bream shows an acceleration of growth after the earliest stages. The other two species show a slight deceleration of growth. At 70-80 mm SL the three species have approximately the same raker length, but at 250 mm SL bream differs clearly from the other two species; the ratio bream to white bream and roach is about 1 : 0.70. Roach and white bream do not differ significantly (p=0.05) but both species differ significantly from bream (p<<0.001).

Gill arch area (A_a, Fig. 8)

Zander (1906) states that roach has a simple branchial sieve with a relatively small area and that bream on the other hand has a relatively large area because of curvature and elongation of the ceratobranchials. Our data confirm this. Apart from elongation of the ceratobranchials we found wider arches in bream. In figure 8 the gill arch areas are plotted on a logarithmic scale. The slope of the curves represents the exponent in the growth curve (table 3). The exponent of roach differs significantly from two (isometry; p=0.001). The gill arch area values of roach are lower than those of white bream and bream. Bream and white bream start to diverge at a SL of 100-120 mm. At 150 mm SL the ratio bream, white bream, roach is about 1 : 0.75 : 0.50 and at 250 mm SL 1 : 0.70 : 0.50. The differences between the three sets of values of area divided by SL^2 are all significant (p=0.001).

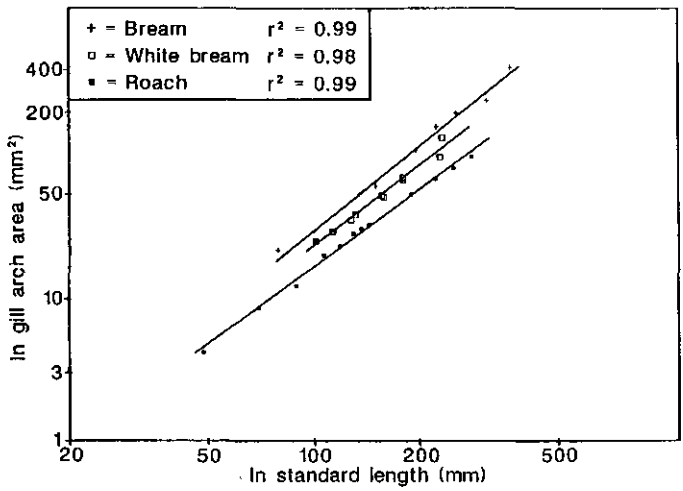

Figure 8
Gill arch area versus standard length plotted on a double logarithmic scale

Table 3
The exponents of standard length in the relation with two filter areas and the energy ratio (Fig. 8, 9, 13). The exponents are derived from the linear regression relations which have the shape:
ln (area) = ln (constant) + exponent · ln(standard length)

	exponent in gill arch area relation	exponent in channel area relation	exponent in energy ratio relation
bream	1.97 ±0.08[a]	2.11 ±0.07	-0.40 ±0.07
white bream	1.86 ±0.09	1.72 ±0.16	-0.71 ±0.19
roach	1.79 ±0.04	2.05 ±0.14	-0.44 ±0.12

a = estimation ± standard error

Channel area (A_c, Fig. 9)

The factor F relating standard measurements of five channel diameters to the total medial channel area is 14.2 for bream, 16.5 for white bream and 12.6 for roach. The differences are a consequence of differences in branchial sieve construction (Fig. 4). The exponent of the growth in white bream is low, 1.72 (table 3); the difference from two is not significant. At 150 mm SL the ratio bream, white bream and roach is about 1 : 0.75 : 0.45 and at 250 mm SL the ratio is 1 : 0.60 : 0.45. The differences between the species are comparable to those of the arch area, but the channel area is smaller than the arch area. The differences between the species are significant (p=0.001).

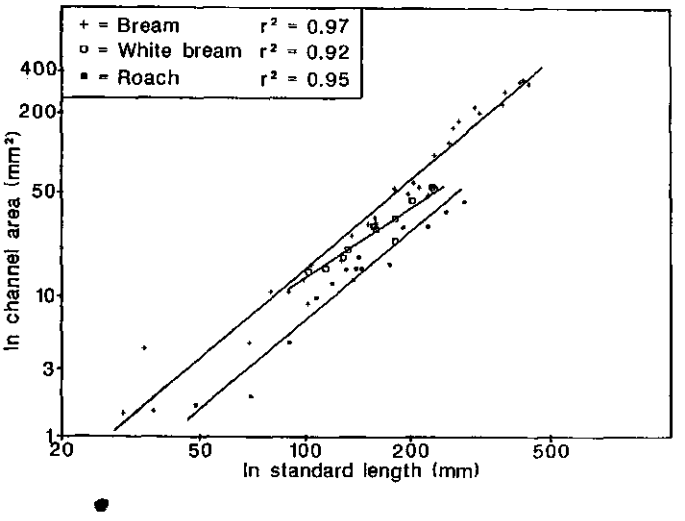

Figure 9 Channel area versus standard length on a double logarithmic scale

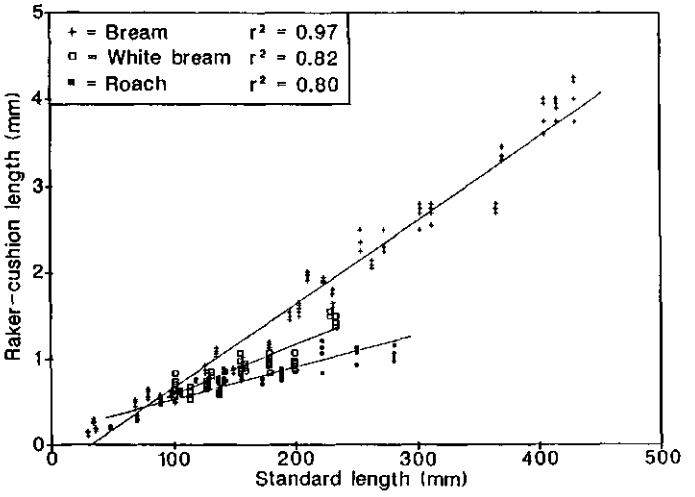

Figure 10 Raker cushion length versus standard length

Raker cushion length (RCL, Fig. 10)

With the same reasoning as above we find an indication of accelerating growth in bream. At 80-90 mm SL the values are equal for the three fishes and at 250 mm SL the ratio is 1 : 0.70 : 0.50 (bream, white bream resp. roach). The accelerating growth rate of bream is in agreement with the observation that the channels are straight at a SL of 55 mm (Fig. 3d); the accelerating growth could be caused by increasing curvature of the channels. The differences between the species are significant (p=0.001).

Table 4
The approximate ratios of gill raker parameters of bream, white bream and roach
A) the ratio of the parameter values at SL 150 mm
B) the ratio of the parameter values at SL 250 mm. The values were determined with the regression data.

	A			B		
	bream	white bream	roach	bream	white bream	roach
inter raker distance (IR)	1	0.85	0.65	1	0.85	0.60
channel width (CW)	1	0.90	0.65	1	0.80	0.65
raker width RW)	1	0.80	0.65	1	0.95	0.65
raker length (RL)	1	0.75	0.75	1	0.70	0.70
gill arch area (A_a)	1	0.75	0.50	1	0.70	0.50
channel area (A_c)	1	0.75	0.45	1	0.60	0.45
raker cushion length (RCL)	1	0.80	0.65	1	0.70	0.50
energy ratio	1	0.65	0.45	1	0.60	0.45

Summary of the results

The pattern of the species differences in gill raker parameter values is the same for all measurements (table 4). In bream the values are about 20% higher than in white bream and about 40% higher than in roach. In the area values the differences are even more pronounced. Furthermore, the branchial arches of bream have more gill rakers than those of white bream and roach. Evidently the branchial sieve of bream is more strongly developed than that of white bream and roach; in other words, bream allocates more room inside its head for the branchial sieve. This is an indication that bream is more adapted to filter feeding than white bream and roach.

We have seen that quite a number of regression lines do not pass the origin closely and we have explained this with differences in early growth of the three species. In fact we do not know a lot about the development of the branchial sieve between SL 0 and 50 mm. In figure 3e the second gill arch of a roach with SL 35 mm is shown. The bony rakers are fully developed but a fleshy cushion is absent. At a SL of 70 mm the raker cushions have emerged and the branchial sieve already looks a lot like the adult form (Fig. 3f and 3c).

Discussion

Filter feeding models: comb model, channel model

The functional anatomy of the branchial sieve has not often been investigated, either only the retention is investigated (Durbin & Durbin 1975, Janssen 1976) or only the anatomy (Beveridge et al. 1988). MacNeill and Brandt (1990) however used a similar approach as in this paper, combining morphology, ontogeny and prey capture efficiency. A model that is often used (sometimes implicitly) as a functional description of mechanical sieving is the comb model or inter raker distance model. In this simple view of filter feeding the inter raker distance or the channel width is a direct measure for the mesh size and retention ability of a filter.

The comb model seems appropriate for clupeid and coregonid filter feeders (e.g. Drenner et al. 1984). In clupeids and coregonids the branchial sieves consist of very

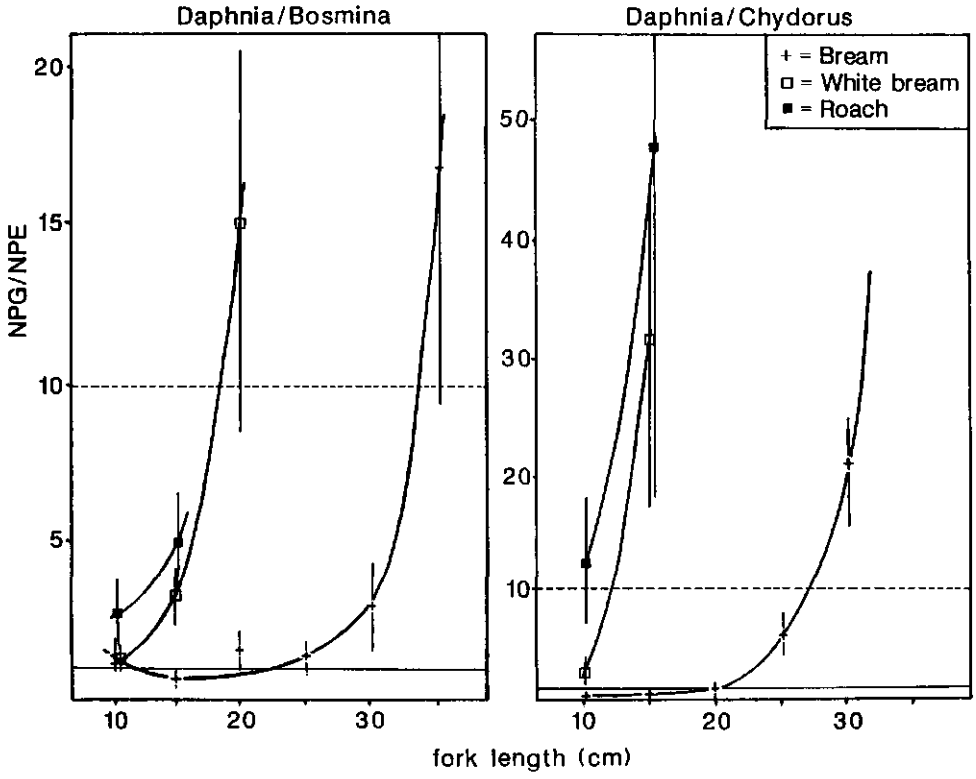

Figure 11

Retention curve based on gut contents of freshly caught fish; the average lengths in Tjeukemeer of the three mentioned cladocerans are: *Daphnia hyalina* 1.11 mm, *Bosmina coregoni* 0.43 mm and *Chydorus sphaericus* 0.28 mm (Lammens et al. 1987). Vertically is plotted the ratio of the numbers of two plankton species in the gut (NPG) divided by the same ratio in the environment (NPE); a value of one means that both species are caught to the same extent, a higher or lower value means that one of the two prey species is preferred or selected; horizontally is plotted the fork length; the horizontal line at 10 is the (arbitrary) limit above which we defined the retention of the smaller species to have stopped being significant. The underlying assumption is that the larger species (*Daphnia hyalina*) is still retained completely (100%) at that point whereas merely 10% of the smaller species is retained.

This figure is redrawn and adapted from figure 1 in Lammens et al. (1987).

long and thin gill rakers mainly on the first arch, very much like a comb (Gibson 1988). However, experimental data do not always fit in with the comb model. Wright et al. (1983) and Gibson (1988) do not find an agreement between the comb model and retention experiments. Drenner et al. (1987) finds that filter feeding of the cichlid *Tilapia galilea* is not hampered by removal of gill rakers and microbranchiospines. The branchial sieves of the cyprinids studied in this paper lack the long specialized branchiospines typical of clupeid and coregonid filter feeders and their systems of branchiospines, cushions and channels are complex; the influence of inter arch distance on the mesh size could be large.

Table 5

The critical standard lengths in this table are based on the data of Lammens et al. (1987) in figure 11 and the average prey lengths on data from the same paper; the average prey length was determined with plankton samples from Tjeukemeer. The critical channel width was calculated from the critical standard length using the regression parameters.

fish species	zooplankton species	average prey length (mm)	critical channel width (mm)	critical standard length (mm)
bream				
	Chydorus sphaericus	0.28 ±0.028[a]	1.05	250
	Bosmina coregoni	0.43 ±0.07	1.31	306
white bream				
	Chydorus sphaericus	0.28 ±0.028	0.40	109
	Bosmina coregoni	0.43±0.07	0.57	164
roach				
	Chydorus sphaericus	0.28±0.028	0.23	85
	Bosmina coregoni	0.43±0.07	0.43	160

a = mean ± standard deviation

The ratio of inter raker distances in bream, white bream and roach is 1:0.85:0.60. This suggests that, applying the comb model, bream has the largest mesh size (lowest retention ability), roach the smallest and white bream is intermediate. This is squarely in conflict with ecological data (Fig. 11). Lammens et al. (1987) counted zooplankton in gut contents of bream, white bream and roach, which were all caught in lake Tjeukemeer. With these data he calculated the numerical proportion (NPG) of pairs of food species in the guts. These proportions he compared to the numerical proportions of the same pairs of food species in the environment (NPE). The ratio of NPG and NPE is a measure for selection of either of the two food species; a value of 1 means that there is no preference for either of the two food species. The food species pairs in figure 11 consist of a large cladoceran (*Daphnia hyalina*) and a small cladoceran (*Chydorus sphaericus* and *Bosmina coregoni*). An increase of the ratio in figure 11 means that the smaller species starts to slip through the branchial sieve. In figure 11 an arbitrary limit of 10 is drawn; at this line, where we assume that 10% of the smaller species is retained and 100% of the larger species, we call the retention of the smaller species critical; the standard length at which this occurs we call the critical standard length.

The guts of bream contained a critical proportion of *Bosmina* at a fork length of 330 mm (SL 306), whereas for white bream the critical FL is 180 mm (SL 164) and for roach 170 mm (SL 160) (Fig. 11); so white bream and roach have a comparable retention ability but bream has a much higher one. The order of retention ability is the reverse of the order mentioned above in connection with the comb model. The differences between these species in success in eutrophic water (Lammens 1986) are in agreement with the retention data of Lammens; bream is very successful in eutrophic lakes, roach and white bream usually are not. However, Lammens data should be used with care because it is not known whether the ingested cladocerans were taken in with gulping or with particulate feeding, the latter involving visual selection (Lammens et al. 1987). Therefore the proportions in the gut do not necessarily reflect the environmental proportions precisely and the retention abilities of the branchial sieves could be higher.

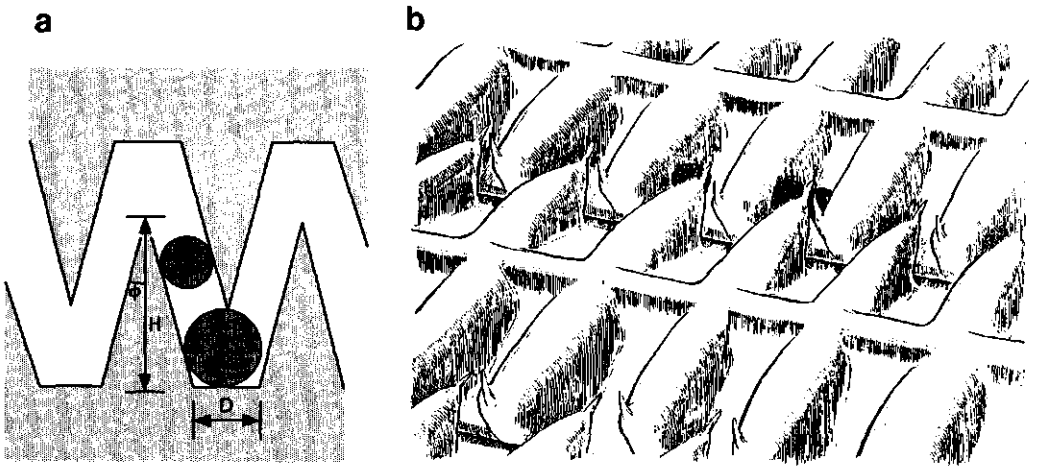

Figure 12

Two filter feeding models predicting the mesh width of the branchial sieve.

a) The saw tooth model or interdigitating model. Notice the importance of gill raker shape and spacing (top angle (φ) and length (H) of the triangular gill raker, distance (D) between the gill rakers) and of the distance between the arches.

b) Schematic drawing to illustrate the channel model. The lateral gill rakers are depressed here, in this position they reduce the mesh size of the medial gill raker channels by at least 50%.

If one compares the critical channel width (defined as the channel width at the critical SL) with the actual prey length (table 5) we find that bream retains prey about three times smaller than its critical channel width, which clearly is not compatible with the comb model. Roach has a critical channel width in the order of magnitude of the prey size, data compatible with the comb model. White bream however has a critical channel width 30-40% wider than the prey size. Because of the above we have doubts about the validity of the comb model in its simplest form for white bream and roach as much as for bream.

The fact mentioned above that the prey size is in the order of magnitude of the mesh size (as predicted by either of the two present models) is a further indication that the branchial sieves of these species are simple sieves (not sticky) as defined by Rubinstein and Koehl (1977), since the critical prey size of sticky sieves will usually be one order of magnitude lower than the physical mesh size (here: channel width or reduced channel width). A second indication for simple sieving is provided by the shape of figure 11, all the curves become very steep beyond the critical point; in other words, small food particles disappear completely from the diet soon after the critical standard length has been reached, which is typical for a simple sieve action, but not for sticky filters.

The channel model (Hoogenboezem et al. 1990) includes a mechanism to reduce the channel width by means of the raker from the opposite side of the gill slit (Fig. 12b). This mechanism is in good agreement with the finding in bream that the critical channel width is about 3x the prey length (table 5); the factor 3 instead of 2 could account for the thickness of the lateral raker. The results of white bream and roach are not in agreement with the channel model (with neither channel width nor reduced channel

width). The present data provide some evidence that this way of filter feeding is unlikely for white bream and roach. Firstly, the raker length of these species is smaller than that of bream (ratio 1 : 0.70, Fig. 7). This means that during filter feeding the gill slits of these species should be 30% narrower than those of bream in order to use the mechanism described above, which would cause a large decrease of filter capacity. Secondly there are differences in the shape of the rakers. In bream the rakers have a clear needle-like point, whereas in white bream and roach the rakers are blunt; in bream the top 1/3 of the bony raker is only covered by a thin layer of tissue, in white bream and roach this is not the case. A needle-like point is a good adaptation to reduce the mesh size of channels without plugging them off completely.

The proper functioning of the channel model depends on the relative position of two arches; the lateral rakers on one side of the slit much reach exactly in the channels on the medial side. This interdigitation can be disturbed by (small) movements of the arches. This factor provides a possible explanation for the relatively large inter raker distance in bream.

A model that might be useful for white bream and roach is mentioned by Sibbing in Nelson & Winfield (in press); the interdigitating or sawtooth model (Fig. 12a). In this planar model the gill rakers are represented as triangles; several parameters describing the shape of the gill slit determine the prey sizes that can be retained. Data about variations in inter arch distance during filter feeding are needed to define the type of filter feeding and the mesh size of white bream and roach. X-ray films are being made in our lab to measure these parameters.

Capacity, filtering area and energy ratio

The capacity of a filter (volume per unit time) is an important property determining (together with the retention ability) the amount of prey that can be retained per unit time. The capacity of a filter is determined by the velocity of the water in the filter and the area through which water flows in the filter (the filtering area).

We want to estimate the ratio of energy intake per unit time through filter feeding and total energy consumption per unit time, in other words, we want to express the filter feeding energy intake as a fraction of total energy consumption. With energy is meant energy per fixed unit of time. When the ratio is high enough the fish can survive on a diet of zooplankton (as far as energy is concerned).

If the concentration and composition of zooplankton in the environment and the retention ability of the filter are constant, then the capacity of the filter is a direct measure of zooplankton and energy intake. If the water velocity in the filter is constant then the capacity is proportional to the filter area. There is some indirect evidence for this. Drenner et al. (1982) found that the filtering rate (= capacity) in gizzard shad (*Dorosoma cepedianum*) is proportional to $SL^{2.08}$ and Smith (1989) found that the filtering rate in silver carp (*Hypophthalmichthys molitrix*) is proportional to $W^{0.713}$. Both values suggest a scaling of capacity with an area. All these points lead to the assumption that energy intake is proportional to the filtering area.

The energy consumption is proportional to the metabolic rate, which is very difficult to measure in fishes, the value of the exponent varies between 0.75 and 0.90 depending on author and taxonomic group (Schmidt-Nielsen 1984). Winberg (1960) found the following relation for cyprinids at 20°C:

$$\text{metabolic rate} = 0.47\ W^{0.80},$$

so in cyprinids the energy consumption is proportional to $W^{0.80}$.

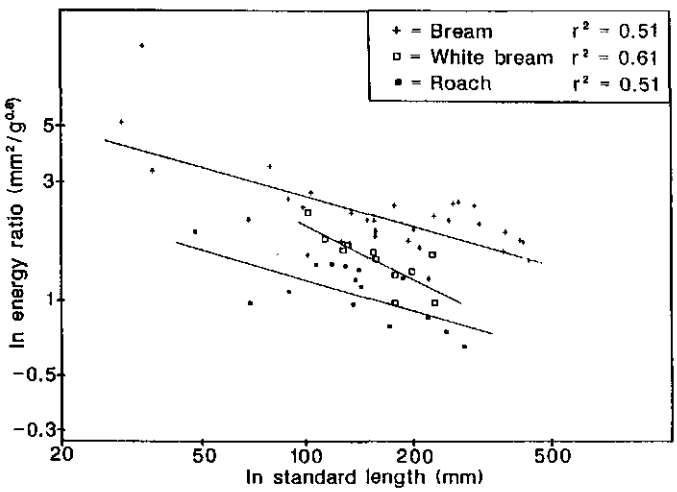

Figure 13

Energy ratio versus standard length on a double logarithmic scale. The energy ratio equals the channel area divided by body weight to the power 0.80; for bream the body weights were not measured but calculated with a separately determined metrical relation.

Combining the above findings we find that the energy ratio is proportional to the filtering area divided by $W^{0.80}$. If the filtering area and the weight increase isometrical then the energy ratio is proportional to $SL^{-0.40}$:

$$\frac{A}{W^{0.80}} = \frac{L^2}{(L^3)^{0.80}} = L^{-0.40}$$

The ratio decreases with increasing length,so filter feeding will become increasingly less suited as sole feeding mode. It should be stressed here that the calculated values of the energy ratio only have a comparative meaning.

In figure 13 the energy ratio (calculated with the channel area) can indeed be seen to decrease with increasing SL. The exponent of this decrease (table 3) is -0.40 for bream and -0.44 for roach, close to the expected value -0.40. For white bream however the exponent is -0.71; this deviation (non-significant, notice the low r^2 values) is caused by the non isometric growth of the channel area in white bream (Fig. 9). At 200 mm SL the ratio bream, white bream, roach is 1 : 0.60 : 0.45. This means that white bream can take in 40% less energy per unit time than bream and roach even 55% less. The differences between the species are significant (p=0.001).

One of the future research subjects is to measure the capacity directly in filter feeding fish in order to test the above ideas.

It seems that the success of bream in eutrophic environments can be explained by a superior ability to exploit zooplankton, i.e. by the efficiency of its branchial sieve. Firstly, there is a strong indication that its capacity is larger than that of white bream and roach and secondly according to Lammens et al. (1987) the retention ability of its branchial sieve is much higher than that of white bream and roach.

List of symbols

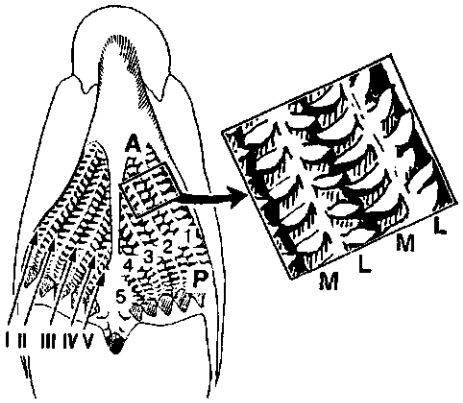

Figure 14
Orientation terms; horizontal section of bream head showing the floor of the mouth cavity and the branchial sieve.
I-V = gill slit 1 to 5
1-5 = gill arch 1 to 5
A = anterior side of gill arch
P = posterior side of gill arch
inset:
L = lateral side of gill arch
M = medial side of gill arch

A_a	= gill arch area
A_c	= sum of the channel diameters on the medial sides of the four arches
AL	= anal length
BAW	= basal arch width
CW	= channel width
ED	= eye diameter
F	= factor relating standard channel diameter measurements to total medial channel area
FL	= fork length
IR	= inter raker distance
LCB	= length of ceratobranchial
NPE	= numerical proportion of a pair of food species in the environment
NPG	= numerical proportion of a pair of food species in the guts
NR	= number of gill rakers
RCL	= raker cushion length
RL	= bony raker length
RW	= raker width
SL	= standard length
SOL	= snout operculum length, head length
TAW	= arch width from raker tip to raker tip
W	= body weight

Acknowledgments

I want to thank Yvette van Vugt and Peter Klinkhamer for doing most of the measurements. Most figures were made by Jos van den Boogaart and Wim Valen. This research is funded by the Dutch organization for Scientific Research (NWO), department BION, project no. 811-428-265.

References cited

Beveridge, M.C.M., M.R.P.Briggs, M.E. Northcott & L.G. Ross. 1988. The occurrence, structure, and development of microbranchiospines among the tilapias (Cichlidae: Tilapiini). Can. J. Zool. 66(11): 2564-2572.

Drenner, R.W., W.J. O'Brien & J.R. Mummert. 1982. Filter feeding rates of gizzard shad. Trans. Amer. Fish. Soc. 111: 210-215.

Drenner, R.W., J.R. Mummert, F.Jr. de Noyelles & D. Kettles. 1984. Selective particle ingestion by a filter-feeding fish and its impact on phytoplankton community structure. Limnol. Oceanogr. 29: 941-948.

Drenner, R.W., G.L. Vinyard, K.D. Hambright & M. Gophen. 1987. Particle ingestion by *Tilapia galilaea* is not affected by removal of gill rakers and microbranchiospines. Trans. Amer. Fish. Soc. 116: 272-276.

Durbin, A.G. & E.G. Durbin.1975. Grazing rates of Atlantic menhaden. Mar. Biol. 33: 265-277.

Gibson, R.N. 1988. Development, morphometry and particle retention capability of the gill rakers in the herring, *Clupea harengus* L.. J. Fish Biol. 32: 949-962.

Goldschmid, A., M. Palzenberger & H. Pohla. 1990. Gill rakers in cyprinids: diversity of morphology and possible function. Environ. biol. fish., this volume.

Hoda, S.M.S. & H. Tsukahara. 1971. Studies on the development and relative growth in the carp (*Cyprinus carpio* (Linne)). J. Fac. Agriculture, Kyushu University16(4): 387-509.

Hoogenboezem, W., F.A. Sibbing, J.W.M. Osse, J.G.M. van den Boogaart, E.H.R.R. Lammens & A. Terlouw. 1989. X-ray measurements of gill-arch movements in filter-feeding bream, *Abramis brama* (Cyprinidae). J.Fish Biol. 36: 47-58.

Hoogenboezem, W. et al.1991 in press. A new model of particle retention and branchial sieve adjustment in filter-feeding bream (*Abramis brama* (L.), Cyprinidae). Can. J. Fisheries Aquat. Sci. 48:

Janssen, J. 1976. Selectivity of an artificial filter feeder and suction feeders on calanoid copepods. Amer. Midland Natur.:491-493.

Lammens, E.H.R.R. 1986. Interactions between fishes and the structure of fish communities in Dutch shallow, eutrophic lakes. Ph.D. thesis Agricultural University Wageningen.

Lammens, E.H.R.R., J. Geursen & P.J. McGillavry. 1987. Diet shifts, feeding efficiency and coexistence of bream (*Abramis brama*), roach (*Rutilus rutilus*) and white bream (*Blicca björkna*) in eutrophicated lakes. Proc. V Congr. Europ. Ichtyol., Stockholm: 153-162.

Lammens, E.H.R.R. 1989. Causes and consequences of the success of bream in Dutch eutrophic lakes. Hydrobiol. Bull. 23: 11-18.

Lindsey, C.C. 1981. Stocks are chameleons: plasticity in gill rakers of coregonid fishes. Can. J. Fisheries Aquat. Sci. 38: 1497-1506.

MacNeill, D.B. & S.B. Brandt. 1990. Ontogenetic shifts in gill-raker morphology and predicted prey capture efficiency of the alewife, *Alosa pseudoharengus*. Copeia 1: 164-171.

Nie, H.W. de, H.J. Bromley & J. Vijverberg 1980. Distribution patterns of zooplankton in Tjeukemeer, the Netherlands. J. Plankton Res. 2: 317-334.

Nie, H.W. de 1987. The decrease in aquatic vegetation in Europe and its consequences for fish populations. EIFAC/CECPI Occasional paper 19: 52 p.

Osse, J.W.M., M.R. Drost, J. Vial & R. Aldunate. 1986. Growth and feeding in larval carp, *Cyprinus carpio* (L). Ann. Mus. Roy. Afr. Centr., Sc. Zool.251: 67-70.

Romeis, B. 1968. Mikroskopische Technik. Oldenbourg, München-Wien.

Rubenstein, D.I. & M.A.R. Koehl.1977. The mechanisms of filter feeding: some theoretical considerations. Amer. Natur. 111, pp. 981-994.

Schmidt-Nielsen, K. 1984. Scaling; why is animal size so important?. Cambridge university press.

Sibbing, F.A. 1982. Pharyngeal mastication and food transport in the carp (*Cyprinus carpio* L.): a cineradiographic and electromyographic study. J. Morph. 172: 223-258.

Sibbing, F.A. & R. Uribe. 1985. Regional specializations in the oropharyngeal wall and food processing in the carp (*Cyprinus carpio* L.). Neth. J. Zool. 35(3): 377-422.

Sibbing, F.A., J.W.M. Osse & A. Terlouw. 1986. Food handling in the carp (*Cyprinus carpio*): its movement patterns, mechanisms and limitations. J. Zool. Lond. (A)210: 161-203.
Sibbing, F.A. 1988. Specializations and limitations in the utilization of food resources by the carp, *Cyprinus carpio*: a study of oral food processing. Environ. Biol. Fish. 22(3): 161-178.
Sibbing, F.A. in press. Food capture and oral processing. In: The Biology of Cyprinids. Eds.: J. Nelson & I.J. Winfield. Chapman & Hall.
Smith, D.W. 1989. The feeding selectivity of silver carp, *Hypophthalmichthys molitrix* Val.. J. Fish Biol. 34: 819-828.
Sokal, R.R. & F.J. Rohlf. 1969. Biometry: The principles and practice of statistics in biological research. W.H. Freeman and company.
Vijverberg, J. & A.F. Richter. 1982a. Population dynamics and production of *Daphnia hyalina* (Leydig) and *Daphnia cucullata* (Sars) in Tjeukemeer. Hydrobiologia 95: 235-259.
Vijverberg, J. & A.F. Richter. 1982b. Population dynamics and production of *Acanthocyclops robustus* (Sars) and *Mesocyclops leuckarti* (Claus) in Tjeukemeer. Hydrobiologia 95: 261-274.
Winberg, C.G. 1960. Rate of metabolism and food requirement of fishes. Fisheries Research Board Translation Services 194.
Wright, D.I., W.J. O'Brien & C. Luecke. 1983. A new estimate of zooplankton retention by gill rakers and its ecological significance. Trans. Amer. Fish. Soc. 112: 638-648.
Zander, E. 1906. Das Kiemenfilter der Teleoster. Zeitschrift für Wissenschaftliche Zoologie 84(4): 619-713.

Chapter 2

Shape of zooplankton and retention in filter-feeding. A quantitative comparison between industrial sieves and the branchial sieves of common bream (*Abramis brama*) and white bream (*Blicca bjoerkna*).

Coen van den Berg, Jos G.M. van den Boogaart, Ferdinand A. Sibbing, Eddy H.R.R. Lammens* and Jan W.M. Osse.
in press Can. J. Fish. Aquat. Sci. 50: ...-... (1993)

Abstract

Industrial sieves retained all cycloid copepods with a width larger than their mesh size, but Daphnia with a width up to 1.4 times the mesh size still passed through them. *Daphnia* have a lower depth/width ratio than copepods (0.599 and 0.882, respectively). Therefore, *Daphnia* could pass the square meshes diagonally. In filter-feeding experiments with common bream, the smallest retained copepods correspondingly were about 35% less wide than the smallest retained *Daphnia*. White bream did not retain smaller copepods than *Daphnia*. In the reducible-channel model of filter-feeding, particles are retained in the channels between the medial gill rakers. The mesh size can be reduced by lowering the lateral rakers into these channels. We calculated that in reduced channels zooplankton depth is the critical size parameter and in unreduced channels zooplankton width. We found that white bream was feeding with unreduced channels, common bream with reduced channels. The depth/width ratio (35% lower in *Daphnia* than in copepods) therefore explains the difference in retention of copepods and *Daphnia* by common bream, whereas for white bream no such difference was expected. The shape of zooplankton thus affects the trophic segregation and the exploitation of food resources by fish.

Introduction

The effective mesh size or retention ability (ability to retain small particles) of the branchial sieve is an important parameter for fish that forage on small particles. This parameter can be determined from the size selectivity of filter-feeding fish in laboratory experiments. One problem in generalizing the results of such experiments, however, is the influence of the shape of zooplankton on retention by the branchial sieve. In previous studies of filter-feeding by coregonids and clupeids, the average of length, width and depth of the zooplankton was used as critical zooplankton size parameter (Wright et al. 1983; Drenner et al. 1984; Mummert and Drenner 1986; Gibson 1988; MacNeill and Brandt 1990), assuming a random orientation of the zooplankton when they meet the comb-like branchial sieve in these fishes. Wright and O'Brien (1984) assumed that the average of width and depth is critical. Wright et al. (1983) suggest that the appendages of the zooplankton may play a role in retention. Mummert and Drenner (1986) found that *Pediastrum* (a circular, flat colony of green algae) was removed by

Dorosoma cepedianum at the same rate as microspheres with a diameter four times smaller. This implies that the depth, not the width of *Pediastrum* is the important factor for retention by *Dorosoma cepedianum*.

To better understand the retention ability of the branchial sieve, the shape of zooplankton clearly deserves more attention. We designed a separation system with industrial sieves (Fig. 1) in order to sieve living zooplankton and to study the relationship between zooplankton shape and mesh size. The results of these sieving experiments were then compared with the results of laboratory experiments with filter-feeding common bream (*Abramis brama*) and white bream (*Blicca bjoerkna*).

Materials and methods

Zooplankton were collected from April to July 1990 in the Dutch lake Tjeukemeer, using hoop nets (mesh size 250 μm) with a collecting bottle at the end. The velocity of the boat was approximately 1 m s^{-1} and each haul lasted approximately half a minute. The zooplankton community is composed of cycloid copepods and cladocerans.

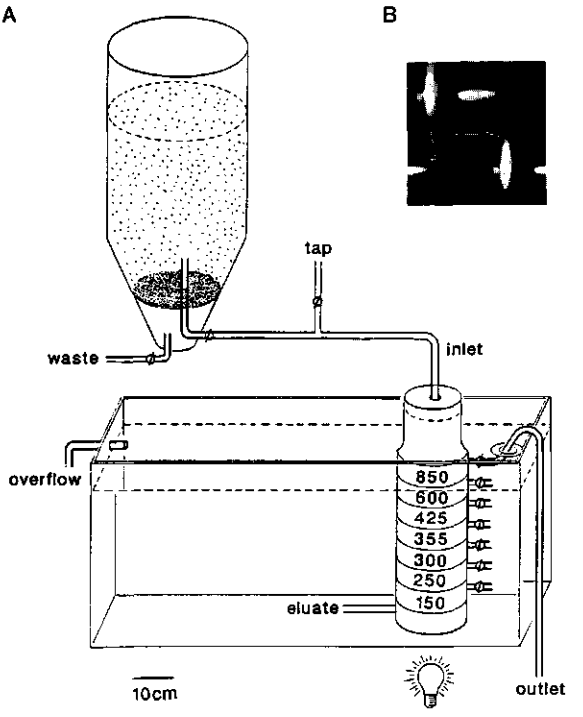

Figure 1

a) The experimental set-up for filtering live zooplankton through industrial sieves. The suspension of zooplankton flows from a storage tank through a stack of industrial sieves with diminishing mesh size (in microns).

b) Detail of an industrial sieve. Mesh size is measured as indicated.

Dominant cladocerans were *Daphnia hyalina, Daphnia cucullata, Bosmina coregoni, Bosmina longirostris, Chydorus sphaericus* and *Leptodora kindtii* (cf. de Nie et al. 1980). In our experiments, we distinguished two groups of zooplankton: the cycloid copepods and the *Daphnia* species. The other species were not considered.

Separation into size classes and measurement of zooplankton

The zooplankton were poured into buckets and the debris (algae, sand and dead zooplankton) was allowed to settle. Floating zooplankters, with an air bubble under their carapace, were removed by skimming them off the surface. The remaining suspension was poured gently in a funnel shaped storage tank (Fig. 1a) and allowed to settle again for about 30 minutes. The zooplankton suspension then flowed from that tank to the uppermost of a stack of sieves through a tube with a tap. The inlet of this tube was above the floor of the storage tank to avoid sucking in debris. To avoid air contact, the stack of sieves was permanently immersed in a large tank of water (Fig. 1a). We used seven stainless steel laboratory test sieves (Endecotts Ltd., London, diameter 200 mm, height 50 mm) arranged with diminishing mesh size (850, 600, 425, 355, 300, 250 and 150 μm respectively) from top to bottom. The sieves are made of interwoven wires in a square pattern (Fig. 1b). Each sieve was provided with an outlet tap. The stack was topped with a 15-cm-high rim to prevent overflowing due to the pressure difference over the sieves. Water and non-retained particles flowed from the bottom of the stack into the large tank. During the filtration trials all the outlet taps of the sieves were closed. Once the zooplankton storage tank was empty, the flow consisted of tap water. The downward flow velocity in the stack averaged approximately 0.5 mm s^{-1} ($\approx$ 15 mL s^{-1}). A higher flow velocity would have resulted in overflowing because of the resistance offered by the sieves, especially when they become clogged. Living zooplankton probably can swim against such a flow, therefore we tried to attract the zooplankton towards the bottom of the stack with a lamp under the large tank (Fig. 1a). The top of the stack was darkened with black plastic. Each filtration trial continued for at least twelve hours, usually at night. The continuous flow of water guaranteed fresh, oxygenated water for the very dense zooplankton population ($1\text{-}2 \cdot 10^4$ per litre) between the sieves; the volume of water in the stack of sieves was replaced every 10 minutes. Following filtration, zooplankton from a particular sieve were collected by opening the outlet tap and siphoning the water with live zooplankton into a bucket, while increasing the flow velocity of the tap water in order to prevent reverse flow in the stack of sieves.

Zooplankton samples were preserved in 4% formalin. The samples were analyzed by counting the zooplankton per species and measuring individual lengths and widths to the nearest 0.03 mm using an ocular micrometer. Measurements are illustrated in figure 2b. If samples contained more than a few hundred specimens a subsample was taken using a whirling apparatus (Kott 1953). Zooplankton lengths were measured following Vijverberg and Richter (1982a, b), Wright et al. (1983) and Wright and O'Brien (1984). For copepods, the length of the cephalothorax was measured. For *Daphnia*, the tail and helmet, when present, were subtracted from the length. On a microscope slide zooplankton always lie on their flattest side. In this orientation zooplankton width equals the minimal distance between two parallel tangents on either side of the body (Fig. 2b). The depth-width ratio was measured with the same zooplankton, floating in a little tray with formol, using an ocular micrometer.

Because of the sequential arrangement of the sieves, the size-frequency distribution of zooplankton passing through a particular sieve is dependent on the sieves above it (with larger mesh size). These sieves set an upper boundary for the size range of zooplankton in each sieve sample. In this set-up the upper boundary is therefore very useful

for interpretation of the results, but the lower boundary is not. The lower boundaries in the sieve samples are influenced by clogging of the sieve, back-swimming of the zooplankton and possibly by zooplankton orientation. These effects can not be distinguished. Therefore, the lower boundaries are not very useful for interpretation of the results.

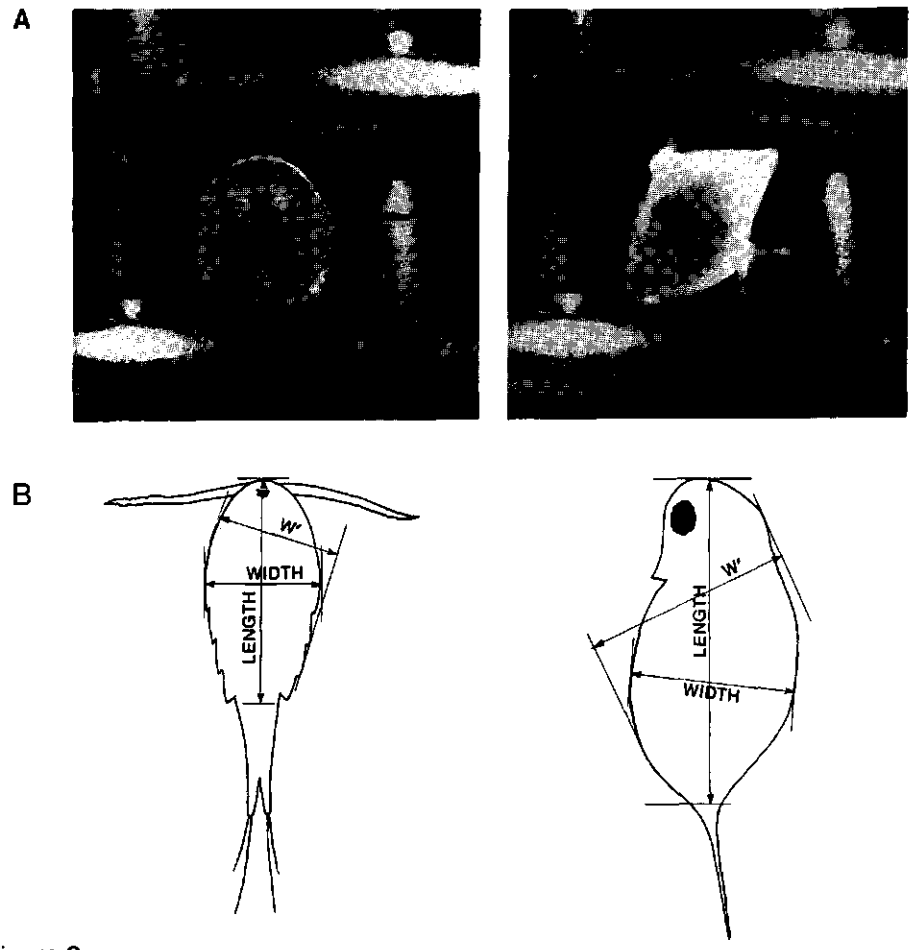

Figure 2

a) Composition photos of an industrial sieve and a copepod and a *Daphnia*.The living zooplankton was embedded in 2% ultra low gelling agarose, which permitted easy handling and a view of all sides of the plankton.This head-on view shows that the depth of *Daphnia* equals about 60% of its width (the d/w ratio is approximately 0.6). The copepod however is almost circular in this view (the d/w ratio is approximately 0.9). Because of this difference in d/w ratio *Daphnia* can pass square meshes diagonally, whereas copepods cannot.

b) The measurement sites of width and length of a copepod and a *Daphnia*. Two sets of parallel tangents on either side of the body of the zooplankton are shown. w' indicates a wrong way to measure width. The set with the shortest distance between the tangents is defined as the plankton width. By definition, width corresponds to the smallest mesh size that the zooplankton can pass through. Note that in *Daphnia* width usually is not perpendicular to length.

Filter-feeding experiments

The common bream, with standard length (SL) 17.6 cm, and the white bream (SL 17.2 cm) were each kept in a tank with a known volume of water (V). A suitable mixture of zooplankton size classes from the industrial sieve system was added to the water, which marked the start of the experiment (t=0 hr.). At eight locations in each tank plankton samples were taken of about 0.15 L each, using a sampling tube (Hoogenboezem et al. subm.). The fish were then allowed to feed for 6 hours. When feeding on zooplankton, common bream and white bream can either use particulate intake or gulping. Because the experiments were performed in the dark the fish were forced to gulp and the prey were not selected visually. The eight samples were lumped and preserved in 4% formalin. Sample volume was measured to the nearest 5 mL. At the end of the experiment (t=6 hr.) another eight samples were taken. The zooplankters were measured and grouped in length classes of 0.06 mm. Their width was calculated from their length using the empirical relationship in Table 1. Zooplankton size classes with less than 5 specimens at t=0 hr. were not included in the analysis.

Zooplankton retention by the branchial sieve

Calculation of zooplankton retention from feeding experiments

The difference between the samples at t=0 hr. and at t=6 hr. in density of a size class of zooplankton represents the fraction of zooplankton from that size class that has been eaten. The experiments were carried out in darkness in order to avoid visual selection and particulate intake of prey and hence to induce continuous, random gulping of the fish. The plankton distribution was kept random with an air bubbler and by movements of the fish. Under these conditions the plankton density will decrease exponentially. Whether this exponential decrease in density is slow or fast for a certain size class of zooplankton depends on the filtering rate of the fish (in litres per hour) and on the retention percentage for the particular size class of zooplankton. This rate of decrease in density of a particular size class is called clearance rate (after Smith 1989). The exponential decrease in density of a particular size class equals (cf. Drenner et al. 1984; Hoogenboezem et al. subm.):

$$D_t = D_0 \, e^{-(CR \cdot t) / V} \qquad (1)$$

where
D_t = density of a particular zooplankton size class at time t
D_0 = initial density of the same zooplankton size class (t=0)
CR = clearance rate (litres per hour)
t = duration of the experiment (hours)
V = tank volume (litres)

If retention is 100 percent, the clearance rate equals the filtering rate of the fish. The filtering rate is therefore estimated in each experiment as the maximal clearance rate that is found. The retention percentage (R) of each size class of zooplankton equals the clearance rate divided by the filtering rate (FR) (cf. Smith 1989):

$$R = CR / FR \qquad (2)$$

The combination of equations 1 and 2 yields:

$$R = \frac{\ln(D_0/D_t) \cdot V}{FR \cdot t} \qquad (3)$$

When D_t is 0, this formula yields $R=\infty$. In these cases we assumed that R=100%.

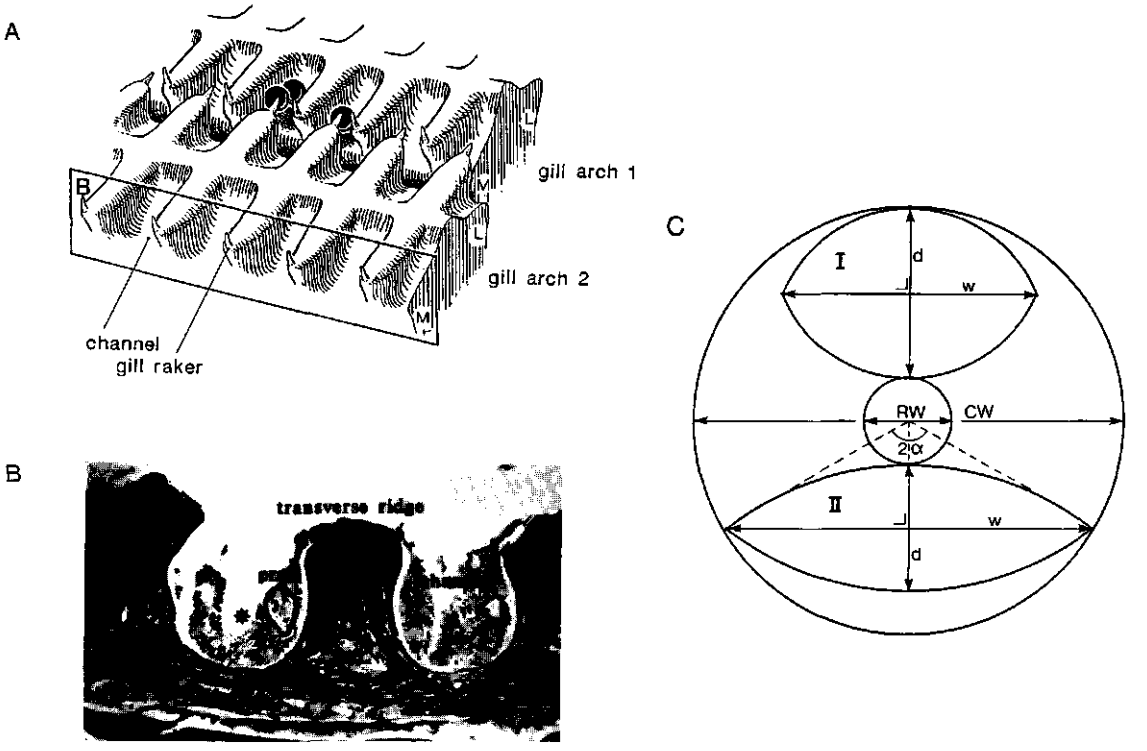

Figure 3

a) The reducible channel model for filter-feeding. The mesh size of the branchial sieve is reduced by depressing the lateral rakers into the medial channels.

b) A longitudinal section (Crossmon staining) of a branchial arch of a common bream. The medial channels appear in cross section and are roughly circular. When the channels are reduced the tips of the lateral rakers of the adjacent arch are positioned as indicated by the stars. A raker cushion, or channel wall, is indicated as transverse ridge.

c) Mathematical model of a reduced channel. A *Daphnia* shaped particle can be retained in two ways, according to depth, d (method I) or according to width, w (method II). The mode of retention depends on the ratio of lateral raker tip width (RW) and channel width (CW) and on the d/w ratio. The value of RW/CW is estimated to be 0.20. In this case particles with d/w > 0.50 will be retained by method I; particles with d/w<0.50 by method II (see appendix). Angle α is used in the calculations in the appendix.

a) adapted from Hoogenboezem et al. submitted

b) adapted from Hoogenboezem et al. 1991

Theoretical retention of zooplankton

We assumed that, during successive gulps, the water flow would reorient the zooplankton until its length axis was lying parallel to the channels. We used the reducible channel model (Hoogenboezem et al. 1991) to obtain theoretical retention values (Fig. 3a). In this model the channels between the medial raker cushions are the site of prey retention. The channel width equals the mesh size. The roof of the channels is formed by the palatal organ. The channels are mostly circular in cross section (Fig. 3b), therefore the diagonal of the channel and its width are equal. This means that zooplankton width is the critical size parameter.

Channel widths (CW) were obtained using the allometric equations CW = -0.104 + 0.00462·SL for common bream and CW = 0.038 + 0.00330·SL for white bream (van den Berg et al. 1992), where SL = standard length (in mm). We found that CW is 0.71 mm for the common bream and 0.61 mm for the white bream. CW was measured only in the middle of the second gill arch. At this position CW is maximal. In fact there is a range of channel widths in the entire branchial sieve, which approximately lies between 60 and 100% of CW (van den Berg et al. 1992). We assumed that the retention curve is a sigmoid curve running from 0% retention at 0.6·CW to 100% retention at CW. This is the theoretical retention curve for unreduced, circular channels.

In the reducible channel model, the mesh size of the branchial sieve can be reduced by lowering the lateral rakers into the medial channels (Hoogenboezem et al. 1991), turning them into reduced channels (Fig. 3a,b). In reduced channels the retention depends on the d/w ratio and on the ratio of the lateral raker radius and the channel radius (Fig. 3c). With a geometrical analysis of the reduced channels (see appendix) we predict that zooplankton depth is the critical size parameter when the d/w ratio is above 0.58 ($1/\sqrt{3}$). The d/w ratio of both copepods and *Daphnia* is above this value (Table 1), therefore zooplankton depth is the critical size parameter for reduced channels. We estimated that the diameter of the lateral raker tip is 20% of the medial channel diameter. The resulting formula for the mesh size of the reduced channels is:

$$\frac{0.40 \cdot CW}{d/w} \qquad (4)$$

For copepods and for *Daphnia* a sigmoid curve was drawn between 60% and 100% of this value. These are the theoretical retention curves for reduced, circular channels.

Note that in unreduced channels zooplankton width is the critical size parameter, whereas in reduced channels zooplankton depth is the critical size parameter.

Results

The ratio of width to length is 0.487 for copepods and 0.468 for *Daphnia* (Table 1). The d/w ratio is 0.882 for copepods and 0.599 for *Daphnia* (Table 1, Fig. 2a). Because these values of the d/w ratio are larger than 0.58, zooplankton depth is the critical zooplankton size parameter in reduced channels for both copepods and *Daphnia*. Using equation 4 we find that the theoretical mesh size of reduced channels is 0.45·CW for copepods and 0.67·CW for *Daphnia*.

It is expected that the size range of zooplankton within a sieve sample is determined by the mesh size of the sample sieve itself and of the sieve above it (with larger mesh size). The mesh size of the sample sieve is the lower boundary of the expected zoo-

plankton size range; the mesh size of the upper sieve is the upper boundary. The upper boundary is absolute; the zooplankton díd pass the upper sieve. The lower boundary is not absolute; zooplankton that did not pass the sample sieve may still be áble to do so.

The average copepod length in each sieve sample (which, in our standard ecological measurements, excludes the tail) generally equals about 1.5 times the upper boundary of the expected size range (Table 1; e.g. average length 360 μm in the 150 μm sample, with upper boundary 250 μm). *Daphnia* length averages almost 2.5 times the upper boundary. Therefore, length clearly is not the critical parameter.

In figure 4 the measured zooplankton width-frequency distribution and the corresponding expected size range of each sieve sample are indicated. There is a good fit between the maximal widths of copepods encountered in the sieve samples and the expected upper boundaries (Fig. 4a). The maximal widths of *Daphnia* however, exceed the upper boundaries by up to 40% (Fig. 4b). Apparently, width is the critical size parameter for copepods. As expected, the lower boundaries are not distinct, for either of the zooplankton. This could be caused both by clogging of the sieves and by the possibility for small zooplankters to remain in or swim back to large sieves. *Daphnia* smaller than 0.18 mm in width (first instar) do not occur, nor do copepods larger than 0.56 mm in width, which probably explains the deviating size-frequency distributions in the smallest and largest sieves.

In Figure 5 zooplankton retention by common bream and white bream is plotted versus plankton width. The results of three experiments are combined in each figure. The initial plankton density was between 100 and 500 per litre in each experiment. Note that the maximum width of the copepods is 0.4 mm and of *Daphnia* 0.7 mm. The copepod retention data of common bream (Fig. 5a) correspond well with the theoretical curve for reduced channels. The data of *Daphnia* are more scattered, but the highest retention data from each size class correspond closely to the theoretical curve for reduced channels. The wide spectrum of retention percentages of *Daphnia* during the six hour

Table 1

Length, width and depth measurements of copepods and *Daphnia* in samples from six industrial sieves. The average of width divided by length is used in the filter-feeding experiments to calculate width from length. The depth/width ratio was measured separately, but using the same plankton. Note the slightly allometric growth of the length/width ratio in *Daphnia*.

sieve mesh size (μm)	copepods length (mm)	width (mm)	n[a]	*Daphnia* length (mm)	width (mm)	n
600	0.832[b]±0.147	0.414±0.087	26	1.285±0.146	0.646±0.119	102
425	0.834±0.148	0.413±0.079	63	1.200±0.111	0.598±0.087	101
355	0.627±0.112	0.302±0.046	99	0.977±0.177	0.420±0.082	49
300	0.597±0.056	0.281±0.044	100	0.752±0.134	0.326±0.062	27
250	0.501±0.061	0.238±0.031	102	0.646±0.105	0.279±0.052	53
150	0.360±0.045	0.184±0.027	38	0.593±0.045	0.268±0.028	113
average width/length	0.487±0.0030		428	0.468±0.0032		445
average depth/width	0.882±0.072		20	0.599±0.066		20

[a] number of measured zooplankters.
[b] mean ± standard deviation

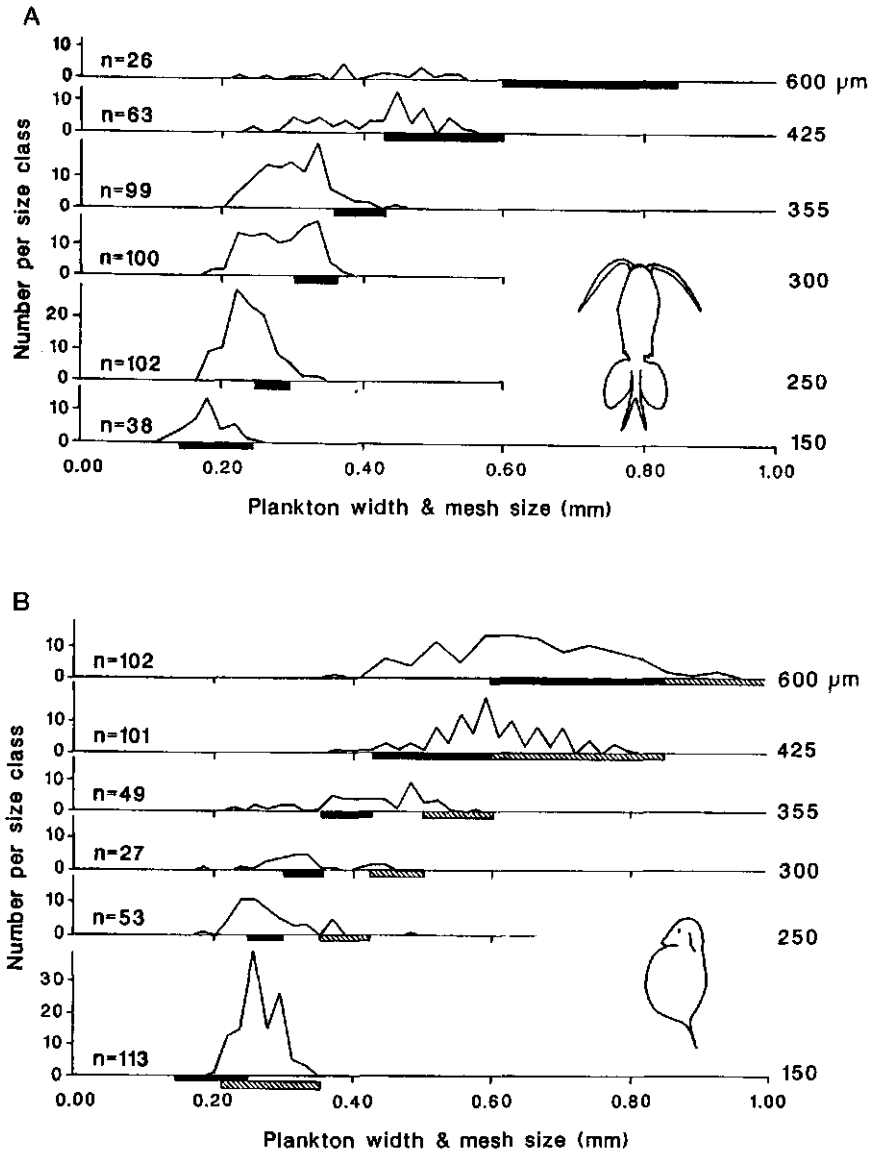

Figure 4

Width-frequency-distributions of zooplankton in samples from six subsequent industrial sieves (600, 425, 355, 300, 250 and 150 µm). The black bars indicate the expected zooplankton size range. The upper boundary is the mesh size of the sieve above the sample sieve: the plankton did pass this sieve. The lower boundary is the mesh size of the sample sieve itself: the plankton did not pass this sieve.

a) The data for copepods. The maximum widths correspond with the upper boundaries of the expected size ranges, indicating that width is the critical size parameter for copepods.

b) The data for *Daphnia*. The cross-hatched bars indicate the expected zooplankton size range when the diagonal of the square meshes is used as mesh size (see discussion). The maximum widths of *Daphnia* correspond with the upper boundaries of these 'diagonal' expected size ranges. Width is the critical size parameter for *Daphnia*, but, unlike copepods, *Daphnia* can pass the sieve diagonally, due to their 3D-shape.

experiments suggests that at the initial high plankton density the common bream was feeding with unreduced channels and later switched to reduced channels. This switch was previously observed in common bream by Hoogenboezem et al. (1991). In white bream (Fig. 5b) we found, in the size range where copepods occurred, no clear difference in retention of copepods and *Daphnia*. The white bream data correspond most closely to the theoretical curve for unreduced channels, though retention is slightly better than expected. The increase in retention from 0 to 100 % is more gradual than predicted.

The average filtering rates of common bream and white bream were 27.5 and 23 litre per hour, respectively. The maximal clearance rate of copepods was about 80% of these filtering rates both for common bream and for white bream.

Discussion

In the industrial sieve experiments the maximal copepod width was equal to the mesh size of the sieve through which it passed, but the maximal *Daphnia* width exceeded the mesh size of the sieve through which it passed by about 40% (Fig. 4). This difference can be explained if one considers the 3D-shape of these organisms. The d/w ratio is about 0.9 in copepods and 0.6 in *Daphnia* (Fig. 2a). Similarly, Wright and O'Brien (1984) found a d/w ratio of about 0.80 in *Mesocyclops edax* and 0.38 in

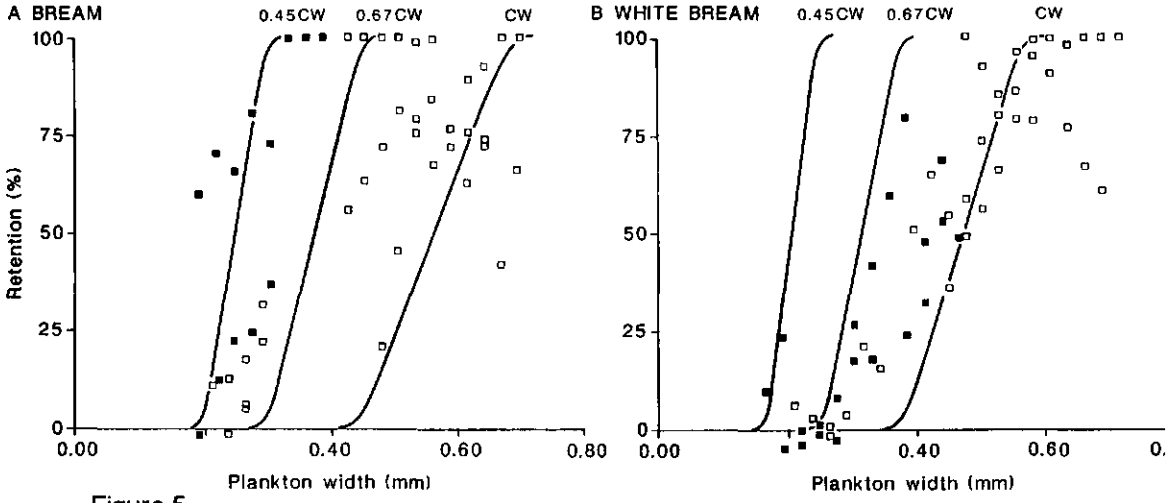

Figure 5

Retention percentage versus plankton width. Data are compiled from three filter-feeding experiments. Note that the maximum width of the copepods is 0.4 mm and of *Daphnia* 0.7 mm. The theoretical retention curve for unreduced channels is indicated (CW, channel width). The theoretical retention curves for reduced channels are indicated with 0.45 CW for copepods and 0.67 CW for *Daphnia*. The multiplication factors of CW are calculated as 0.40 divided by the d/w ratio (0.882 for copepods and 0.599 for *Daphnia*) since depth is the critical size parameter.

a) common bream, SL=17.6 cm

b) white bream, SL=17.2 cm.

■ = copepods □ = *Daphnia*

Daphnia parvula. Because of its low d/w ratio *Daphnia* can pass square meshes diagonally (Fig. 2a). We calculated the expected plankton size ranges using the diagonal mesh size (cross-hatched bars in Fig. 4b), which equals $\sqrt{2}$ times the original mesh size. As expected, the maximum widths of *Daphnia* correspond with the upper boundaries of these 'diagonal' expected size ranges.

The relationship between plankton width and the mesh size it can pass is very close. Apparently the antennae of copepods and of *Daphnia* do not prevent the plankton from passing through the sieves, even at the very low experimental flow velocity. Kerfoot (1978) describes the 'dead-man response' in *Bosmina longirostris*. When it perceives a predator it folds its antennae into its carapace and passively sinks away from the predator, thus avoiding mechano-receptive perception of its exact location. This phenomenon may also explain why the antennae do not influence retention.

Both the copepod and the *Daphnia* retention data of common bream correspond closely to the reduced channel (RC) curves. Therefore, the reducible channel model appears to be valid for common bream (cf. Hoogenboezem et al. 1991). The common bream retained copepods of about 65% of the width of the smallest retained *Daphnia*. There is a similarity with the industrial sieves; *Daphnia* are more difficult to retain than copepods of the same width because of their low d/w ratio. The maximal clearance rate for copepods was about 80% of the filtering rate. This could indicate that the high escape velocity of copepods (Kerfoot 1978: 35 cm s^{-1}) has some influence on retention by the fishes. Janssen (1976) showed that *Daphnia* do not escape at all, whereas copepods are negatively rheotactic. The different retention of copepods and *Daphnia* by common bream can not be caused by this difference in escape behaviour. If it were, we would expect copepods to be retained less well than *Daphnia*, whereas we found the opposite. Furthermore, we would expect the larger, quicker copepods to be retained less than the small ones. Again, we found the opposite (Fig. 5).

The retention data of white bream correspond most closely to the unreduced channel (URC) curve. In white bream we found only a minor difference in retention of copepods and *Daphnia*, as was expected theoretically for unreduced channels. The white bream probably did retain zooplankton in its channels, but it did not reduce its channels. Hoogenboezem et al. (1991) showed that the lateral gill rakers of common bream have a *musculus abductor branchiospinalis*, capable of abducting (lowering) the lateral rakers into the medial channels. This tiny muscle is not present in white bream (unpubl. res.), indicating that white bream is unable to reduce its channels. This clearly corroborates with the present results.

An important conclusion is that zooplankton depth is the critical size parameter only when the channels are reduced (see Appendix). Therefore, both the shape of the biological sieve and the shape of zooplankton should be examined in order to predict retention accurately.

We have predicted that in unreduced channels zooplankton width is the critical size parameter, since the channels are mostly circular in cross section (Fig. 3b). The roof of the channels however is formed by the muscular palatal organ (Sibbing et al. 1986; Sibbing 1991). Possibly, the roof is not circular. This means that zooplankton depth could play a role in unreduced channels as well, which might explain the slightly better retention of copepods by white bream (Fig. 5b).

In previous experiments (Hoogenboezem et al. subm.) formalin preserved zooplankton was sieved by pouring the zooplankton over an industrial sieve and rinsing the sieve with water. In this way, a wider size range of zooplankton was retained than by using the present method and the relationship between mesh size and particle size was less clear. The orientation of the dead plankton is probably more random than that of live ones. In our opinion, the present underwater method with live zooplankton is

more similar to the actual events in the branchial sieve. Although the orientation of the zooplankters when entering a channel is unknown, plankton width and depth are more important than length. The forces exerted by the water during gulping will reorient a prey until its length axis is parallel to the direction of flow and to the channel walls. Drost et al. (1988) found that carp larvae always take in elongated prey items with their length parallel to the flow, because of the steep velocity gradients within the flow. They concluded that prey width is critical. The lack of knowledge about flow pattern and prey orientation in the branchial sieve stresses the need for measuring water flow profiles in live fish. Unfortunately, this requires highly complicated experiments (e.g. Sanderson 1991). It is likely that prey orientation is more random when the branchial sieve is comb shaped, like in many clupeids and coregonids. In that case, a combination of zooplankton size parameters is probably more meaningful than just zooplankton width or depth (Wright et al. 1983; Drenner et al. 1984; Mummert and Drenner 1986; Gibson 1988; MacNeill and Brandt 1990).

The complex and variable shape of zooplankton makes it difficult to predict retention accurately. Experiments have been performed with mixtures of zooplankton and microspheres of different sizes (Drenner et al. 1984; Mummert and Drenner 1986). The well defined diameter of microspheres makes the assessment of a mesh size of the branchial sieve comparatively easy. During natural functioning, however, the branchial sieve is not retaining spheres but zooplankton. The relationship between the shape of zooplankton and of the branchial sieve is crucial to understand filter-feeding. We found that different zooplankton size parameters may be critical depending on the species of fish and zooplankton and on the filtering mode. In unreduced channels, zooplankton width is critical. In reduced channels, zooplankton depth is critical, provided that the d/w ratio is higher than 0.58. The metrical relationships between length, width and depth of the zooplankton are, therefore, essential to interpret filter-feeding experiments in fish. In fact, the differential retention of copepods and *Daphnia*, which only occurs in common bream, strongly supports the reducible channel model (Hoogenboezem et al. 1991). Our results have implications for the zooplankton as well. Differently shaped species will have a different chance of predation depending on the shape of the sieve of the predator. The flat shape of *Pediastrum*, for example, might be an adaptation to prevent ingestion by *Dorosoma cepedianum* (Mummert and Drenner 1986). The present study of the interaction between live zooplankton and sieves shows that the shapes of both are essential to test theoretical filter-feeding models in order to understand filter-feeding in fishes. Such detailed knowledge is fundamental to trophic segregation and the exploitation of food resources by fish.

Acknowledgements

We want to express our thanks to two anonymous referees for their useful and detailed comments and to Kristin Abbott and Dr. M. Moir for their thorough editorial work. The experiments were carried out in the field laboratory of the Limnological Institute in Oosterzee, the Netherlands. The institute provided the zooplankton and much of the materials used. W. Valen and K. Boekhorst prepared the figures. The research is supported by the Foundation for Fundamental Biological Research (BION), which is subsidized by the Dutch Organization for Scientific Research (NWO), project 811-428-265.

References

Berg, C. van den, F.A. Sibbing, J.W.M. Osse and W. Hoogenboezem.1992. Structure, development and function of the branchial sieve of common bream, *Abramis brama*, white bream, *Blicca bjoerkna*, and roach, *Rutilus rutilus*. Env. Biol. Fish. 33: 105-124.

Drenner, R.W., J.R. Mummert, F.Jr. de Noyelles and D. Kettles. 1984. Selective particle ingestion by a filter-feeding fish and its impact on phytoplankton community structure. Limnol. Oceanogr. 29(5): 941-948.

Drost, M.R., J.W.M. Osse and M. Muller. 1988. Prey capture by fish larvae, water flow patterns and the effect of escape movements of prey. Neth. J. Zool. 38: 23-45.

Gibson, R.N. 1988. Development, morphometry and particle retention capability of the gill rakers in the herring, *Clupea harengus* L.. J. Fish Biol. 32: 949-962.

Hoogenboezem, W., J.G.M. van den Boogaart, F.A. Sibbing, E.H.R.R. Lammens, A. Terlouw and J.W.M. Osse. 1991. A new model of particle retention and branchial sieve adjustment in filter-feeding bream (*Abramis brama* (L.), Cyprinidae). Can. J. Fish. Aquat. Sci. 48: 7-18.

Hoogenboezem, W., E.H.R.R. Lammens, P.J. McGillavry and F.A. Sibbing. submitted. Prey-size selectivity and sieve adjustment in filter-feeding bream (*Abramis brama* (L.), Cyprinidae). Can. J. Fish. Aquat. Sci.

Janssen, J. 1976. Selectivity of an artificial filter feeder and suction feeders on calanoid copepods. Amer. Midland Natur. 95: 491-493.

Kerfoot, W.C. 1978. Combat between predatory copepods and their prey: *Cyclops*, *Epischura*, and *Bosmina*. Limnol. Oceanogr. 23: 1089-1102.

Kott, P. 1953. A modified whirling apparatus for subsampling of plankton. Aust. J. Mar. Freshwat. Res. 4: 387-393.

MacNeill, D.B. and S.B. Brandt. 1990. Ontogenetic shifts in gill-raker morphology and predicted prey capture efficiency of the alewife, *Alosa pseudoharengus*. Copeia 1: 164-171.

Mummert, J.R. and R.W. Drenner. 1986. Effects of fish size on the filtering efficiency and selective particle ingestion of a filter-feeding clupeid. Trans. Amer. Fish. Soc. 115: 522-528.

Nie, H.W. de, H.J. Bromley and J. Vijverberg. 1980. Distribution patterns of zooplankton in Tjeukemeer, the Netherlands. J. Plankton Res. 2: 317-334.

Sanderson, S.L., J.J. Cech Jr. and M.R. Patterson. 1991. Fluid dynamics in suspension-feeding blackfish. Science 251: 1346-1348.

Sibbing, F.A., J.W.M. Osse and A. Terlouw. 1986. Food handling in the carp (*Cyprinus carpio*): its movement patterns, mechanisms and limitations. J. Zool. Lond. (A)210: 161-203.

Sibbing, F.A. 1991. Food capture and oral processing. p 377-412. *In* I.J. Winfield and J. Nelson (Ed.). Cyprinid fishes; systematics, biology and exploitation. Chapman & Hall.

Smith, D.W. 1989. The feeding selectivity of silver carp, *Hypophthalmichthys molitrix* Val.. J. Fish Biol. 34: 819-828.

Vijverberg, J. and A.F. Richter. 1982a. Population dynamics and production of *Daphnia hyalina* (Leydig) and *Daphnia cucullata* (Sars) in Tjeukemeer. Hydrobiologia 95: 235-259.

Vijverberg, J. and A.F. Richter. 1982b. Population dynamics and production of *Acanthocyclops robustus* (Sars) and *Mesocyclops leuckarti* (Claus) in Tjeukemeer. Hydrobiologia 95: 261-274.

Wright, D.I., W.J. O'Brien and C. Luecke. 1983. A new estimate of zooplankton retention by gill rakers and its ecological significance. Trans. Amer. Fish. Soc. 112: 638-648.

Wright, D.I. and W.J. O'Brien. 1984. The development and field test of a tactical model of the planktivorous feeding of white crappie (*Pomoxis annularis*). Ecol. Monogr. 54(1): 65-98.

Appendix

Square meshes of the industrial sieves

Particles should fulfil two conditions to pass a square mesh diagonally:

1) The d/w ratio should not exceed $1/\sqrt{2}$ (≈ 0.71)

2) The profile edges in the width direction should be be able to pass the rectangular corners of the mesh. The angle of the profile edges should therefore be less than 90°.

Daphnia meet both of these demands, copepods meet neither of them (Fig. 2a).

Mathematical model for retention in a reduced channel (Figure 3c)

The channel is a circle with diameter CW, the lateral raker tip is a smaller circle in the centre of the channel, with diameter RW. The particle has depth d and width w. The contours of the particle are formed by two identical circle segments. A particle can be critically retained in two ways, according to d (I), then d = 0.5CW - 0.5RW or according to w (II), with a complex relationship to CW. The relationship for method II is obtained using angle 2α, which is the angle between the contact points of a critical particle with the channel wall and the centre of the channel. It can be shown that:

$$\cos \alpha = \frac{d + RW}{CW} \qquad \text{and} \qquad w = CW \sin \alpha$$

rewritten:

$$d/w = \frac{\cos \alpha - RW/CW}{\sin \alpha}$$

With given ratios d/w and RW/CW the value of α can be determined iteratively, with α the value of d and w can be determined. If the value of d obtained in this way exceeds 0.5CW - 0.5RW, method II is invalid and method I should be used.
At the transition of method I and II both formulas should apply. It follows:

$$\cos \alpha = 0.5\, RW/CW + 0.5 \qquad \text{and} \qquad d/w = \frac{0.5}{\sin \alpha}(1 - RW/CW)$$

some values of RW/CW and d/w at this transition point are given in the table below:

RW/CW	**d/w**
0	$1/\sqrt{3}$ ≈ 0.58
0.1	$\sqrt{(9/31)}$ ≈ 0.54
0.2	$1/2$ $= 0.50$
0.5	$1/\sqrt{7}$ ≈ 0.38

For example, when RW/CW equals 0.10 and d/w > 0.54 method I is appropriate(retention according to d) and when d/w < 0.54 method II is appropriate (retention according to w). When d/w exceeds $1/\sqrt{3}$ method I is always appropriate, independent of the value of RW/CW.

Chapter 3

Filter-feeding in common bream (*Abramis brama*), white bream (*Blicca bjoerkna*) and roach (*Rutilus rutilus*): experiments, models and energy intake.

Coen van den Berg, Jos G.M. van den Boogaart, Eddy H.R.R. Lammens
Ferdinand A. Sibbing and Jan W.M. Osse
subm. Can. J. Fish. Aquat. Sci.

Abstract

Three models of the sieving mechanism of the branchial sieve were used to predict the ability to retain zooplankton of three sympatric cyprinids: common bream, white bream and roach. The model predictions were tested with filter-feeding experiments, using three size classes of each species. Results of experiments in darkness corroborated with the reducible-channel model for common bream, with the unreducible-channel model for white bream and possibly with the saw-tooth model for roach. Common bream can adjust the mesh size of its branchial sieve, thus achieving a higher flexibility in food uptake than the other two species. In light experiments, roach and the small common and white bream switched to particulate intake, characterized by a lower retention ability and a higher filtering rate than during gulping. The retention ability was used to calculate the percentage of the available zooplankton energy, that the three cyprinids can retain as a function of their length. The retained energy percentage decreases sigmoidly with increasing fish length. At any length between 10-50 cm, common bream has the highest retained energy percentage, white bream the lowest and roach is intermediate. The population of common bream will therefore be at an advantage when competition for zooplankton is strong, like in eutrophic lakes.

Introduction

Common bream (*Abramis brama*), white bream (*Blicca bjoerkna*) and roach (*Rutilus rutilus*) are opportunistic feeders and their diets show a considerable degree of overlap (Lammens and Hoogenboezem 1991). A certain amount of niche segregation is required for species to coexist in an ecosystem. Common bream, white bream and roach can coexist in a diversified habitat with both vegetation and open water. This situation has become rare in the Netherlands due to eutrophication. In Tjeukemeer (a eutrophic lake in the north of the Netherlands) large numbers of algae and suspended particles reduce the light level strongly and macrophytes have almost disappeared (Lammens 1989, 1986; de Nie 1987). Chironomid larvae, buried in the soft substrate, and zooplankton are the major food resources for the fishes. The competition for food has increased, due to this limited spectrum of food resources. Common bream has become the dominant fish species, while other cyprinid species have decreased sharply in number and average size. The efficiency of filter-feeding probably plays an important role in this shift in the fish fauna (Hoogenboezem et al. 1991, in press) because zooplankton is a major food resource.

Filter-feeding fishes exert a positive size selection on the zooplankton and will therefore change the size-frequency distribution of the zooplankton population. The average size of each zooplankton species in Tjeukemeer is smaller than in non-eutrophic lakes (de Nie et al., 1980; Lammens 1985). In the summer, the average length of *Daphnia hyalina* is reduced from about 1.5 to 0.7 mm, which is caused by plankton feeding of the new 0^+ fish generation (Vijverberg and Richter 1982a) and by the poor food conditions for the zooplankton (Boersma et al. 1991). Therefore, the ability to retain the smaller zooplankters, as well as the larger ones (retention ability) is an important factor in the competition for zooplankton.

To better understand the dominance of common bream in eutrophic lakes, we measured the differences in retention ability of common bream, white bream and roach. Three fish sizes of each species were tested. Experiments were performed both in darkness and in light to test whether visual clues are important for zooplankton feeding and whether different feeding modes are used in these circumstances. The experimental retention data were used to test retention models, based on the morphology of the branchial sieve. With these retention models we could estimate the fraction of the available zooplankton energy that the fishes can retain as a function of their length. In this way we could roughly quantify the effect of differences in retention ability on competition for zooplankton.

Models of the filter-feeding mechanism

Hoogenboezem et al. (1991) presented a new model of the filter-feeding mechanism of common bream, the reducible-channel model (Fig. 1a). In this model, the branchial sieve has two discrete mesh sizes. The channels between the medial raker cushions are the site of prey retention. In the first filter-feeding mode, with unreduced channels (URC), the medial channel width is the mesh size of the sieve. The second filter-feeding mode is with reduced channels (RC). In this mode, the lateral rakers are abducted (lowered) into the medial channels of the opposite arch, reducing their mesh size (Hoogenboezem et al. 1991). In the unreducible-channel model this second filter-feeding mode is not possible.

The gut contents of common bream contain much smaller particles than would be expected from its (unreduced) channel width (Lammens et al. 1987). This can be explained with the reducible-channel model. The morphology and functioning of the branchial sieve of common bream corroborate with the reducible-channel model. Hoogenboezem et al. (1991) found a previously undescribed muscle (*m. abductor branchiospinalis*) which can abduct the lateral rakers, thus reducing the medial channels. X-ray films showed that marked food particles are retained in the medial channels and filter-feeding experiments proved that common bream switches between the two predicted mesh sizes of its branchial sieve (Hoogenboezem et al. 1991, in press).

In the two-dimensional saw-tooth model (Sibbing 1991; Van den Berg et al. 1992), particles are retained on the gill slit, which is lined with interdigitating rakers (Fig. 1b). The mesh size of this sieve is dependent on the shape of the rakers and the distance between the gill arches. Another possible filter-feeding mechanism in cyprinids is retention between the gill arch surface and the palatal organ. The palatal organ is capable of local, detailed movements and can hold small food particles, while debris is removed by rinsing (Sibbing and Uribe 1985; Sibbing et al. 1986). Predictions about the retention ability of the fishes were formulated using the reducible- and unreducible-channel models and the saw-tooth model.

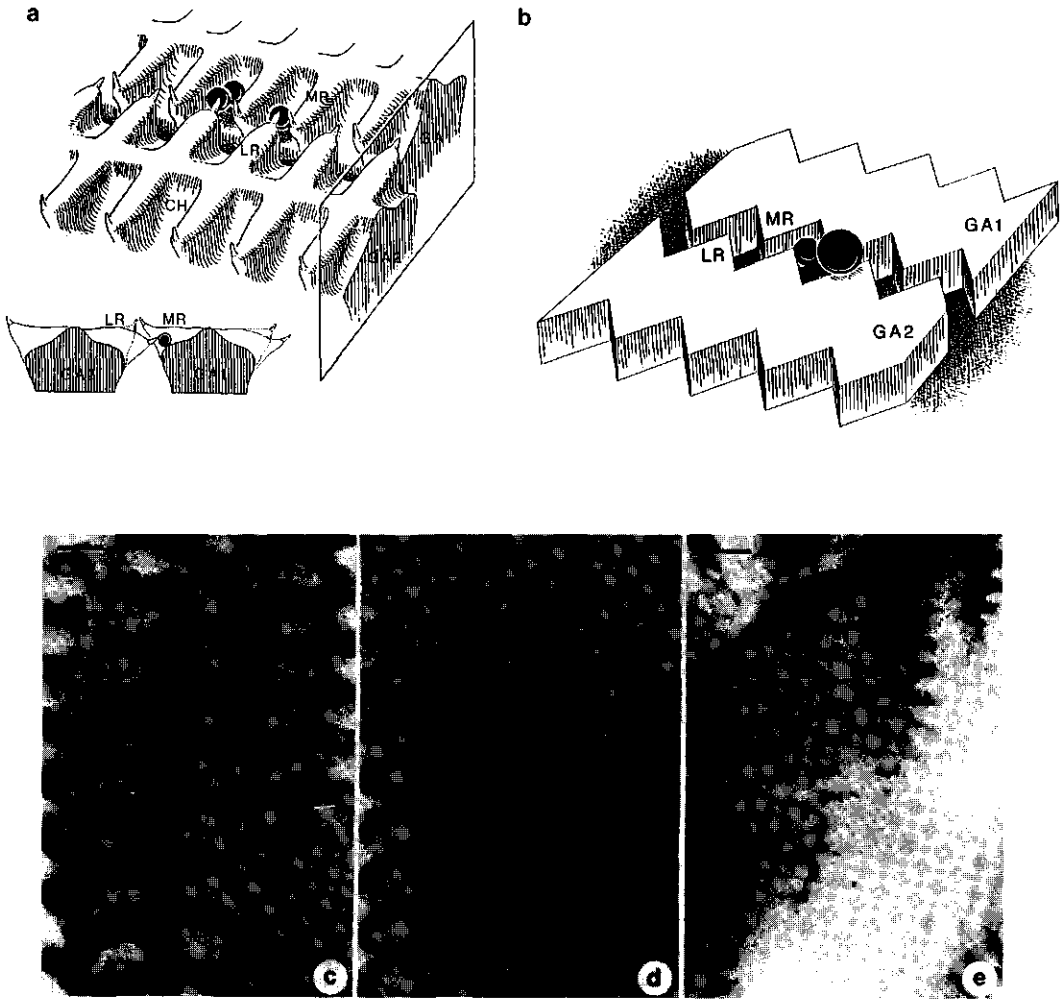

Figure 1

a) The reducible-channel model of filter-feeding. The top picture shows a portion of two neighbouring gill arches. Particles are retained in the medial channels. According to this model, the mesh size of the branchial sieve can be reduced by lowering the lateral rakers on the other side of the gill slit into these medial channels. In the figure below, the lowering of a lateral raker is shown in cross section.

b) The saw-tooth model of filter-feeding. In this 2D model, the gill rakers are represented by triangular projections in the gill slit. Particles are retained on the gill slit. According to this model, the mesh size of the sieve can be adjusted over a continuous range by altering the distance between the gill arches.

c) Detail of the branchial sieves of common bream

d) white bream and

e) roach (each with SL≈23 cm). Scale bar represents 1 mm. Note the deep, curved channels in common bream, the straight channels in white bream and the irregular, small channels in roach.

CH, channel; GA1,2, gill arch 1,2; LR, lateral gill raker and cushion; MR, medial gill raker and cushion.

a) and b) adapted from Hoogenboezem et al. (1991)

c), d) and e) adapted from Van den Berg et al. (1992).

Materials and methods

Fishes and zooplankton

Common bream (*Abramis brama*), white bream (*Blicca bjoerkna*) and roach (*Rutilus rutilus*) were trawled in two lakes in the north of the Netherlands, Tjeukemeer and Beulaker Wijde. Prior to the experimental period they were kept in 250 litre tanks for at least one year to acclimatize to laboratory circumstances and tap water. The experimental tanks (volume c. 42 litres) were connected to a recirculation system, which included a pump, UV tubes and a cooling device. Circulation was stopped during experiments. We used nine tanks for three size classes of each species, and a control tank containing no fish. Food consumption in a tank will roughly be proportional to the total metabolic weight of the fishes in that tank. The basal metabolism of cyprinid fishes is proportional to $W^{0.80}$ (at 20°C; Winberg 1960). To facilitate comparison of the experiments we put groups of experimental fishes with about equal total metabolic weight in each tank (Table 1).

Zooplankton was collected in Tjeukemeer from April to July 1990, using hoop nets (mesh size 250 μm) with a collecting bottle at the end. The velocity of the boat was approximately 1 m s^{-1} and each haul lasted approximately half a minute. The zooplankton consisted mainly of cycloid copepods and cladocerans. Dominant cladocerans were *Daphnia hyalina*, *Daphnia cucullata*, *Bosmina coregoni*, *Bosmina longirostris*, *Chydorus sphaericus* and *Leptodora kindtii* (cf. de Nie et al. 1980). In the experiments, we distinguished two groups of zooplankton: the cycloid copepods (length ~0.3-0.8 mm) and the two *Daphnia* species (length ~0.4-1.6 mm).

Table 1

Mean standard length, number, total metabolic weight and two branchial sieve parameters of the fishes in each experimental tank.

	mean SL (mm)	number	total metabolic weight ($g^{0.80}$)	CW1M[a] (mm)	IR1M[b] (mm)
common bream	99	2[c]	14.6	0.35	0.66
	132	2	37.9	0.51	0.88
	176	1	31.7	0.71	1.16
white bream	99	4	39.7	0.37	0.56
	135	2	47.7	0.48	0.76
	172	1	42.1	0.60	0.97
roach	103	4	42.5	0.27	0.46
	131	2	39.4	0.35	0.56
	172	1	44.1	0.46	0.72

[a] = Channel width of the medial side of the first gill arch (Van den Berg et al. 1992)
[b] = Inter raker distance of the medial side of the first gill arch (" ")
[c] = a sufficient number of appropriately sized fishes was not available

Experimental procedures

Prior to each experiment the fishes were starved for 48 hours. Experiments were either performed in complete darkness or in light. We tried to obtain a zooplankton mixture with sufficient numbers of zooplankton in a range of size classes. Therefore, the zooplankton were sieved in a submersed stack of industrial sieves with diminishing mesh size from top to bottom (Van den Berg et al. in press). Sufficient numbers of zooplankton could often not be obtained due to the unequal and unpredictable size-frequency distribution of the zooplankton in the lake. The selected mixture of zooplankton was stirred gently and distributed over the experimental tanks. During experiments, random distribution of the zooplankton in the tanks was enhanced with air stones.

A zooplankton sample was taken from each tank at t=0 hr, marking the start of an experiment. Further samples were taken at t=3 hr and t=6 hr. The zooplankton was sampled with a tube of 20 cm length and 3 cm diameter (Hoogenboezem et al. in press; Van den Berg et al. in press). This sampler tube was lowered quickly into the tank and the lower opening was closed with a cork on a string. This was done eight times in each tank, in a fixed order and at fixed positions. The total of the eight tube contents is the tank sample. We found that the sampler tube is only reliable when the movement is performed quickly.

The volume of the samples was measured to the nearest 5 mL, the zooplankton in the samples was concentrated and stored in 5% formalin. If samples contained more than a few hundred specimens, a subsample was taken using a whirling apparatus (Kott 1953). For up to 100 *Daphnia* and up to 50 copepods, the number of specimens in length classes of 0.06 mm was determined with an ocular micrometer. Zooplankton lengths were measured following Vijverberg and Richter (1982a, b), Wright et al. (1983) and Wright and O'Brien (1984). For copepods, the length of the cephalothorax was measured. For *Daphnia*, the tail and helmet were subtracted from the length. Zooplankton width was calculated using the average ratio of width to length (Van den Berg et al. in press).

Calculation of retention percentage

To determine the retention ability of the fishes we measured the rate of decrease of each size class of zooplankton in the experimental tanks (the clearance rate). The clearance rate (CR) is related directly to the retention percentage by the fish. Size classes that are retained completely will have the highest CR, size classes retained less than 100% will have a proportionally lower CR.

The density of a zooplankton size class as a function of time is (Van den Berg et al. in press):

$$D_t = D_0 \, e^{-(CR \cdot t) / V} \qquad (1)$$

where
D_t = density of a particular zooplankton size class at t=t
D_0 = initial density of the same zooplankton size class (t=0)
CR = clearance rate (L hr^{-1})
t = duration of the experiment (hr)
V = tank volume (L)

The filtering rate (FR) in each experimental tank was defined as the average of the five highest clearance rates among all zooplankton size classes. The retention percentage (R) is the clearance rate divided by the filtering rate. Hence, the retention percentage for each size class of zooplankton is (Van den Berg et al., in press):

$$R = \frac{\ln (D_0/D_t) \cdot V}{FR \cdot t} \qquad (2)$$

Size classes with less than 5 specimens at t=0 were omitted from the figures. The retention data were smoothed by averaging the zooplankton number in each size class and its two neighbours. When the filtering rate in a tank was lower than 10 L hr^{-1}, the data were omitted, since this is a sign of poor eating (checked with video recordings made during light experiments) and hence of increased data scatter.

Theoretical retention of zooplankton

In the channel models (Fig. 1a) of filter-feeding the mesh size of the branchial sieve is related to the channel width (CW). Therefore, the cumulative frequency of CW was used to calculate the theoretical retention curves (cf. Boyd 1976; Drenner et al. 1984; Gibson 1988). The cumulative frequency of the widths of all channels of the branchial sieve was determined in one specimen of each species; these data were scaled to the size of the experimental fishes, using the relation between CW and standard length (Van den Berg et al. 1992). Common bream has the largest relative channel width of the three species, roach the smallest (Van den Berg et al. 1992).

The mesh size of unreduced channels is CW and zooplankton width is the critical size parameter for retention (Van den Berg et al. in press). Since we study the relation between retention and zooplankton width, the theoretical retention curve for unreduced channels is simply the cumulative frequency of CW. In reduced channels however, zooplankton depth is the critical size parameter for retention (Van den Berg et al. in press). The average depth/width ratio is 0.882 for copepods and 0.599 for *Daphnia*. With these ratios, it was shown that the mesh size of reduced channels is 0.45CW for copepods and 0.67CW for *Daphnia* (Van den Berg et al. in press). Therefore, the theoretical retention curves for reduced channels are the cumulative frequency of 0.45CW (copepods) and of 0.67CW (*Daphnia*).

In reduced channels the retention ability for copepods is higher than that for *Daphnia*, but not in unreduced channels. This difference is very useful to discriminate between the two sieving modes of the reducible-channel model (see 'model predictions').

In the saw-tooth model, zooplankton depth is the critical size parameter for retention because the sieve is a slit (Fig. 1b). Copepods have a higher depth/width ratio than *Daphnia* (see above). Therefore, the retention ability for copepods will be higher than that for *Daphnia*. The mesh size of the sieve can be adjusted over a continuous range by changing the distance between the gill arches.

The agreement between experimental and theoretical retention data was quantified statistically with the maximum likelihood method (MLM) (for details, see Appendix). The original, non-smoothed numbers of zooplankton per size class were used for this test. Retention was described with a likelihood function with two parameters. Up to plankton width μ nothing is retained at all. Above μ the retention curve goes up as a straight line with angle α. The MLM basically looks for a peak of the likelihood function by gradually changing the values of μ and α. This peak likelihood is compared with the like-

lihood of the theoretical values of μ and α. When the difference is too large, the theory is rejected. This method could not be applied to the difference in retention of copepods and *Daphnia*, because the fraction of measured specimens was different in each zooplankton group. Instead, this difference was analyzed with the non-parametric rank test of Wilcoxon. The test parameter is the ratio of retention percentage and zooplankton width in a width interval where both copepods and *Daphnia* are present. In order to get a sufficient number of data, the data of all dark experiments were lumped.

Model predictions of zooplankton retention

In the retention models we assume that the branchial sieve is the only size selective step during feeding on zooplankton. This is presumably true during feeding in the dark. When the fish use particulate feeding (in light) visual selection plays a role, as well. In that case, the predictions, stated below, can still be applied to the difference between the visually selected and the retained fraction of zooplankton.

If the reducible-channel model applies (Fig. 1a), we predict:
1) agreement of the results with the theoretical retention curve for unreduced channels or with that for reduced channels, or in the area between these curves (if the fish has switched between unreduced and reduced channels during the experiment).
2) the ability to adjust the branchial sieve to two distinct mesh sizes.
3) an equal retention ability for copepods and *Daphnia* when the channels are unreduced, but a higher retention ability for copepods when the channels are reduced.

If the unreducible-channel model applies, we predict:
1) agreement of the results with the theoretical retention curve for unreduced channels.
2) no ability to adjust the mesh size of the branchial sieve.
3) no difference in retention ability for copepods and *Daphnia*.

If the saw-tooth model applies (Fig. 1b), we predict:
1) position of the retention curve unknown, since the distance between the gill arches during filter-feeding is unknown.
2) the ability to adjust the mesh size of the branchial sieve over a continuous range.
3) a higher retention ability for copepods than for *Daphnia*.

Results

General

We assumed that in darkness particulate intake of zooplankton can not occur, because visual stimuli are absent. Infra-red video recordings of fishes feeding on zooplankton in darkness (no visible light) confirmed that their feeding mode was always gulping. Particulate feeding was never observed in darkness. In light, the feeding behaviour of the fishes often changed. In particular the behaviour of roach changed markedly from regular gulps, which were directed forward (gulping) in darkness, to swift, upward, aiming snaps (particulate intake) in light.

Two dark experiments and two light experiments will be discussed. The other experiments proved to have insufficient numbers of small zooplankton to test the retention models properly. The available data from these experiments agreed with the conclusions from the discussed ones. In both dark experiments the total filtering rate in

each experimental tank was high (15-30 L hr^{-1}) (Fig. 2). Apparently, all fishes were able and willing to feed on zooplankton in complete darkness. In general, the filtering rate increased when the initial zooplankton density was higher (Fig. 2) (on average 23.8 L hr^{-1} in experiment 2 versus 18.1 L hr^{-1} in experiment 1). Video recordings showed that in the light experiments the white bream and roach were often stressed, which resulted in low filtering rates. Common bream ate very well in all experiments.

In the dark experiments (Fig. 2), the retention data of the largest *Daphnia* were often very 'noisy', especially in the tanks with small fishes. In the light experiments (Fig. 3) this phenomenon did not occur. Possibly, filter-feeding is less effective for very large zooplankton. Since the small zooplankters show the limit of what the fish can retain, the large ones are less important for determining the retention ability. The interpretation of the light experiments is difficult, because of the occurrence of both particulate feeding and gulping. The results of the dark experiments facilitated the interpretation of the light experiments.

Dark experiments

The experimental data are compared with the predictions of the retention models (see 'methods'). The statistical data in table 2a are used for this comparison, while figure 2 is a visual aid. One should be aware that the graphs in figure 2 give a distorted view of the deviations from the predictions. The logarithmic transformation of the original data (cf. formula 2) tends to exaggerate the deviations at high retention values and to underestimate the deviations at low retention values.

Experiment 1 and 2 had an initial total zooplankton density of approximately 200 L^{-1} resp. 500 L^{-1} These experiments therefore potentially show the influence of zooplankton density on the adjustment of the mesh size of the branchial sieve.

Table 2 (see overleaf)

a) The maximum likelihood method was used to quantify the correspondence between the dark experiments and the theoretical retention curves (see Appendix). The difference between the likelihood of the theoretical values of μ and α and the maximum likelihood was calculated. In the table the chance of falsely rejecting the model (= type I error) because of this difference is indicated. When the chance of this error is lower than 0.05 the data justify rejection of the model. Values larger than or equal to 0.05 are printed in bold, indicating that the model is not rejected. The conclusions indicate the position of the data with respect to the theoretical curves.

RC	= data correspond to the reduced channel curve
URC	= data correspond to the unreduced channel curve
←	= data slightly to the left of the curve, i.e. with a slightly better retention ability
→	= data slightly to the right of the curve, i.e. with a slightly worse retention ability
RC↔ URC	= data in between the reduced and unreduced channel curves
*	= the maximum could not be found
[....]	= dubious result since there was an insufficient number of small zooplankters (see Fig 2b,c,g,i).

Table 2 a)

		D_0 (L^{-1})	type I error reduced	type I error unreduced	conclusion
COMMON BREAM					
SL 176 mm:					
Daphnia	○	191	**0.05**	0.005	RC
	△	445	0.01	<0.005	RC→
copepods	●	191	0.04	<0.005	←RC
	▲	445	<0.005	<0.005	RC↔URC
SL 132 mm:					
Daphnia		219	[*	**0.25**	URC]
		583	*	0.025	URC→
copepods		219	**0.4**	<0.005	RC
		583	*	<0.005	←URC
SL 99 mm:					
Daphnia		185	[<0.005	<0.005	?]
		541	*	<0.005	URC→
copepods		185	**0.3**	0.005	RC
		541	*	**0.05**	URC
WHITE BREAM					
SL 172 mm:					
Daphnia		238	<0.005	0.01	←URC
		652	<0.005	<0.005	←URC
copepods		238	<0.005	<0.005	←URC
		652	*	**0.08**	URC
SL 135 mm:					
Daphnia		136	<0.005	<0.005	←URC
		539	*	**0.05**	URC
copepods		136	*	0.005	RC↔URC
		539	*	0.02	←URC
SL 99 mm:					
Daphnia		238	<0.005	0.005	←URC
		474	*	<0.005	URC→
copepods		238	<0.005	<0.005	←URC
		474	*	*	?
ROACH					
SL 172 mm:					
Daphnia		190	[*	<0.005	URC→]
		543	<0.005	<0.005	URC→
copepods		190	*	**0.06**	URC
		543	*	*	URC→
SL 131 mm:					
Daphnia		179	*	*	?
		575	<0.005	<0.005	URC→
copepods		179	<0.005	**0.1**	URC
		575	*	<0.005	URC→
SL 103 mm:					
Daphnia		250	[*	<0.005	URC→]
		592	<0.005	<0.005	URC→
copepods		250	<0.005	**0.2**	URC
		592	*	*	URC→

Table 2b) Summary of the results of the experiments in light.

	SL ≈ 17 cm	SL ≈ 13 cm	SL ≈ 10 cm
common bream	gulping, RC	gulping, RC/URC	partic. intake; gulping, RC
white bream	-	-	feeding mode unclear
roach	particulate intake	particulate intake	particulate intake

The retention data of the 176 mm common bream (Fig. 2a) agree quite well with the theoretical retention curves. The data from experiment 1 (low density) agree with the RC curves; those from experiment 2 (high density) are intermediate between the URC and the RC curve (Table 2a). The retention data of the 132 mm and 99 mm common bream (Fig. 2b,c) show similar trends. The copepod retention data of experiment 1 (low density) clearly agree with the RC curves (Table 2a). The *Daphnia* retention data do not show this, because there are hardly any data points from *Daphnia* size classes small enough to test the retention models (Fig. 2b,c). The *Daphnia* retention data in experiment 2 (high density) are slightly to the right of the URC curve (Table 2a). The copepod retention data in experiment 2 are slightly to the left (SL 132 mm) or agree with (SL 99 mm) the URC curve (Table 2a). In experiment 1 the retention ability was always higher than in experiment 2, so common bream can adjust the mesh size of its branchial sieve. In all size classes of common bream the retention ability was significantly higher for copepods than for *Daphnia* ($p<0.025$). In experiment 2 this difference was always smaller than in experiment 1. Considering all retention characteristics, the data of common bream clearly corroborate with the predictions of the reducible-channel model.

The retention data of all size classes of white bream (Fig. 2d,e,f) agree rather well with the URC curve, but in most cases the retention ability is better than predicted (Table 2a). The slope of the retention data is less steep than predicted, possibly indicating that the mesh size throughout the branchial sieve of white bream is less homogeneous than predicted. The retention ability is the same in both experiments; there is no indication that white bream can adjust the mesh size of its branchial sieve. In all size classes of white bream the retention ability for copepods and *Daphnia* did not differ significantly ($p>0.10$). Considering all retention characteristics, the data of white bream corroborate most closely with the predictions of the unreducible-channel model.

The retention data of all size classes of roach (Fig. 2g,h,i) show the same pattern. The copepod data of experiment 1 (low density) agree with the URC curve (Table 2a). In experiment 2 the retention ability for copepods is worse than predicted from the URC curve. In both experiments the retention ability for *Daphnia* is much worse than according to the URC curve (Table 2a). In experiment 1 (low density) roach retained copepods better than in experiment 2 (high density). This difference is not noticeable for *Daphnia*. In all size classes of roach the retention ability was significantly higher for copepods than for *Daphnia* ($p<0.025$). Considering all retention characteristics, the data of roach corroborate most closely with the predictions of the saw-tooth model.

Figure 2 (see overleaf)

a-i) Retention percentage versus zooplankton width calculated from the zooplankton feeding experiments in darkness. The theoretical retention curves are indicated with lines, the experimental data are indicated with symbols (see legend in top left corner). The initial zooplankton density (D_0) and the filtering rate (FR) of the fish are indicated in the lower right corners of each graph.

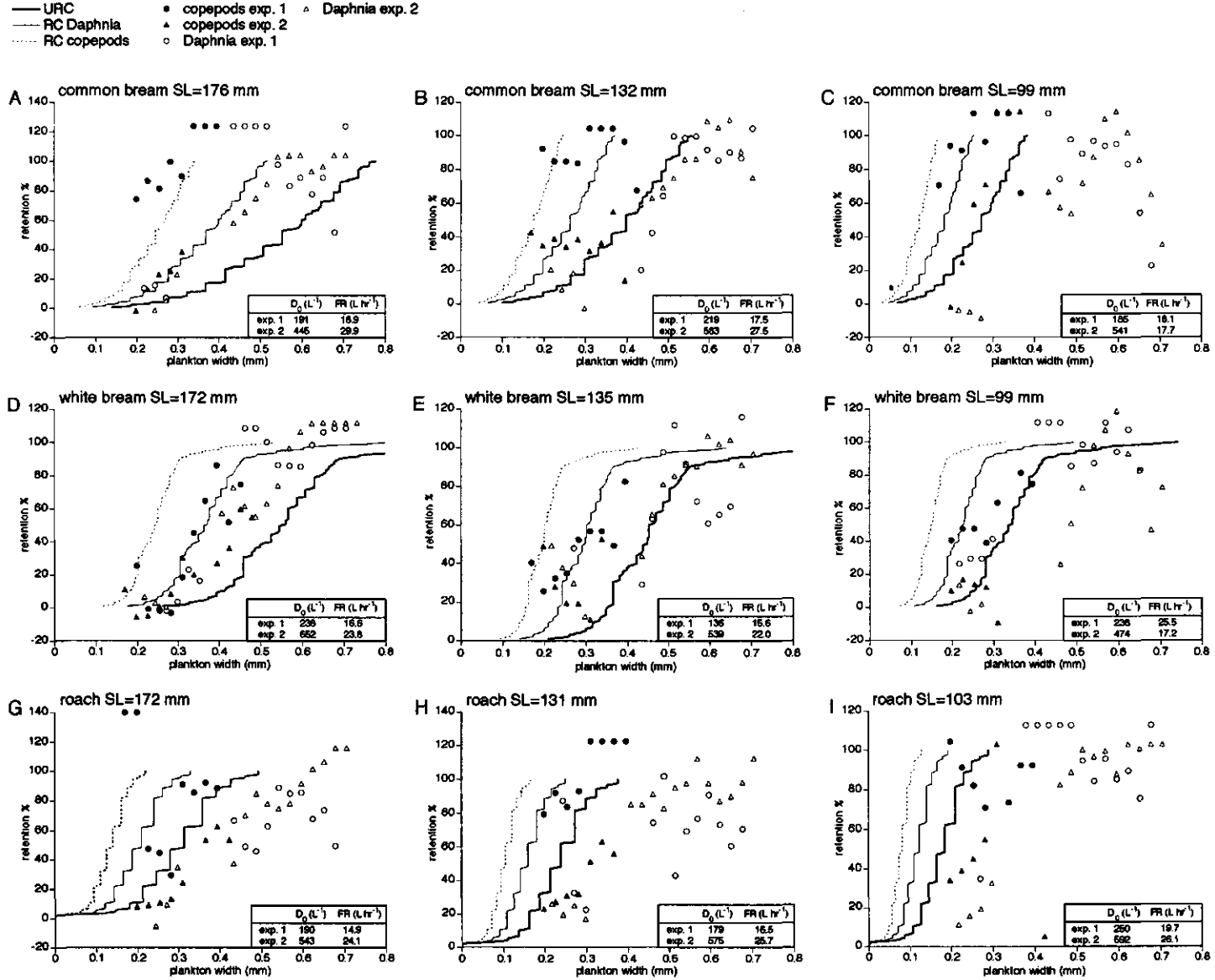
URC
RC Daphnia
RC copepods
copepods exp. 1
copepods exp. 2
Daphnia exp. 1
Daphnia exp. 2
A common bream SL=176 mm
B common bream SL=132 mm
C common bream SL=99 mm
D white bream SL=172 mm
E white bream SL=135 mm
F white bream SL=99 mm
G roach SL=172 mm
H roach SL=131 mm
I roach SL=103 mm
retention %
plankton width (mm)
D0 (L-1) FR (L hr-1)
exp. 1 191 18.9
exp. 2 445 29.9
exp. 1 219 17.5
exp. 2 563 27.5
exp. 1 185 18.1
exp. 2 541 17.7
exp. 1 236 16.6
exp. 2 652 23.6
exp. 1 136 15.6
exp. 2 539 22.0
exp. 1 236 25.5
exp. 2 474 17.2
exp. 1 190 14.9
exp. 2 543 24.1
exp. 1 179 16.5
exp. 2 575 25.7
exp. 1 250 19.7
exp. 2 592 26.1

Light experiments

The light experiments are more difficult to interpret than the dark experiments because particulate intake of zooplankton does occur, which causes errors in the calculations. The filtering rate will be overestimated because an aiming fish will process less water for one zooplankter than a random gulping filter-feeder. The retention ability will be underestimated because a particulate feeder will aim at the largest zooplankters. Differences in retention ability for copepods and *Daphnia* can have multiple causes in light. The shape of the zooplankton and of the meshes of the branchial sieve play a role (Van den Berg et al. in press), but also copepods are more conspicuous in appearance and in their movements than *Daphnia* (Wright and O'Brien 1984). By comparison with the results of the dark experiments we can determine whether the fish in a tank have switched from gulping to particulate intake of zooplankton.

In Table 2b the feeding mode during the light experiments is indicated for each experimental group of fishes. The zooplankton in light experiment 1 consisted of more than 99% copepods. In both experiments the retention data of the 176 mm common bream (Fig. 3a) agree extraordinarily well with the RC curve. The data of the 132 mm common bream (Fig. 3b) agree with the RC curve in experiment 1. The *Daphnia* retention data of experiment 2 agree with the URC curve, but the copepod retention data are intermediate between the RC and URC curves. The retention data of experiment 1 of the 99 mm common bream agree with the RC curve. In experiment 2, the retention ability of the 99 mm common bream for *Daphnia* (Fig. 3c) is much worse than according to the URC curve, which indicates particulate intake. The copepod retention data of experiment 2 are slightly to the left of the URC curve.

The retention data of the 99 mm white bream (Fig. 3d) possibly agree with the URC curve. However, the retention ability is worse than in darkness (Fig. 2f), which indicates particulate intake. The other two size classes of white bream always had a low filtering rate in the light experiments (lower than 10 L hr^{-1}). Therefore, these data are not presented. In our experimental set-up, white bream apparently prefers to feed in the dark. Video recordings of the experiments show that these fishes behaved agitated and stressed during the light experiments.

In experiment 1 (>99% copepods) the 172 mm roach seems to have retained copepods much better (Fig. 3e) than in the dark experiments (Fig. 2g). However, this graph should be considered with care, since no large particles were present and hence the calculated 100% retention level might well be wrong. The filtering rate is very high (35.4 L hr^{-1}), which can only be explained if the fish was particulate feeding. The retention data of the 131 mm and 103 mm roach (Fig. 3f,g) indicate particulate intake, since the retention ability for copepods is much worse than in the dark experiments. Each size class of roach had a filtering rate lower than 10 L hr^{-1} in one of the two experiments. Again, video recordings showed that the roach were agitated during these light experiments.

Figure 3 (see overleaf)

a-g) Retention percentage versus zooplankton width calculated from the zooplankton feeding experiments in light. The theoretical retention curves are indicated with lines, the experimental data are indicated with symbols (see legend in top left corner). The initial zooplankton density (D_0) and the filtering rate (FR) of the fish are indicated in the lower right corners of each graph.

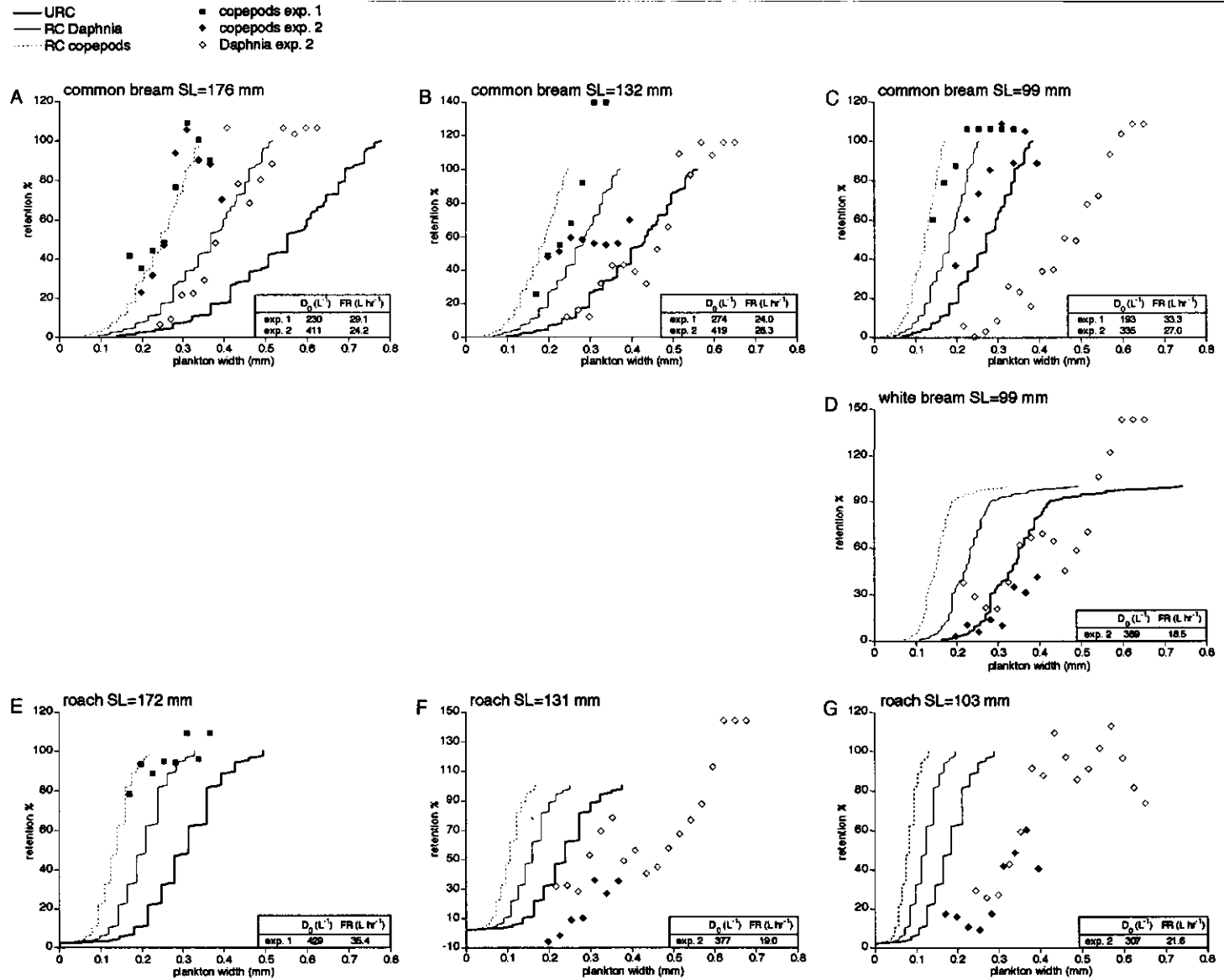
URC
RC Daphnia
RC copepods
copepods exp. 1
copepods exp. 2
Daphnia exp. 2
A common bream SL=176 mm
B common bream SL=132 mm
C common bream SL=99 mm
D white bream SL=99 mm
E roach SL=172 mm
F roach SL=131 mm
G roach SL=103 mm
retention %
plankton width (mm)
D_0 (L^{-1}) FR ($L\ hr^{-1}$)
exp. 1 230 29.1
exp. 2 411 24.2
exp. 1 274 24.0
exp. 2 419 25.3
exp. 1 193 33.3
exp. 2 335 27.0
exp. 2 389 18.5
exp. 1 429 35.4
exp. 2 377 19.0
exp. 2 307 21.6

Discussion

Using the data from the dark experiments we have concluded on a different retention model for each of the three species. These models are compared with the morphology of the branchial sieve of each species. The significance of a retention mechanism with two mesh sizes is discussed. The choice between two feeding modes is discussed briefly and some comments are made on the natural light conditions in eutrophic lakes. In the final part of this discussion the retention models are used to quantify the role of the retention ability in interspecific competition for zooplankton.

Retention models and the morphology of the branchial sieve

In the dark experiments all experimental fishes were feeding on zooplankton. White bream and roach even had a higher average filtering rate in the dark experiments than in the light experiments. Therefore, in the range between 10 and 17.5 cm SL, all three species are able to filter-feed. We have seen that the retention data of common bream corroborate with the predictions of the reducible-channel model, whereas those of white bream agree with the predictions of the unreducible-channel model. The retention data of roach do not corroborate with the channel model at all; the saw-tooth model seems more appropriate. Unfortunately, the theoretical retention curves for the saw-tooth model are unknown because the maximal distance between the gill arches of roach during filter-feeding is unknown. In general, it can be concluded that the saw-tooth model results in a retention ability in the same order of magnitude as that of the channel models.

When its channels are reduced, the retention ability of common bream is the highest of the three species, but when its channels are unreduced it is similar to that of white bream. The retention ability of roach is slightly higher than that of white bream for *Daphnia* and much higher for copepods (Fig. 2d-i, cf. Fig. 5). When copepods are dominant prey items roach will tend to be at an advantage compared to white bream.

Interspecific differences in morphology of the branchial sieve support the above conclusions about the retention models for each species. *M. abductor branchiospinalis* (MAB) is a tiny muscle, running between the lateral gill raker feet and the *radii branchiales*. MAB can abduct the lateral rakers and is therefore essential for reducing the mesh size of the medial channels on the neighbouring gill arch (Hoogenboezem et al. 1991). MAB is present on gill arch 1 to 4 in common bream, but only on the first gill arch in white bream and roach (Van den Berg et al. subm.). Since there are no medial channels opposite the lateral side of the first gill arch, the reducible-channel model can not be applied to white bream and roach. Furthermore, the comparatively larger length and slender tip of the lateral rakers of common bream are especially suited for the reducible-channel model (Van den Berg et al. 1992). The channels of common bream are deep, curved and circular in cross section[3] (Fig. 1c). They are well suited to guide water and particles into them. The channels of white bream are deep, circular and not curved. They are, nevertheless, also suited to retain prey. The channels of roach however, are not deep, curved or circular in cross section. Considering this branchial sieve morphology, both the URC and the RC model are unlikely for roach.

[3]Among seven cyprinid species, common bream and carp (*Cyprinus carpio*) were the only species with deep, curved channels and MABs on the lateral side of gill arch 1 to 4. Both of these characteristics are adaptations to the reducible-channel model (Van den Berg et al. subm.)

Adjustment of the mesh size of the branchial sieve

The results of the dark experiments showed that common bream can adjust the mesh size of its branchial sieve. At comparatively low experimental zooplankton density (~200 L^{-1}) they mainly used reduced channels, whereas at high density (~500 L^{-1}) they mainly used unreduced channels (Fig. 2a-c, Table 2a). The same trend is found in the retention data of roach (Fig. 2g-i). Hoogenboezem et al. (1991) found that common bream fed with unreduced channels during the first hour of a filter-feeding experiment, strongly reducing the frequency of the size classes of large zooplankton, and switched to reduced channels during the second hour. Apparently, common bream switches from URC to RC below a certain threshold density of zooplankton. The present retention data suggest that this threshold is at a lower zooplankton density for small than for large common bream. Probably however, the threshold should be related to the number of retained particles per gulp (the retained zooplankton density) and not to the total zooplankton density. Since small fishes have comparatively small channels (Van den Berg et al. 1992), they can retain more size classes of zooplankton than large fishes and the retained zooplankton density will be comparatively high for them. The switching threshold might well be at the same retained zooplankton density for all size classes of common bream.

Since common bream do not always reduce their channels, the choice to feed with reduced channels is probably a cost/benefit problem. When common bream is feeding with reduced channels extra energy will be required to pump water through the reduced channels (extra cost) and the filtering rate might decrease (reduced benefit). At low 'retained zooplankton density' the benefit of extra food (energy) intake will outweigh the above disadvantages, whereas above the threshold density of zooplankton (see above) it will be more advantageous to feed with unreduced channels.

Facultative versus obligate filter-feeders

The question arises as to why common bream has such an elaborate sieving mechanism and not a fine comb like many clupeid and coregonid filter-feeders. An important clue is that common bream are not pelagic, obligate filter-feeders (like most clupeid and coregonid filter-feeders), but demersal, opportunistic feeders (like most cyprinids), who versatilely combine fast suction, filter-feeding and sieving of chironomid larvae from the substrate (cf. Sibbing 1991). If the sieve is too fine, separating food from substrate becomes difficult (Janssen 1978). The reducible-channel mechanism is probably a compromise between conflicting ecological demands. Feeding with unreduced channels allows fast suction during particulate feeding on larger prey and separation of chironomid larvae from coarse substrate. Whereas, feeding with reduced channels, common bream greatly improve their retention ability for smaller prey.

Particulate intake versus gulping

The light experiments provide the opportunity to study the choice between alternative feeding modes: particulate feeding and gulping. A model for the relation between the size of common bream, the density of zooplankton and the feeding mode was presented by Hoogenboezem et al. (1992). In this model common bream is expected to use gulping if a random gulp contains on average one prey item or more. The number of prey in a random gulp is proportional to the product of zooplankton density and the mouth volume of the fish. The threshold density above which common bream is expected to use gulping will be higher for small fishes than for large ones because small fishes have a comparatively small mouth volume. In other words, at a certain zooplank-

ton density there will be a threshold fish size above which common bream is expected to use gulping rather than particulate feeding.

In the light experiments common bream preferred gulping. Only the smallest size class of common bream used particulate intake in one experiment (Table 2b). This is in agreement with the prediction from Hoogenboezems model that small fishes are more likely to use particulate feeding. It does not agree with the more specific prediction in Hoogenboezem et al. (1992) that fishes smaller than 15 cm SL are expected to use gulping below densities of 500 L^{-1}. Common bream seems to switch to gulping even when a random gulp contains on average less than one prey item. This might be related to the higher cost of an aimed snap (particulate feeding) than of a gulp.

In the light experiments, roach always used particulate feeding, irrespective of their size (Table 2b). The infra-red video recordings showed that roach switch to directed snaps as soon as the light is turned on. There are insufficient data of white bream to be able to make any statements about switching of feeding mode.

Natural light conditions

The previous paragraph showed that feeding behaviour and zooplankton retention are strongly dependent on the light conditions. Therefore, it is important to know whether the light conditions for fish in a eutrophic lake are comparable to the dark or to the light experiments. Many factors play a role: turbidity and light level in the water at various depths; size, transparency and behaviour of zooplankton; visual threshold and reaction distance of the fish. Confer et al. (1978) give a review on this subject. Small common bream has a visual threshold of 1.25 lux (Townsend and Risebrow 1982). Vinyard and O'Brien (1976) found 5 cm as the reaction distance of bluegill (*Lepomis macrochirus*) at high turbidity (30 Jackson Turbidity Units). At high turbidity, the reaction distance in their experiments was hardly dependent on prey size. There may be no visual prey selection by the fish at high turbidity, since only one prey may be visible at a time (Confer et al. 1978). Like other eutrophic lakes, Tjeukemeer is turbid; it has a Secchi disc depth of about 25 to 40 cm. Algae and suspended bottom material cause this turbidity. Bottom material is whirled up by the wind and by common bream, digging for chironomid larvae. The above literature data all use different units for which no conversion factors are given, hence no coherent picture of the light conditions can be distilled. A preliminary conclusion is that the light conditions for fish in eutrophic, turbid lakes are probably more comparable with the dark experiments than with the light experiments. The fish are therefore expected to use gulping rather than particulate feeding.

Retained zooplankton energy and interspecific competition

When competition for zooplankton is high, the proportion of small zooplankters will increase, because fishes are positively size selective (Vijverberg and Richter 1982a, b). A high retention ability will be important for the competing fish species. In order to quantify the profitability of filter-feeding and the role of the retention ability in competition, we must think in terms of energy. Which fraction of the available zooplankton energy can be utilized given a certain retention ability?

The relation between energy content and zooplankton length was determined for *Daphnia hyalina*, cycloid copepods, *Bosmina coregoni* and *Chydorus sphaericus* by Vijverberg and Frank (1976), using the population from Tjeukemeer. With these energy relations and the zooplankton data from Tjeukemeer in 1987, we calculated the zooplankton energy content per litre Tjeukemeer water, considering the above zooplankton species (Fig. 4). On average, *Daphnia* and copepods represent hardly 50% of the total energy. The small zooplankters of the genera *Bosmina* and *Chydorus* also represent

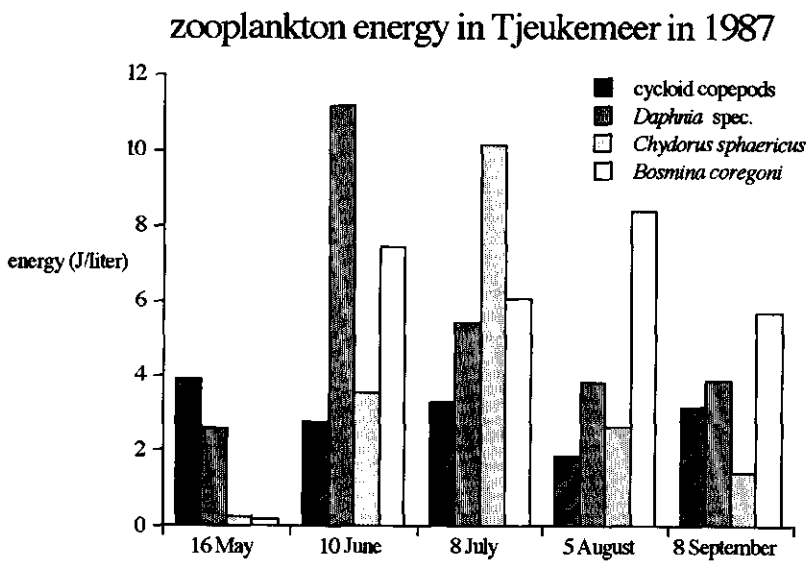

Figure 4

The contributions of four zooplankton species (categories) to the zooplankton energy content of Tjeukemeer at five sample dates in 1987. The distribution over the four categories and the total energy content per litre are strongly dependent on the sample date. *Chydorus sphaericus* and *Bosmina coregoni* are comparatively small zooplankton species. Nevertheless, on 8 July and 5 August they form the majority of the total energy content of the lake. Therefore, it is highly profitable for filter-feeding fish to be able to retain these small organisms.

50%. Unfortunately, there were very few *Bosmina* and *Chydorus* in our experiments. We could therefore not determine the retention characteristics of these prey species. They will only be discussed qualitatively.

We used the appropriate retention models to describe the retention ability of each species. The retention curves were scaled to different fish lengths using the equations in Van den Berg et al. (1992). For common bream we used the reduced channel curve and for white bream the unreduced channel curve. Even though the channel model does not apply to roach, it can be used to describe the retention ability of roach. We estimated (from Fig. 2g-i) that the retention ability of roach can be described with 1.5 times CW for *Daphnia* and CW for copepods. The retained energy of each size class of zooplankton was calculated as retention percentage times zooplankton density times energy content of that size class. The total retained energy is the sum of the retained energy of all size classes of zooplankton. This total retained energy divided by the total available zooplankton energy is the retained energy percentage (REP).

Not unexpectedly, the relation between fish length and REP turns out to be an S-shaped curve (Fig. 5). Up to a certain standard length (SL) a fish can retain 100% of the available zooplankton. After this point, REP decreases with increasing speed down to a percentage of about 50% and finally approaches 0% more or less asymptotically. At any SL, common bream has the highest REP. Roach has a higher REP than white bream, especially for copepods.

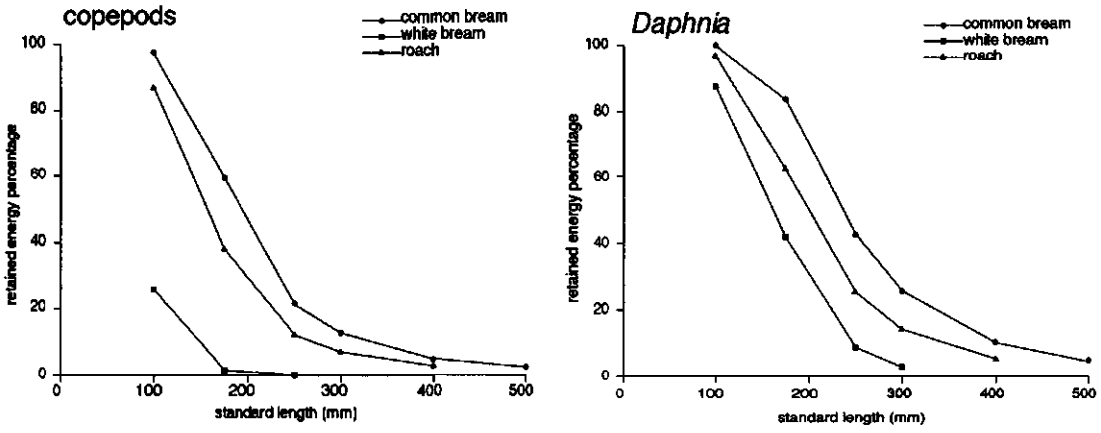

Figure 5

The retained energy percentage (REP) for copepods and *Daphnia*. REP is the retained zooplankton energy per litre divided by the total zooplankton energy per litre. REP is plotted as a function of standard length for common bream, white bream and roach, using data of the Dutch, eutrophic lake Tjeukemeer on June 10th, 1987 (cf. Figure 4).

Lammens et al. (1987) showed that common bream up to 25 cm SL still retain *Chydorus sphaericus* and common bream up to 30 cm still retain *Bosmina coregoni*, whereas these prey species are absent in gut contents of white bream and roach larger than 15 cm SL. Since these zooplankton species represent about 50% of the available zooplankton energy in Tjeukemeer (Fig. 4), the REP differences between common bream, white bream and roach will be larger than shown in Figure 5.

Regarding its ability to retain the available zooplankton energy, common bream is at an advantage in the whole range of size classes from 10 cm SL up to 50 cm SL (Fig. 5). This means that the total population of common bream has an advantage over white bream and roach in its access to zooplankton. This advantage of the common bream population is probably an important factor in explaining its dominance in eutrophic lakes, where zooplankton is an important food resource.

Obviously, zooplankton is not the only food resource in eutrophic lakes. Chironomid larvae are important as well, and to a lesser extent freshwater mussel (*Dreissena polymorpha*). Common bream is less efficient than white bream and roach in feeding on *D. polymorpha* (Nagelkerke et al. 1991), but it is more efficient in digging up chironomid larvae and in separating them from the substrate, than white bream and roach (Lammens et al. 1987). Apparently, the branchial sieve of common bream is adapted to exploit both zooplankton and chironomid larvae efficiently. As discussed earlier, the reducible-channel model is an effective mechanism to exploit both these food resources.

The mechanisms for retention of zooplankton in cyprinids cannot be described with one model. Three different retention models were needed to explain the retention data of the three species under study. This variety of retention mechanisms might be the reflection of differences in ecomorphological demands, which in turn originate in the opportunistic life style of cyprinid fishes (cf. Sibbing 1991). However, the variety of

mechanisms may also represent alternative solutions for the same problem, as a result of differences in the phylogenetic history of these species. Whatever the reason for the variety of mechanisms, during the process of eutrophication the reducible-channel mechanism may well have given common bream a crucial advantage over cyprinid species that use other retention mechanisms. This advantage may have led to the dominance of common bream in eutrophic lakes.

Acknowledgements

Peter McGillavry patiently measured and counted the majority of zooplankton samples. The experiments were carried out in the former field laboratory of the Limnological Institute in Oosterzee, the Netherlands. The Limnological Institute provided the live zooplankton and the zooplankton data of Tjeukemeer from 1987. The RIN in Arnhem lent us the infra-red video camera and lamp. A.P.T. Vervuurt and M.A.J. van Montfort solved the statistical problems, the former wrote the FORTRAN maximum likelihood program. This research was supported by the Foundation for Fundamental Biological Research (BION), which is subsidized by the Netherlands Organization for Scientific Research (NWO), project number 811-428-265.

References cited

Boersma, M., W.L.T. van Densen and J. Vijverberg. 1991. The effect of predation by smelt (*Osmerus eperlanus*) on *Daphnia hyalina* in a shallow eutrophic lake. Verh. Internat. Verein. Limnol. 24: 2438-2442.

Boyd, C.M. 1976. Selection of particle sizes by filter-feeding copepods: A plea for reason. Limnol. Oceanogr. 21: 175-180.

Confer, J.L., G.L. Howick, M.H. Corzette, S.L. Kramer, S. Fitzgibbon and R. Landesberg. 1978. Visual predation by planktivores. Oikos 31: 27-37.

De Nie, H.W. 1987. The decrease in aquatic vegetation in Europe and its consequences for fish populations. EIFAC/CECPI Occasional paper 19: 1-52.

De Nie, H.W., H.J. Bromley and J. Vijverberg. 1980. Distribution patterns of zooplankton in Tjeukemeer, the Netherlands. J. Plankton Res. 2: 317-334.

Drenner, R.W., J.R. Mummert, F.Jr. de Noyelles and D. Kettles. 1984. Selective particle ingestion by a filter-feeding fish and its impact on phytoplankton community structure. Limnol. Oceanogr. 29(5): 941-948.

Gibson, R.N. 1988. Development, morphometry and particle retention capability of the gill rakers in the herring, *Clupea harengus* L.. J. Fish Biol. 32: 949-962.

Hoogenboezem, W., J.G.M. van den Boogaart, F.A. Sibbing, E.H.R.R. Lammens, A. Terlouw and J.W.M. Osse. 1991. A new model of particle retention and branchial sieve adjustment in filter-feeding bream (*Abramis brama* (L.), Cyprinidae). Can. J. Fish. Aquat. Sci. 48: 7-18.

Hoogenboezem, W., E.H.R.R. Lammens, Y. van Vugt and J.W.M. Osse. 1992. A model for switching between particulate-feeding and filter-feeding in the common bream *Abramis brama*. Env. Biol. Fish. 33: 13-21.

Hoogenboezem, W., E.H.R.R. Lammens, P.J. McGillavry and F.A. Sibbing. in press. Prey-size selectivity and sieve adjustment in filter-feeding bream (*Abramis brama* (L.), Cyprinidae). Can. J. Fish. Aquat. Sc.

Janssen, J. 1978. Feeding-behavior repertoire of the alewife, *Alosa pseudoharengus*, and the ciscoes *Coregonus hoyi* and *C. artedii*. J. Fish Res. Bd. Canada 35: 249-253.

Kott, P. 1953. A modified whirling apparatus for subsampling of plankton. Aust. J. Mar. Freshwat. Res. 4: 387-393.

Lammens, E.H.R.R. 1985. A test of a model for planktivorous filter-feeding by bream *Abramis brama*. Env. Biol. Fish. 13: 288-296.

Lammens, E.H.R.R. 1986. Interactions between fishes and the structure of fish communities in Dutch shallow, eutrophic lakes. Ph.D. thesis. Agricultural University Wageningen.

Lammens, E.H.R.R., J. Geursen and P.J. McGillavry. 1987. Diet shifts, feeding efficiency and coexistence of bream (*Abramis brama*), roach (*Rutilus rutilus*) and white bream (*Blicca björkna*) in eutrophicated lakes. Proc. V Congr. Europ. Ichtyol., Stockholm: 153-162.

Lammens, E.H.R.R. 1989. Causes and consequences of the success of bream in Dutch eutrophic lakes. Hydrobiol. Bull. 23: 11-18.

Lammens, E.H.R.R. and W. Hoogenboezem. 1991. Diets and feeding behaviour. p 353-376 *in* I.J.Winfield and J.S.Nelson [ed.] Cyprinid fishes; systematics, biology and exploitation. Chapman and Hall, London.

Nagelkerke, L.A.J., F.A. Sibbing and C. van den Berg. 1991. Efficiency of molluscivory in bream, white bream and roach. Abstracts of the seventh International Ichthyology Congress of the European Ichthyological Union. Bulletin Zoologisch museum. ISSN 0165-9464.

Scales, L.E. 1985. Introduction to non-linear optimization. MacMillan Publishers Ltd.

Sibbing, F.A. and R. Uribe. 1985. Regional specializations in the oropharyngeal wall and food processing in the carp (*Cyprinus carpio* L.). Neth. J. Zool. 35(2): 377-422.

Sibbing, F.A., J.W.M. Osse and A. Terlouw. 1986. Food handling in the carp (*Cyprinus carpio*): its movement patterns, mechanisms and limitations. J. Zool. Lond. (A)210: 161-203.

Sibbing, F.A. 1991. Food capture and oral processing. p 377-412 *in* I.J. Winfield and J. Nelson [ed.] Cyprinid fishes; systematics, biology and exploitation. Chapman and Hall, London.

Townsend, C.R. and A.J. Risebrow. 1982. The influence of light level on the functional response of a zooplanktivorous fish. Oecologia (Berl) 53: 293-295.

Van den Berg, C., F.A. Sibbing, J.W.M. Osse and W. Hoogenboezem. 1992. Structure, development and function of the branchial sieve of common bream, *Abramis brama*, white bream, *Blicca bjoerkna*, and roach, *Rutilus rutilus*. Env. Biol. Fish. 33: 105-124.

Van den Berg, C., J.G.M. van den Boogaart, F.A. Sibbing, E.H.R.R. Lammens and J.W.M. Osse. in press. Shape of zooplankton and retention in filter-feeding. A quantitative comparison between industrial sieves and the branchial sieves of common bream (*Abramis brama*) and white bream (*Blicca bjoerkna*). Can. J. Fish. Aquat. Sci.

Van den Berg, C., G. van Snik, F.A. Sibbing, J.W.M. Osse. subm. Comparative micro anatomy of the branchial sieve of common bream (*Abramis brama*), white bream (*Blicca bjoerkna*) and roach (*Rutilus rutilus*), and its implications for the reducible-channel model of filter-feeding. J. Morph.

Vijverberg, J. and T.H. Frank. 1976. The chemical composition and energy contents of copepods and cladocerans in relation to their size. Freshwater Biology 6: 333-345.

Vijverberg, J. and A.F. Richter. 1982a. Population dynamics and production of *Daphnia hyalina* (Leydig) and *Daphnia cucullata* (Sars) in Tjeukemeer. Hydrobiologia 95: 235-259.

Vijverberg, J. and A.F. Richter. 1982b. Population dynamics and production of *Acanthocyclops robustus* (Sars) and *Mesocyclops leuckarti* (Claus) in Tjeukemeer. Hydrobiologia 95: 261-274.

Vinyard, G.L. and W.J. O'Brien. 1976. Effects of light and turbidity on the reactive distance of bluegill (*Lepomis macrochirus*). J. Fish. Res. Board Can. 33: 2845-2849.

Winberg, C.G. 1960. Rate of metabolism and food requirement of fishes. Fisheries Research Board Translation Services 194.

Wright, D.I., W.J. O'Brien and C. Luecke. 1983. A new estimate of zooplankton retention by gill rakers and its ecological significance. Trans. Amer. Fish. Soc. 112: 638-646.

Wright, D.I. and W.J. O'Brien. 1984. The development and field test of a tactical model of the planktivorous feeding of white crappie (*Pomoxis annularis*). Ecological Monographs 54(1): 65-98.

Appendix

The Maximum Likelihood Method

N_x is the number of zooplankton particles in size class x at the beginning of the experiment, n_x is the number at the end of the experiment. It is assumed that sample n_x has a Poisson distribution:

$$P(n_x = n_x) = \frac{e^{-\lambda}\lambda^{n_x}}{n_x!} \tag{3}$$

where λ is the expected value of n_x as a function of N_x and x. The zooplankton retention is described with two parameters. The number of zooplankton is constant up to plankton width μ, above μ the number of zooplankton decreases exponentially as a function of plankton width. The rate of decrease is expressed as parameter α. λ equals:

$$\lambda = \begin{cases} f*N_x & ,x \le \mu \\ f*N_x e^{-\alpha(x-\mu)} & ,x > \mu \end{cases} \tag{4}$$

where: f = factor compensating for sample volume and measured fractions of zooplankton

Parameters μ and α are estimated using the maximum likelihood method (Scales 1985). This method looks for a combination of μ and α that maximizes the total likelihood (L) of the experimental realization of n_x of all zooplankton size classes. The method starts at some reasonable values of μ and α and then searches with small steps for the direction in which L increases, until a maximum is found. The function to be maximized is:

$$L^*(\alpha,\mu) = \prod_{x\le\mu} \frac{e^{-fN_x(i)}(fN_x(i))^{n_x(i)}}{n_x(i)!} * \prod_{x>\mu} \frac{e^{-fN_x(i)*e^{-\alpha(x(i)-\mu)}}\{fN_x(i)e^{-\alpha(x(i)-\mu)}\}^{n_x(i)}}{n_x(i)!} \tag{5}$$

By taking the logarithm of L one obtains:

$$L = \ln(L^*) = \sum_{x\le\mu} \ln\left[\frac{e^{-fN_x(i)}fN_x(i)^{n_x(i)}}{n_x(i)!}\right] + \sum_{x>\mu} \ln\left[\frac{e^{-fN_x(i)e^{-\alpha(x(i)-\mu)}} * (fN_x(i)*e^{-\alpha(x(i)-\mu)})^{n_x(i)}}{n_x(i)!}\right]$$

$$= \sum_{x\le\mu} [-fN_x(i) + n_x(i)\ln(fN_x(i)) - \ln(n_x(i)!)] +$$
$$\sum_{x>\mu} [-fN_x(i)e^{-\alpha(x(i)-\mu)} + n_x(i)\ln(fN_x(i)) - n_x(i)\alpha(x(i)-\mu) - \ln(n_x(i)!)] \tag{6}$$

The maximization of this function with respect to μ and α was done with a FORTRAN program (using the DBCONF-routine of the IMSL MATH-LIBRARY).

We want to test whether the retention data are in agreement with the theoretical retention curves. In order to do that, we must simplify the theoretical retention curves to theoretical values of μ and α. Formula 2 (see Materials and Methods) can be rewritten to:

$$R = C_1 \cdot \ln(f \cdot N_x / n_x)$$

where,

$C_1 = V/(FR \cdot t)$

Formula 4 can now be transformed to retention percentage:

$R = 0$ for $x < \mu$
$R = \alpha \cdot C_1 \cdot (x - \mu)$ for $x \geq \mu$

In the retention graphs, μ is the intercept with the plankton width axis and $\alpha \cdot C_1$ is the slope of the curve. The theoretical values of α and μ were estimated with linear regression of the cumulative frequency of the channel width.

The likelihood (L) is calculated with the theoretical values of α and μ and compared with the maximum likelihood (L_{max}). The value of $2(L_{max}-L)$ has a χ^2-distribution. The difference between the theoretical and maximal values of α and μ is significant ($p=0.05$) when this value exceeds 5.99.

Chapter 4

Comparative micro anatomy of the branchial sieve of three sympatric cyprinid species in relation to filter-feeding mechanisms.

Coen van den Berg, Geert J.M. van Snik, Jos G.M. van den Boogaart, Ferdinand A. Sibbing and Jan W.M. Osse
subm. J. Morphology

Abstract

In the reducible-channel model of filter-feeding (Hoogenboezem et al., '91), the mesh size of the branchial sieve can be reduced by lowering the lateral gill rakers into the channels between the medial rakers. This movement requires that all lateral gill rakers have a *m. abductor branchiospinalis* (MAB). MAB runs from the *radii branchiales* to the raker feet. It is present on the lateral side of all four gill arches of common bream and carp, but only on the first arch of white bream, roach, grass carp, asp and rudd. Therefore, the latter species do not fulfil the structural requirement for the reducible-channel model, whereas common bream and carp do. Laboratory and field data confirm that common bream and carp can reduce their mesh size according to this model and are the better filter-feeders. The seven cyprinid species studied show the same principal micro anatomy of their branchial sieve. *M. abductor filamenti* is a sheet of muscle fibres between the lateral *radii branchiales* and the ceratobranchial bone. *M. branchialis superficialis* is a specialized region of the subepithelial muscle fibre network, with origos along both sides of the ceratobranchial bone. In most cyprinids, the lateral gill rakers of the first gill arch differ conspicuously from all other rakers. They are longer, flattened and they point anteriorly. They probably form a sieve across the wide slit between the first gill arch and the operculum. The most revealing anatomical feature is the presence of MABs on gill arches 1 to 4. It is a suitable bio-assay for identifying the better facultative filter-feeders.

Introduction

Eutrophication has profound effects on freshwater ecosystems. In Tjeukemeer, a well studied eutrophic lake in the Netherlands, some of the most important changes have been an increase in number of blue-green and green algae and of zooplankton, reduced visibility, disappearance of macrophytes and shifts in the composition of the fish fauna (Lammens, '89; de Nie, '87). Common bream (*Abramis brama*) have become very dominant, whereas other cyprinid species are strongly reduced in number. Common bream up to 25 cm SL still retain small zooplankton, whereas white bream (*Blicca bjoerkna*) and roach (*Rutilus rutilus*) larger than 15 cm SL do not (Lammens et al., '87). This helps to explain the dominance of common bream in eutrophic water, where zooplankton is a major food resource. We aim to gain more insight into the filter-feeding mechanisms employed by cyprinids by studying the micro anatomy and function of the branchial sieve of common bream and two sympatric cyprinid species, white bream and roach.

A frequently used model of filter-feeding is the comb model, where the inter-raker distance is assumed to be the mesh size of the branchial sieve. Considering the morphology of their branchial sieve, the comb model seems appropriate for clupeid and coregonid filter-feeders (e.g. Drenner et al., '84). However, the results of experiments with filter-feeding common bream cannot be explained with the comb model. Hoogenboezem et al. ('91; in press a) showed that common bream can retain particles that are much smaller than its inter raker distance and also, that the mesh size of its sieve is adjustable.

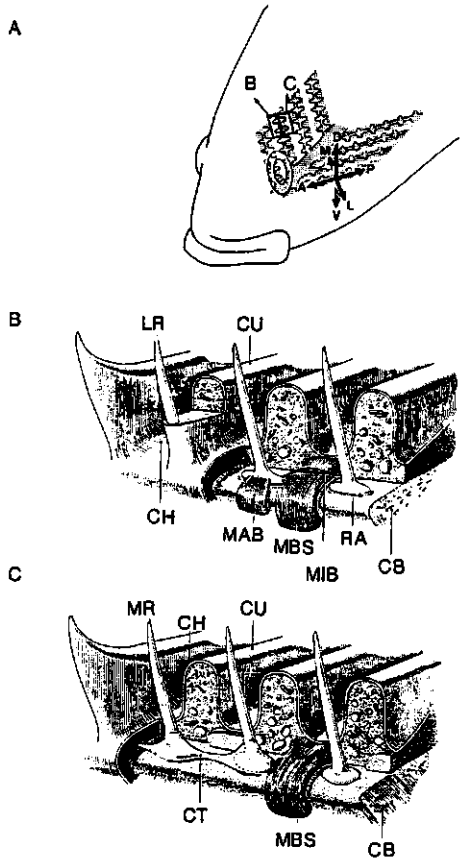

Figure 1

A) the position of the branchial sieve in the fish head and the orientation terms for the gill arches. The position of Figure B and C in the branchial sieve is indicated, as well.
a/p, anterior/posterior; d/v, dorsal/ventral; l/m, lateral/medial.
B) the lateral side of the gill arch according to Hoogenboezem et al. ('91).
C) the medial side of the gill arch according to Hoogenboezem et al. ('91).
M. constrictor canalis interbranchiospinalis was renamed as *m. branchialis superficialis*. Figure adapted from Hoogenboezem et al. ('91).
CB, ceratobranchial bone; CH, channel; CT, compact connective tissue; CU, raker cushion; LR, lateral gill raker; MAB, *m. abductor branchiospinalis*; MBS, *m. branchialis superficialis* (was *m. constrictor canalis interbranchiospinalis*); MIB, *m. interbranchiospinalis*; MR, medial gill raker; RA, raker articulation.

In cyprinids a cushion is attached to each gill raker. The depressions between these cushions are called channels (Fig. 1). In the reducible-channel model of filter-feeding, particles are retained in the medial channels (Hoogenboezem et al., '91). The channel width is the mesh size of the branchial sieve. By abducting the lateral gill rakers of the next gill arch into the medial channels, the mesh size can be reduced. The fish can thus adjust the mesh size of its sieve to the size and density of the available zooplankton (Hoogenboezem et al. in press a). In order to reduce the medial channels, the lateral gill rakers must have abductor muscles. Hoogenboezem et al. ('91) found that the lateral gill rakers of each gill arch of common bream have abductor muscles, whereas the medial gill rakers do not, which is a strong support for the reducible-channel model. The model was further supported for common bream with X-ray analysis of the movements of the gill arches and with aquarium experiments (Hoogenboezem et al., '90; in press a).

The micro anatomy of the branchial sieve clearly provides important information to validate the reducible-channel model. We studied the micro anatomy of the branchial sieve of common bream, white bream and roach, mainly to discover whether white bream and roach can reduce their channels, just like common bream. Ultimately, we want to explain why the filter-feeding performance of common bream is better than that of white bream and roach (Lammens et al., '87) and why common bream is dominant in eutrophic lakes.

State of the art

Hoogenboezem et al. ('91) were the first to give a detailed description of the micro anatomy of the gill arches of common bream. This paragraph is a summary of the results of these authors (Fig. 1). The feet of the lateral gill rakers are spindle-shaped and are thus suited for articulation during gill raker abduction. The feet of the medial gill rakers are

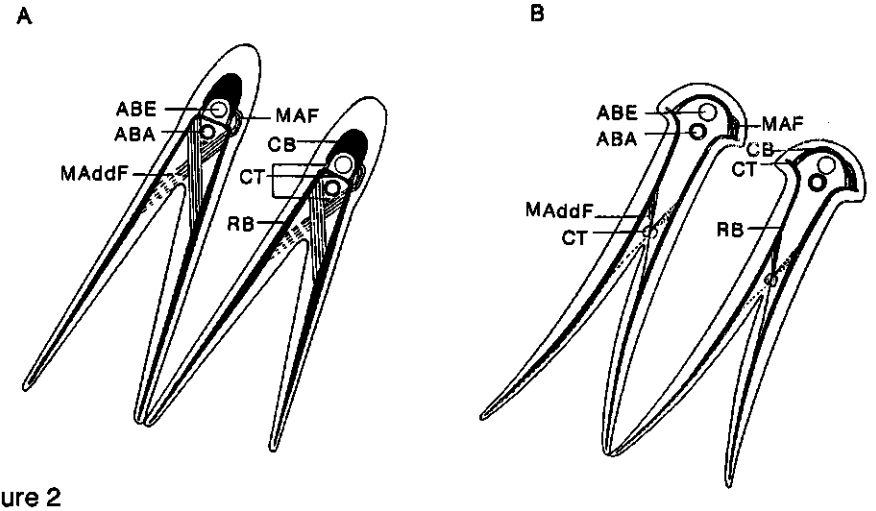

Figure 2

Gill ray musculature in gill arches of the *Perca* type (A) and the *Salmo* type (B). Cyprinids belong to the *Salmo* type. N.B.: these schemes do not show the real proportions; gill rakers are not indicated. Figure adapted from Bijtel ('49).

ABA, *arteria branchialis afferens*; ABE, *a. branchialis efferens*; CB, ceratobranchial bone; CT, compact connective tissue; MAddF, *m. adductor filamenti*; MAF, *m. abductor filamenti*; RB, *radius branchialis*, gill ray.

broadened, flat and imbedded in a continuous connective tissue sheet, which impedes raker movement. *M. abductores branchiospinales* (MABs) are only present on the lateral side of the gill arches. They insert on the feet of the lateral gill rakers. The function of MAB is to abduct the lateral gill raker. Hoogenboezem et al. consider it to be identical to *m. abductor filamenti* (MAF) as described by Bijtel ('49). *M. interbranchiospinalis* is only present on the lateral side of the gill arches. It is a tiny muscle, which runs between adjacent lateral gill raker feet, attaching at slightly different levels on each foot. This muscle may well be able to position the abducted lateral gill raker tips exactly in the centre of the opposite medial channels. *M. constrictor canalis interbranchiospinalis* is present on both the lateral and the medial side of the gill arches. The muscle runs under the floor of each channel and radiates into the gill raker cushions on either side of the channel.

Bijtel ('49) distinguished two types of organization of the muscular system of the teleost gill, the *Perca* type and the *Salmo* type (Fig. 2). The hemibranchs of the *Perca* type are separate and *m. adductor filamenti*, which runs cross wise between the lateral and medial gill rays (*radii branchiales*), is situated near the base of the hemibranchs. Only the top parts of the hemibranchs of the *Salmo* type are separate and *m. adductor filamenti* is situated near this separation point. In both types *m. abductor filamenti* is present at the lateral side of the gill arch only. *M. abductor filamenti* runs between the feet of the lateral gill rays and the lateral gill rakers in perch (*Perca fluviatilis*) (Dunel-Erb and Bailly, '87). This is far less common for the *Salmo* type, to which cyprinids belong: "...muscle fibres now and then originate from these [the lateral gill rakers]..." (Bijtel, '49); the fibres usually originate from the ceratobranchial bone.

Materials and methods

Common bream, white bream and roach were trawled in September 1990 in the Dutch lake Beulaker Wijde and stored in 7% formol. From each of these species, one specimen of 14.9 cm standard length (SL) was selected. The branchial baskets of these specimens were fixed in Bouin's fixative for 6 days, decalcified in a 50/50 mixture of 99% formic acid and 70% ethanol, dehydrated and embedded in paraffin. The embedded branchial baskets were then cut in half through the *copula communis*. One half of each branchial basket was cut into approximately 300 serial sections (5 μm), perpendicular to the ceratobranchial bones. The first and second of every five sections were Crossmon stained (Romeis, '68). The first series was used for three-dimensional computer reconstruction. Hence, the distance between sections in each reconstruction is 25 μm. The second series was only used if the neighbouring section in the first series was damaged or lost. For comparison, we also made series of longitudinal sections which were not reconstructed.

The gill rakers in the middle of the second gill arch were selected for reconstruction since they are representative for most of the branchial sieve. The other gill rakers and arches were examined as well, but not reconstructed. Important spatial differences will be treated in the results. Each section was projected on a data tablet (Calcomp 9100) using a projection microscope. Deformation due to projection was maximally 1.5%. The relevant contours were digitized with AnyTablet 3.4 on a Macintosh IIfx computer (Fig. 3). Three-dimensional reconstructions were made with the program MacReco 3.4.

Whole mount bone and cartilage stained branchial sieves were made of a common bream of 25 cm SL and a white bream and a roach of 22 cm SL, using the method of Simons and Van Horn ('71). The micro anatomy of the branchial sieve of grass carp

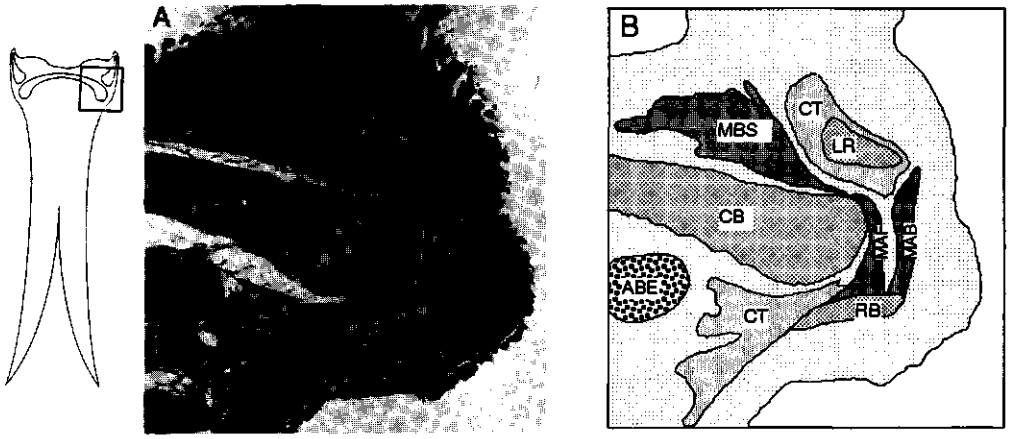

Figure 3

A) Lateral part of a Crossmon stained cross section of the second gill arch of common bream (SL 14.9 cm). The MAB fibres can be followed from the fork of a gill ray to the foot of a lateral gill raker. MBS is thin and tendinous directly under the raker. The inset shows the position of this photo in a cross section of a gill arch.

B) Digitized version of photo A).

ABE, branch of *arteria branchialis efferens*; CB, ceratobranchial bone; CT, compact connective tissue; LR, lateral gill raker foot; MAB, *m. abductor branchiospinalis*; MAF, *m. abductor filamenti*; MBS, *m. branchialis superficialis*; RB, *radius branchialis*, gill ray.

(*Ctenopharyngodon idella*), asp (*Aspius aspius*), rudd (*Scardinius erythrophthalmus*) and carp (*Cyprinus carpio*) was studied with Crossmon stained, transverse, serial sections of their heads.

Results

The anatomical features shared by common bream, white bream and roach are described first, followed by interspecific differences and a survey of four other cyprinid species.

Generalized micro anatomy

Bones

The full shape of the bony elements was studied in whole mount alizarine stained branchial sieves (Figs. 6-9). The ceratobranchial bone in cross section is arched and has thickened rims (Figs. 4, 5). The gill rakers consist of a conical needle and a broad foot. The gill rays, which support the gill filaments on the lateral and medial side of the gill

arch, are flattened in the direction of the gill filaments. They curve outwards near the ceratobranchial bone and end in a forked foot. The forked feet are joined by a syndesmosis (cf. Bijtel '49). There are about three gill rays per gill raker in each species.

Muscles

The muscles of the branchial sieve described below are all striated. Contrary to Hoogenboezem et al. ('91), we found that *m. abductor filamenti* (MAF) and *m. abductor branchiospinalis* (MAB) are two individual muscles (Figs. 3-5). If present, these muscles are only found at the lateral side of the gill arch. MAF is a sheet of muscle fibres which inserts on the forked feet of the lateral gill rays. The sheet runs over the lateral edge of the ceratobranchial bone and has its origo latero-dorsally on the ceratobranchial bone. The origo is a continuous line along the ceratobranchial bone. If MABs are present on the gill arch, the MAF muscle sheet is interrupted by MAB at every gill raker. The origo of the MABs is on the feet of the lateral gill rays. The fibres of MAB and MAF are not clearly separated at their attachment to the gill ray feet (Fig. 3). The insertion of MAB is on the lateral side of the feet of the lateral gill rakers.

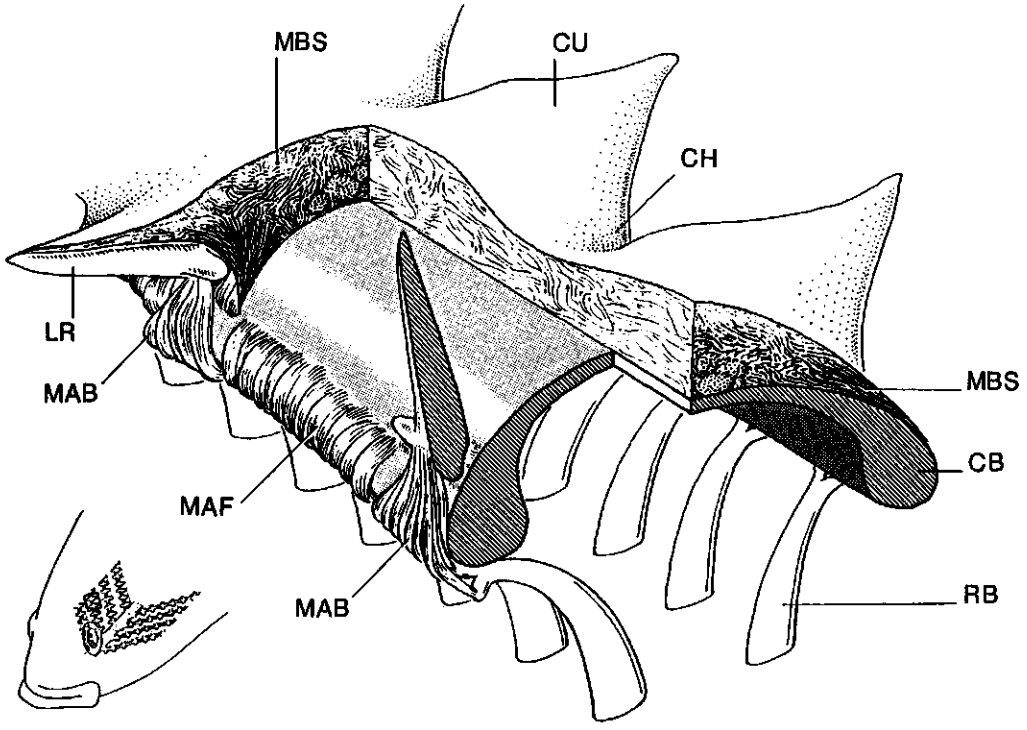

Figure 4

Lateral view of a part of a typical cyprinid gill arch with MABs. The inset shows the position of this scheme in the branchial sieve.

CB, ceratobranchial bone; CH, channel; CU, raker cushion; LR, lateral gill raker; MAB, *m. abductor branchiospinalis*; MAF, *m. abductor filamenti*; MBS, *m. branchialis superficialis*; RB, *radius branchialis*, gill ray.

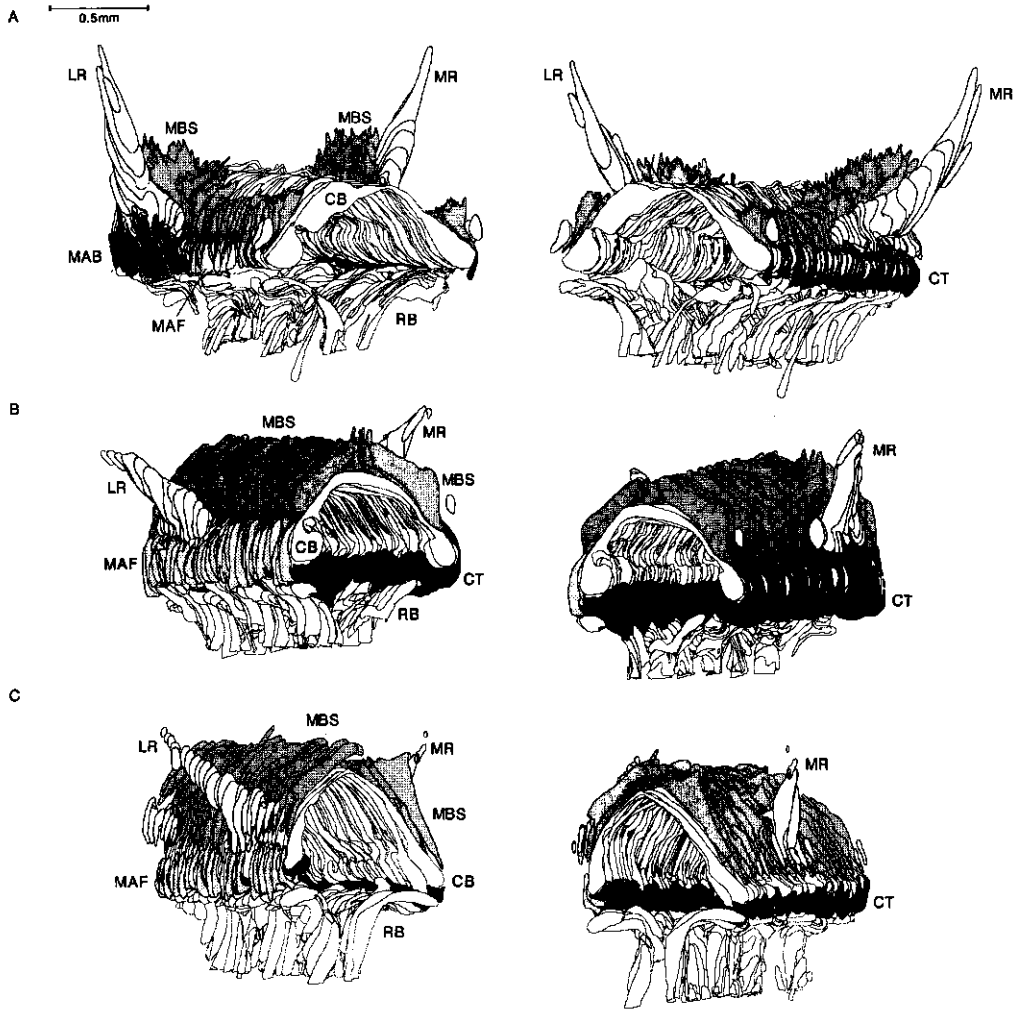

Figure 5

Three-dimensional computer reconstructions of a part of the second gill arch of common bream (A), white bream (B) and roach (C) (each with SL 14.9 cm). The pictures on the left show the lateral side of the gill arch, those on the right the medial side. The distance between the sections is 25 μm.
CB, ceratobranchial bone; CT, compact connective tissue; LR, lateral gill raker; MAB, *m. abductor branchiospinalis*; MAF, *m. abductor filamenti*; MBS, *m. branchialis superficialis*; MR, medial gill raker; RB, *radius branchialis*, gill ray.

We renamed *m. constrictor canalis interbranchiospinalis* as *m. branchialis superficialis* (MBS). The old name suggests a function which has not yet been confirmed by observations. Therefore, a topographical name is preferable. Fibres of MBS traverse the entire subepithelial space on the dorsal side of the ceratobranchial bone. The muscle is continuous with the postlingual organ (Sibbing and Uribe, '85) on one side and with *m. adductor arcus branchialis* (Vetter, 1878), between the cerato- and epibranchial bones, on the other side. MBS seems to be a local specialization of the subepithelial muscle fibre network (similar to the postlingual organ and the palatal organ), rather than a distinct muscle (cf. Sibbing and Uribe, '85). Nevertheless, it has two clear origo lines, on the latero- and medio-dorsal side of the ceratobranchial bone. From these origo lines compact bundles of muscle fibres radiate into the gill raker cushions and the channel floor. The origo at the lateral side is shared with MAF. MBS is very thin and tendinous directly under the gill rakers (Figs. 3, 5).

We could identify *m. interbranchiospinalis* (Hoogenboezem et al., '91) in the first and possibly the second and third gill arch of Hoogenboezems sections of a common bream of 30 cm SL. However, we could not distinguish this tiny muscle in our sections, not even in those of common bream, possibly due to the smaller size of the fishes (14.9 cm SL).

Connective tissue

The transition between loose and compact connective tissue cannot be determined properly with Crossmon stained sections, since the intensity of coloration of connective tissue is highly variable. A detailed study of connective tissue requires other staining or EM techniques. However, a general picture can be given (Figs. 3, 5). Each gill raker foot is enveloped by dense connective tissue. Both on the lateral and the medial sides, a connective tissue cushion is interposed between the ventral side of the ceratobranchial bone and the gill rays. On the medial side, this cushion extends dorsally to the medial origo line of MBS, thus taking the space that is, on the lateral side, taken up by MAF.

Blood vessels

The *a. branchialis afferens* and *efferens* have a protected position in the curve of the ceratobranchial bone. The efferent filamental branches run through the forks of the gill ray feet to the *a. branchialis efferens* (Fig. 10). The vessels are much wider before the fork than beyond it. The blood flow in the gills is very slow, which improves gas exchange. At the position of the forks the flow speed of the blood is apparently increased again. In perch (*Perca fluviatilis*), the branches of *a. branchialis efferens* run through a slit-like depression of the gill rays and have sphincter muscles (Dunel-Erb and Bailly, '87).

Interspecific variation

Gill rakers

The gill rakers of common bream are longer than those of white bream and roach (Fig. 5). In the reconstructions we measured a length of 1.04 and 1.01 mm (laterally resp. medially) in common bream, 0.67 resp. 0.61 mm in white bream and 0.75 resp. 0.55 mm in roach. Using the equations in Van den Berg et al. ('92), which relate gill raker length to fish standard length, a gill raker length of about 1.0 mm in the common bream and of about 0.75 mm in the white bream and roach was expected, which is in good agreement with the measurements in the reconstructions.

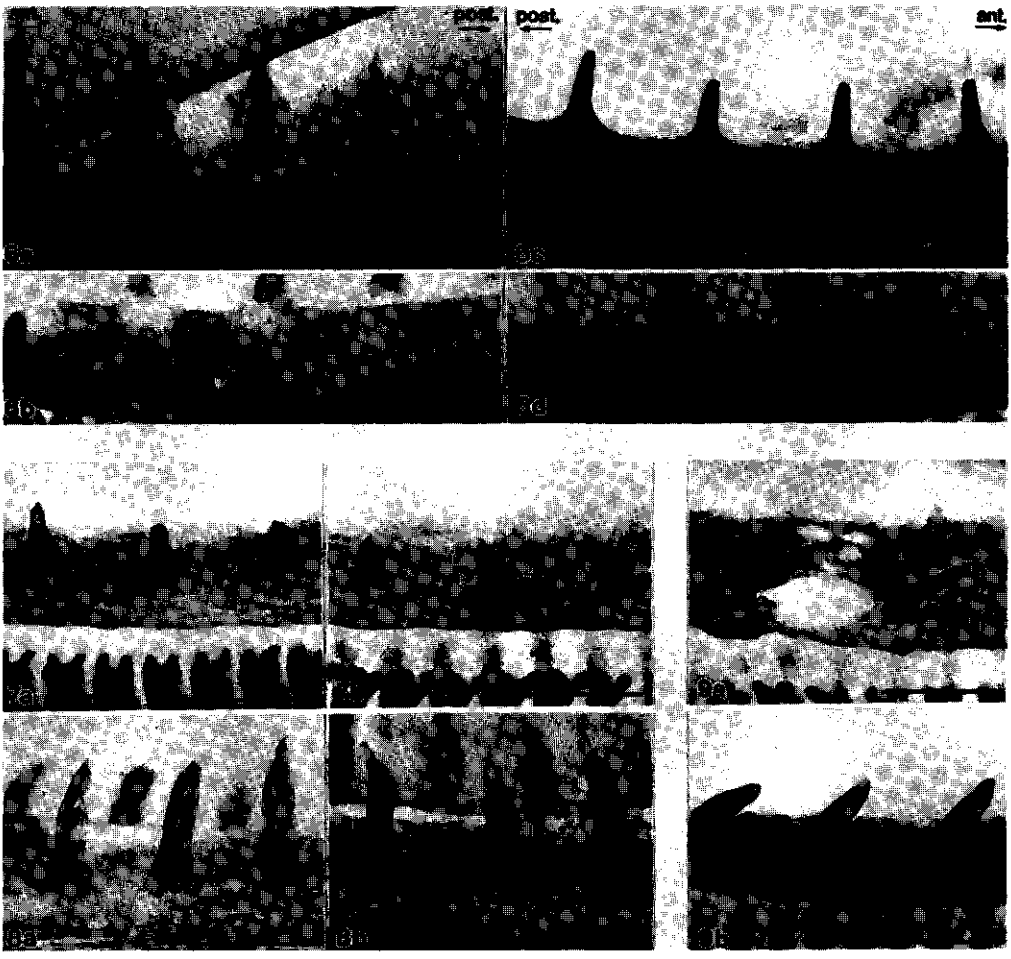

Figure 6

Second gill arch of common bream (SL 25 cm); whole mount alcian blue staining. Figure B and D are a top view of the gill rakers in Figure A and C. The medial gill rakers feet (A, B) are flat and the lateral ones (C, D) are spindle-shaped. At the medial side, the posterior raker feet are less flat than the anterior ones. Note the forked feet of the gill rays. Scale bars in figure 6-9 indicate 1 mm.

Figure 7

Second gill arch of white bream (SL 22 cm); whole mount alcian blue staining. Some gill raker needles are incompletely ossified. The medial and lateral side do not differ.
A medial side; B lateral side.

Figure 8

Second gill arch of roach (SL 22 cm); whole mount alcian blue staining. The gill rakers are perforated with tiny holes. The raker feet have root-like extensions. The medial and lateral side do not differ.
A medial side; B lateral side.

Figure 9

The lateral side of the first gill arch of white bream (A) and common bream (B); whole mount alcian blue staining. Note the anterior orientation of the gill rakers and the tilted implantation of their feet.

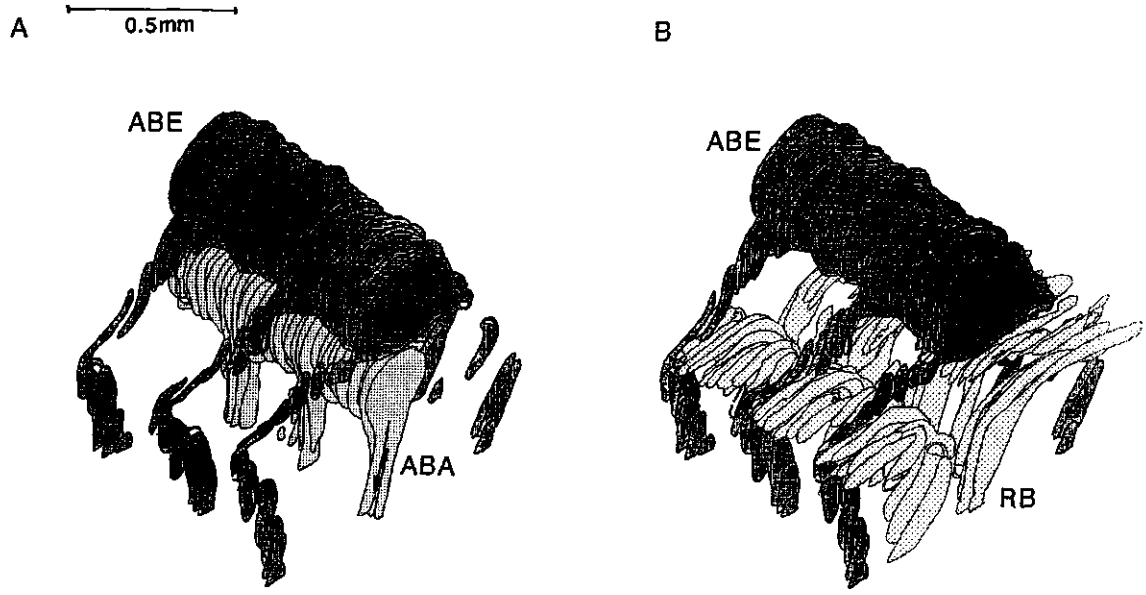

Figure 10

A) The large arteries in the second gill arch of roach (SL 14.9 cm). The arrows indicate the direction of the blood flow in the branches of these arteries.

B) The filamental branches of *a. branchialis efferens* run through the forks of the gill ray feet. Beyond the forks their diameter is strongly reduced.

ABA, *arteria branchialis afferens*; ABE, *arteria branchialis efferens*; RB, *radius branchialis*, gill ray.

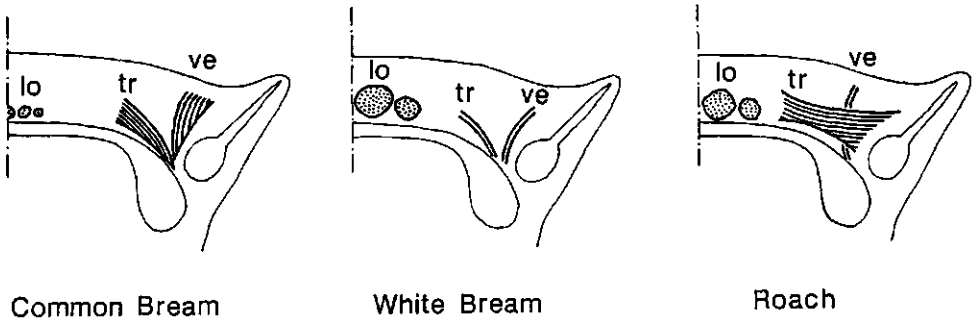

Figure 11

Scheme of the main muscle fibre directions of *m. branchialis superficialis* in common bream, white bream and roach.

lo, longitudinal fibres; tr, transversal fibres; ve, vertical fibres

In common bream there is a continuous range of shapes of the raker feet. Two extremes can be distinguished, spindle-shaped feet and flat feet. The flat feet are possibly less mobile than the spindle-shaped ones, because the former are more firmly anchored in connective tissue. All lateral gill raker feet are spindle-shaped and the medial ones are flat (Fig. 6) (cf. Hoogenboezem et al., '91). On the medial side, the raker feet posteriorly on the gill arch are slightly more spindle-shaped. The difference between the gill raker feet on the medial and the lateral sides suggests that the lateral rakers can be more easily moved than the medial ones, which strongly supports the reducible-channel theory. On the other hand, both gill rakers with flat feet and with spindle-shaped feet can easily be abducted in freshly killed common bream.

In white bream the raker needles are often incompletely ossified. The raker feet of white bream resemble the medial ones of common bream (Fig. 7). The gill rakers of roach are entirely different (Fig. 8). They contain numerous holes and have various root-like extensions at their feet, giving them the appearance of firmly anchored structures. However, the gill rakers of freshly killed white bream and roach can easily be abducted. No gradient in raker foot shape was observed in white bream and roach.

Muscles

All lateral gill rakers of the four gill bearing gill arches of common bream have a MAB (Fig. 5A) (cf. Hoogenboezem et al., '91). In white bream and roach MAB is only present at the lateral side of the first gill arches. On the gill arches of white bream and roach that lack MABs, MAF is an uninterrupted muscle sheet (Fig. 5B,C).

The pattern of fibres of MBS is complex, but we can qualitatively divide the fibres in three groups based on their direction: 1) transversal fibres (tr, from lateral to medial), 2) longitudinal fibres (lo, from anterior to posterior) and 3) vertical fibres (ve, from ventral to dorsal). By studying the perpendicular and the longitudinal serial sections of the gill arches we could determine the relative importance of these fibre directions in each species. Common bream has mainly tr- and ve-fibres (Fig. 11A). The tr-fibres are concentrated at the bottom of the cushions, most of them run in the length direction of the cushions. Most ve-fibres are close to the gill rakers, radiating from the origo lines on the ceratobranchial bone. White bream has mainly lo-fibres, which are concentrated in bundles at the central dorsal side of the gill arch (Fig.11B). Roach has mainly tr- and lo-fibres (Fig. 11C). The lo-fibres of roach are also concentrated in bundles at the central dorsal side of the gill arch. Many of the tr-fibres of roach are high in the cushions; several of these fibres are attached to the central side of the gill rakers. In common bream and white bream just a few tr-fibres are attached to the gill rakers, and near the base of the raker feet.

Micro anatomy of other cyprinid species

The four additionally studied cyprinid species have the same principal micro anatomy as described above. MABs are present on the lateral side of the first gill arches. In grass carp, asp and rudd MABs are not present on gill arches 2, 3 and 4, but they are in carp. Within the examined group, common bream and carp are the only species with conspicuously curved and deep channels between their cushions. Alizarine material of carp showed that its lateral gill rakers have rather large, circular feet, but its medial gill rakers have even larger feet. Regarding the micro anatomy of their gill arches, cyprinids can be divided into two groups, species with MABs on all four gill arches and species with MABs on the first gill arch only.

Discussion

The reducible-channel model

The reducible-channel model can only be applied if the lateral gill rakers can be abducted into the medial channels. This implies that *m. abductores branchiospinales* (MABs) should be present on gill arches 2, 3 and 4. This structural requirement for the reducible-channel model only holds true for common bream and carp, but not for white bream, roach, grass carp, asp and rudd. Filter-feeding experiments (unpublished results) have shown that the retention ability of white bream and roach is far worse than predicted by the reducible-channel model. Common bream however, has a retention ability which does agree with the reducible-channel model (cf. Hoogenboezem et al., in press a). These experiments clearly corroborate with the present results. Filter-feeding experiments (Uribe-Zamora, '75, p. 37-43) showed that carp can adjust the mesh size of their branchial sieve from about 500 to 250 μm when small zooplankters are abundant. As found for common bream, carp can sieve with two distinct mesh sizes that differ by a factor of two. Considering the following characteristics of carp:

1) the ability to diminish the mesh size of the branchial sieve by a factor of two,
2) the presence of MABs on the lateral side of gill arches 1 to 4,
3) the deep, curved channels and
4) the smaller lateral gill raker feet,

it seems justified to conclude that the reducible-channel model can be applied to carp, as well.

White bream and roach may either retain zooplankton with unreduced channels, without the possibility to adjust the mesh size of their branchial sieve, or use an entirely different retention technique, like the saw-tooth (interdigitation) model (Sibbing, '91). In the saw-tooth model the slits between the gill arches (gill slits) are the site of retention. The mesh size of the sieve is dependent on the shape of the gill rakers and on the distance between successive gill arches. Analysis of gill arch movements of each species during filter-feeding is necessary to test this model.

The first gill slit

All seven studied cyprinid species have MABs at the lateral side of the first gill arch. The lateral side of this gill arch faces the operculum, not another gill arch. Therefore, the function of MAB on the first gill arch cannot be channel reduction. The shape of the lateral gill rakers on the first gill arch of the seven species differs from the gill rakers on the other gill arches. They are flattened and longer than all other rakers (about 110% in white bream and roach and 165% in common bream; Van den Berg et al., '92) and lie flat against the gill arch, pointing anteriorly (Fig. 9). This shape of the gill rakers on the first gill arch appears to be common among cyprinids.

During breathing and feeding the first gill slit becomes about two times wider than the other gill slits, in common bream (Hoogenboezem et al., '90) and white bream (unpublished results). A retention structure is necessary to prevent loss of food particles through this slit. Also, the delicate gill filaments could be damaged by large particles. The MABs might well rotate the lateral gill rakers of the first gill arch latero-posteriorly, towards the operculum, thus forming a sieve. A sieve between the first gill arch and the palatal organ, with gill rakers pointing upwards (Hoogenboezem et al., '91) is less likely, since the rakers are implanted in such a way that MAB will move them sidewards, not upwards (Fig. 9). The comparatively large length of these gill rakers will be an adaptation to the large width of the first slit.

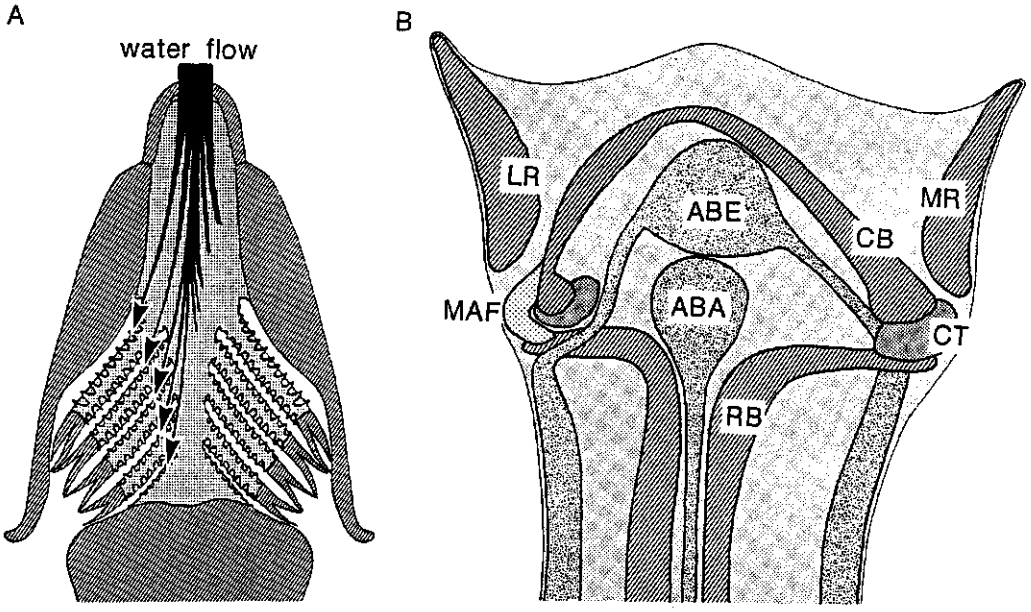

Figure 12

A) Dorsal view of the floor of the buccal and pharyngeal cavities of a schematical cyprinid fish head. The arrows indicate the expected direction of the water flow. The inertial force exerted by the backward flowing water will tend to rotate the hemibranchs towards the fish axis.

B) Schematical cross section of a gill arch, based on a computer reconstruction of the second gill arch of a roach (SL 14.9 cm). The inset shows the position of this picture in a cross section of a gill arch. The connective tissue cushions between the gill rays and the ceratobranchial bone provide the stiffness needed to prevent rotation of the hemibranchs (A). During vigorous breathing, contraction of MAF could increase this stiffness, which would explain the uniquely lateral position of MAF. Another possible function of MAF is regulation of the blood flow. The filamental branches of ABE run through the forks of the gill rays. When MAF contracts, these branches will be pressed more tightly against the connective tissue cushions, thereby reducing their diameter.

ABA, *arteria branchialis afferens*; ABE, *arteria branchialis efferens*; CB, ceratobranchial bone; CT, compact connective tissue; LR, lateral gill raker; MAF, *m. abductor filamenti*; MR, medial gill raker; RB, *radius branchialis*, gill ray.

The inter raker distance is probably the mesh size of this sieve. In common bream, this inter raker distance is only about 75% of that on the other gill arches. However, in white bream and roach it is 125% resp. 145% of the distance on the other gill arches (Van den Berg et al., '92). Since common bream can reduce the mesh size of its channels to 50%, this means that in all three species the mesh size of the sieve of the first gill slit is about 50% larger than that of the rest of the branchial sieve. The significance of this difference is unclear. Possibly the palatal organ can adjust the mesh size of the sieve across the first gill slit.

The function of the gill arch muscles

The function of the tiny gill arch muscles can not easily be checked experimentally. Electrical stimulation of the gill arches of freshly killed specimens could give some impression of the possible movements, but with this method too large of an area is activated at the same time. Therefore, we resorted to deduction of the muscle functions.

Contraction of *m. abductor branchiospinalis* will lead to abduction of the lateral gill raker. MAB will also apply an abducting force on the lateral gill rays. In the common bream of 149 mm SL one MAB has a cross-sectional area of about 0.0235 mm^2. With isometric contraction this muscle can develop a maximum force of 0.0235x12.10 = 0.28 N (using data of Granzier et al., '83). By means of scaling we estimated that this force is enough to abduct the gill raker. Increasing the scale from 1 mm (gill raker) to 500 mm (human fore-arm) we find a corresponding area of 5875 mm^2 and a maximal force of 70 kN, which is more than enough for fore-arm abduction.

How are the lateral gill rakers adducted? The transversal fibres of *m. branchialis superficialis* (MBS) that are attached to the lateral gill rakers are suited for raker adduction, but this kind of fibre is mainly present in roach, which has no abductor muscle on gill arches 2, 3 and 4. Common bream has hardly any of such fibres, but it might adduct its gill rakers indirectly by deforming its cushions using transversal and vertical fibres. As observed in freshly killed fishes, adduction might also be a passive, elastic property of the gill raker cushion.

Cyprinids have gills of the *Salmo* type, therefore the lower half of each pair of hemibranchs is fused (Fig. 2B). As a result, *m. abductor filamenti* (MAF) will move both hemibranchs together with respect to the ceratobranchial bone. According to Bijtel ('49), MAF prevents rotation of the hemibranchs during coughing. MAF may be used during hyperventilation as well, to maintain the position of the hemibranchs. Due to inertia of the water, which flows from front to back, the water pressure on the lateral hemibranchs will be larger than on the medial ones (Fig. 12A). During normal ventilation this pressure difference will be absorbed by the connective tissue cushions (Fig. 12B). When the pressure difference is larger, due to hyperventilation, rotation of the hemibranchs can be prevented by contraction of MAF, which would explain the uniquely lateral position of MAF. Another possible function of MAF is to aide in the regulation of blood flow within the gills. The filamental branches of *a. branchialis efferens* run through the forks of the *radii branchiales* (Fig. 10B). Contraction of MAF will press these branches into the connective tissue cushions, thus possibly reducing their diameter (Fig. 12B).

Since MAF is a continuous muscle sheet, only interrupted when MAB is present, and since MABs and MAF both attach to the gill ray feet, it seems reasonable to suggest that the MABs have developed as specialized sections of the muscle as a whole.

M. branchialis superficialis (MBS) has a number of possible functions:

1) Gill raker adduction (see above)

2) Contraction of the cushion may lead to extrusion of mucus from the numerous mucus cells in the cushion epithelium. It has been proposed (Hoogenboezem and Van den Boogaart, in press b), that small food particles, that are trapped in the channels, stimulate contraction of MBS and become encapsulated in a mucus layer. During back-washing, the encapsulated particles stick together and form a large mucus ball. The multi-layered structure of the mucus balls, which are frequently found in freshly caught common bream, provided support for this hypothetical prey transport mechanism.

3) The muscle fibres of the free surface of the gill arches and the postlingual organ may cooperate with the palatal organ in selection, manipulation and transport of food particles (Sibbing and Uribe, '85). Most muscle fibres in the gill arches make an angle of

about 45° with those in the palatal organ. The longitudinal fibres seem particularly suited for this function.
4) Constriction of the channels and hence a change of their diameter (= the mesh size of the sieve).

With its transversal and vertical fibres, common bream can easily deform its cushions (Fig. 11A). However, most fibres of white bream are not suited to deform the cushions, since they are concentrated along the central dorsal axis (Fig. 11B). The functions 1, 2 and 4 stated above are therefore not likely to apply to white bream.

Because of gill arch movements during feeding, the interdigitation of the gill rakers on either side of a gill slit is disturbed (unpublished results). Small corrections of the position of the lateral raker tip in the medial channels are therefore necessary. In the absence of *m. interbranchiospinalis*, common bream can still adjust the position of its lateral gill rakers by using MAB. The longitudinal sections of the gill arches reveal that the fibres of MAB fan out from their insertion at the gill raker foot to several feet of the gill rays (Fig. 4). If a segment of MAB is contracted separately, the gill raker will turn anteriorly or posteriorly, as well as abduct.

From micro anatomy to ecology

The gill arch anatomy of cyprinids, with an intricate musculature, gill rays, rakers and cushions, provides the fish with a subtle and flexible system to retain and manipulate small food particles. It would be interesting to study the micro anatomy of the branchial sieve of a wider range of cyprinids, and possibly other families, in relation to the filter-feeding performance. The presence of MAB is easy to study using standard histological techniques. Its presence on gill arches 2, 3 and 4 is a suitable bio-assay to identify the better facultative filter-feeders in a group of otherwise similar species (eco-typing), who will be successful in lakes where zooplankton is a dominant food resource, e.g. man-made reservoirs.

Acknowledgments

This research was supported by the Foundation for Fundamental Biological Research (BION), which is subsidized by the Netherlands Organization for Scientific Research (NWO), project no.: 811-428-265. The reconstruction programs AnyTablet 3.4 and MacReco 3.4 can be purchased from E. Otten, Bloemsingel 10, 9712 KZ, Groningen, the Netherlands, tel. (31)-(0)50-632768.

Literature cited

Bijtel, J.H. (1949) The structure and the mechanism of movement of the gill-filaments in Teleostei. Extrait des Archives Néerlandaises de Zoologie 8(3):1-22.

Drenner, R.W., J.R. Mummert, F.Jr. de Noyelles and D. Kettles (1984) Selective particle ingestion by a filter-feeding fish and its impact on phytoplankton community structure. Limnol. Oceanogr. 29(5):941-948.

Dunel-Erb, S. and Y. Bailly (1987) Smooth muscles in relation to the gill skeleton of *Perca fluviatilis*: organization and innervation. Cell Tissue Res. 247:339-350.

Granzier, H.L.M., J. Wiersma, H.A. Akster and J.W.M. Osse (1983) Contractile properties of a white- and a red-fibre type of the *m. hyohyoideus* of the carp (*Cyprinus carpio* L.). J. Comp. Physiol. 149:441-449.

Hoogenboezem, W., F.A. Sibbing, J.W.M. Osse, J.G.M. van den Boogaart, E.H.R.R. Lammens and A. Terlouw (1990) X-ray measurements of gill-arch movements in filter-feeding common bream, *Abramis brama* (Cyprinidae). J.Fish Biol. 36:47-58.

Hoogenboezem, W., J.G.M. van den Boogaart, F.A. Sibbing, E.H.R.R. Lammens, A. Terlouw and J.W.M. Osse (1991) A new model of particle retention and branchial sieve adjustment in filter-feeding common bream (*Abramis brama* (L.), Cyprinidae). Can. J. Fish. Aquat. Sci. 48:7-18.

Hoogenboezem, W., E.H.R.R. Lammens, P.J. McGillavry and F.A. Sibbing (in press a) Size selectivity and sieve adjustment in filter-feeding common bream *Abramis brama* (L.), Cyprinidae. Can J. Fish. Aquat. Sci.

Hoogenboezem, W. & J.G.M. van den Boogaart (in press b) The role of oro-pharyngeal mucus in filter-feeding of common bream (*Abramis brama*). Can. J. Fish. Aquat. Sci.

Lammens, E.H.R.R., J. Geursen and P.J. McGillavry (1987) Diet shifts, feeding efficiency and coexistence of common bream (*Abramis brama*), roach (*Rutilus rutilus*) and white bream (*Blicca bjoerkna*) in eutrophicated lakes. Proc. V Congr. Europ. Ichtyol., Stockholm:153-162.

Lammens, E.H.R.R. (1989) Causes and consequences of the success of bream in Dutch eutrophic lakes. Hydrobiol. Bull. 23:11-18.

Nie, H.W. de (1987) The decrease in aquatic vegetation in Europe and its consequences for fish populations. EIFAC/CECPI Occasional paper 19:52 p.

Romeis, B. (1968) Mikroskopische Technik. München-Wien, Oldenbourg.

Sibbing, F.A. and R. Uribe (1985) Regional specializations in the oropharyngeal wall and food processing in the carp (*Cyprinus carpio* L.). Neth. J. Zool. 35(2):377-422.

Sibbing, F.A. (1991) Food capture and oral processing. In I.J. Winfield and J. Nelson (eds): Cyprinid Fishes; Systematics, Biology and Exploitation. London: Chapman and Hall, pp. 377-412.

Simons, E.V. and J.R. van Horn (1971) A new procedure for whole mount alcian blue staining of the cartilaginous skeleton of chicken embryos, adapted to the clearing procedure in potassium hydroxide. Acta Morphol. Neerl.-Scand. 8:282-291.

Uribe-Zamora, M. (1975) Selection des proies par le filtre branchial de la carpe miroir (*Cyprinus carpio* L.). Doctoral thesis. University of Lyon.

Van den Berg, C., F.A. Sibbing, J.W.M. Osse and W. Hoogenboezem (1992) Structure, development and function of the branchial sieve of common bream, *Abramis brama*, white bream, *Blicca bjoerkna*, and roach, *Rutilus rutilus*. Env. Biol. Fish. 33:105-124.

Vetter, B. (1878) Untersuchungen zur vergleichende Anatomie der Kiemen- und Kiefermuskulatur der Fische. Jenaische Zeitschrift für Naturwissenschaften 12:431-550.

Chapter 5

A quantitative, 3D method to analyze rotational movement from single view movies, exemplified with the gill arch movements of white bream (*Blicca bjoerkna*).

Coen van den Berg
To be submitted to the Journal of Experimental Biology

Abstract

Cinematography is an important tool in the study of animal movement. A major problem in the analysis of films is that three-dimensional movements are projected on two-dimensional film frames. In studies of animal movement one usually tries to reduce the projection errors by careful experimental design. Reconstruction of the 3D movements from a single 2D projection is rarely done. A related problem in film analysis is how to calculate movements relative to a moving reference structure (e.g. the skull). In this paper a general 3D method is presented which solves these problems for rotational movements. A major requirement of this method is that in each film frame at least two marker points can be identified on each structure. The distance between these markers should be accurately known. The method is illustrated with the analysis of gill arch movements in white bream (*Blicca bjoerkna*). This example demonstrates clearly that the 3D aspect of movements can be of paramount importance for both a quantitative and a qualitative analysis of animal movement.

Introduction

The study of animal movement is an important aspect of functional morphological research. Movements of (parts of) animals are usually studied with either light- or X-ray cinematography. This means that 3D movements are recorded on 2D film frames. For a quantitative analysis the real movements should be reconstructed from their projections. Examples of the need for quantitative data are the experimental verification of four bar linkage models (Westneat 1990) and the accurate measurement of the variation of the distance between the gill arches to verify theoretical filter-feeding mechanisms (Hoogenboezem et al. 1990, Van den Berg et al. in prep.). A quantitative method is also required for a functional analysis of muscle/skeleton complexes. Such an analysis is complicated by shortening of the muscles. The direction of the action lines of the muscles should be inferred from the orientation of the skeletal elements.

If movements occur in one plane their projection is distorted only if this plane is not parallel to the film-plane. The maximal projection error is proportional to the cosine of the angle between these planes (e.g. an angle of 30° causes a maximal projection error of 13%). In studies of movements of animals projection errors are usually assumed to be negligible (e.g. Videler 1981 and Batty 1981 (locomotion of fish larvae), Jenkins 1981 (wrist movements in monkeys), Gambaryan 1974 (running in mammals)). The underlying assumption is that the movement is in one plane, which is parallel to the film-plane.

Unfortunately, many movements are not even nearly in one plane, which means that considerable distortions of lengths and angles in the projected image are unavoidable.

The movements of skeletal elements of the fish head during suction feeding are usually not in one plane. In general, these movements are a combination of abduction/adduction and depression/levation. Such movements have been studied with X-ray cinematography (e.g. Sibbing 1982, Sibbing et al. 1986, Hoogenboezem et al. 1990, Westneat 1990, Claes and de Vree 1991). Again, a 2D method of analysis of the films was always used. These authors minimized the projection errors by carefully selecting scenes:
1) with a minimum of pitch, yaw and roll (inset of Fig. 3) of the fish and
2) which were filmed as much as possible perpendicular to the plane of the movement under study.

Clearly, the 2D method of analysis results in a severe restriction on the number of scenes that are suited for analysis. Furthermore, structures moving in different planes can not be studied simultaneously. For a qualitative description of movement patterns the 2D method can be a valid approximation, although one should be very careful not to mistake movements of the whole animal for those of a particular element. However, the 2D method is inappropriate for quantitative analysis, even when scenes and experimental conditions are selected carefully (Sibbing 1982, Hoogenboezem et al. 1990). The 2D method is also inappropriate when the movement under study is not approximately in one plane.

When two (or more) views of a movement can be recorded simultaneously, e.g. with the aid of mirrors, the 3D movements can be fully reconstructed from the two 2D images (Zarnack 1972, Nachtigall 1983, Van Leeuwen 1984, Drost and Van den Boogaart 1986). However, due to technical (and budget) limitations simultaneous views of a movement cannot always be shot, e.g. when X-ray cinematography is used (X-ray mirrors do not exist).

In this paper a method is presented to reconstruct 3D rotational movement using single view films and to determine rotation relative to a moving reference structure (e.g. the skull), i.e. in an object-bound frame. Earlier, Ellington (1984) presented a method to determine 3D wing movements from single view films of flying insects. The present method is similar to his method, but more generally applicable. Ellingtons method for determining wing movements relative to the body axis of an insect can only be applied to symmetrical movements, it is "based upon bilateral symmetry of the wing motions" (Dudley and Ellington 1990). The present method however does not depend on symmetry, but on the presence of two markers in each structure under study, with a known distance. Hence, the method can be applied to a variety of kinematic investigations.

3D method of film analysis

General requirements

The 3D method of analysis can only be applied when some general requirements are fulfilled:

1. The magnification of the projection of the object should be known.

2. At least two markers should always be visible in each structure to be analyzed. These markers should be as far apart as possible in the direction of the movement under study. Markers may be conspicuous and well-defined anatomical points or artificial points (e.g. surgically implanted pieces of platinum, which are commonly used in X-ray cinematography).

3. The distance between the markers in each structure should be known accurately in each frame (a constant distance is most convenient).
4. One should know whether the structures are pointing 'up' or 'down' with respect to the film-plane. This cannot be determined from their 2D projection. The easiest way to solve this problem is to make sure that the angle between each structure and the film-plane stays well within the range from 0 to 180°; in other words, to make sure that the structure is either pointing 'up' or 'down' during the entire scene.

If a structure has only two marker points, axial rotation (rotation around the line that connects the markers) cannot be measured. If this movement component is object of study a third marker point (obviously not in line with the other two markers) is necessary. I will only discuss the calculations for structures with two markers. The calculations with three markers are essentially the same.

The calculation of 3D orientation and angles between structures

To avoid an entirely abstract treatment of the method, it is illustrated with an example. The movements of the gill arches of a white bream (*Blicca bjoerkna*) were analyzed with dorsal X-ray films (Van den Berg et al. in prep.). Accurate measurements with a resolution of less than 50 μm were required in this detailed study of the retention mechanism of the branchial sieve. Two platinum markers were inserted in each gill arch, the *copula communis* (the fused basibranchials that connect the gill arches mid-ventrally) and the skull. The skull was the reference structure. All the above general requirements were fulfilled (for technical details and error analysis see Van den Berg et al. in prep.).

The film-plane is the xy-plane. The z-axis is perpendicular to this plane. All calculations in this paper are performed in this xyz-frame. The two markers in each structure define a vector, **G**. For example, let **G** be a gill arch. One marker is translated to the origin (0,0,0). The coordinates of the other marker are (x,y,z). **G** can now be expressed in terms of x, y and z. Coordinate x and y are determined directly from each film frame (Fig. 1a,b). The value of z is calculated with Pythagoras' rule (Fig. 1c):

$$z = \pm \sqrt{G^2 - x^2 - y^2} \qquad (1)$$

where G^2 (= the length of **G** squared) and the sign of z are known (general requirement 3 and 4) (see Ellington 1984).

When two structures are connected with a single joint, the 3D angle α between these structures can be calculated. If there is no marker exactly in the joint, the coordinates of the joint should be calculated with the coordinates of other marker points. In the example, let $\mathbf{G}_1$ be a gill arch and $\mathbf{G}_2$ the *copula communis*, connected by a joint. The cosine of the angle α between these structures equals:

$$\cos \alpha = \frac{\mathbf{G}_1 \cdot \mathbf{G}_2}{G_1 \cdot G_2} = \frac{x_1x_2 + y_1y_2 + z_1z_2}{G_1 \cdot G_2} \qquad (2)$$

where

$x_1,y_1,z_1; x_2,y_2,z_2$ = coordinates of vector $\mathbf{G}_1$; $\mathbf{G}_2$
G_1, G_2 = length of vector $\mathbf{G}_1$, $\mathbf{G}_2$ (scalar)

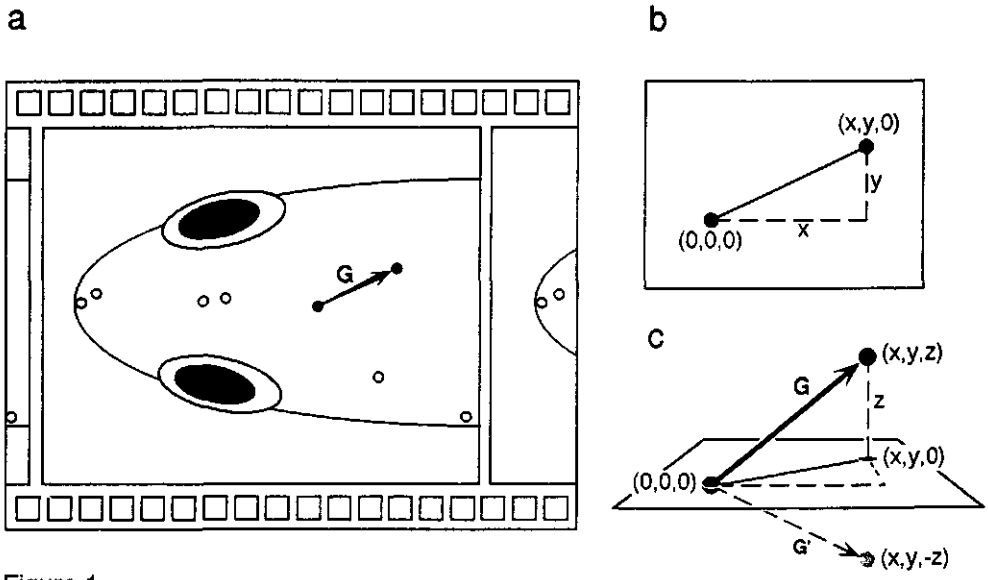

Figure 1

a) The markers in the fish head are indicated as small circles in this schematic film frame. The two black markers (at opposite ends of a gill arch) define a vector **G** (not in the film-plane).
b) The x- and y-coordinate of **G** are calculated from its projection on the film-plane (= xy-plane).
c) In this view the film-plane from (b) is shown from the side. The z-coordinate of **G** is calculated with Pythagoras' rule, given the length of **G** and the orientation of **G** with respect to the film plane. The wrong orientation is indicated as **G'**.

Rotation relative to a reference structure

This paragraph will be illustrated with the example mentioned above. The movement of a gill arch in a series of film frames (a film scene) is the sum of its movement with respect to the skull and the movement of the skull with respect to the film frame. The separate components are interesting, their sum is not. Therefore, we want to separate these two components.

The movement of the skull can be split in a translation and a rotation component. The distance between the skull and the gill arches is not constant and unknown. Therefore, the position (translation component) of the gill arches cannot be calculated relative to the skull[4]. However, the depression angle of the gill arches *can* be corrected for rotation of the skull.

The vector representing the skull in frame number n is S_n. The vector representing a gill arch is **G**. The angle between **G** and **S** might easily be calculated with formula (2). However, we want to know the depression angle of **G**, which is the angle between **G** and a horizontal plane (plane H) in the fish (Fig. 2 a,b). The calculation of such a depression angle is more complicated. First, one film frame is chosen as reference frame (Fig. 2a). In this frame plane H is parallel to the xy- (or film-)plane (by definition). All vectors (**G**, S_n etc.) in the other film frames (Fig. 2b) must be transformed to the orientation of the reference frame (the method is described below). The depression angle of **G**

[4] When two (preferably perpendicular) views are filmed simultaneously, general requirements 3 and 4 can be dropped. Using both views, the x, y and z coordinates of the marker points that are visible in both views can be determined directly. Hence, all distances and angles between structures can be calculated and movements of structures can be corrected for both rotation and translation of a reference structure.

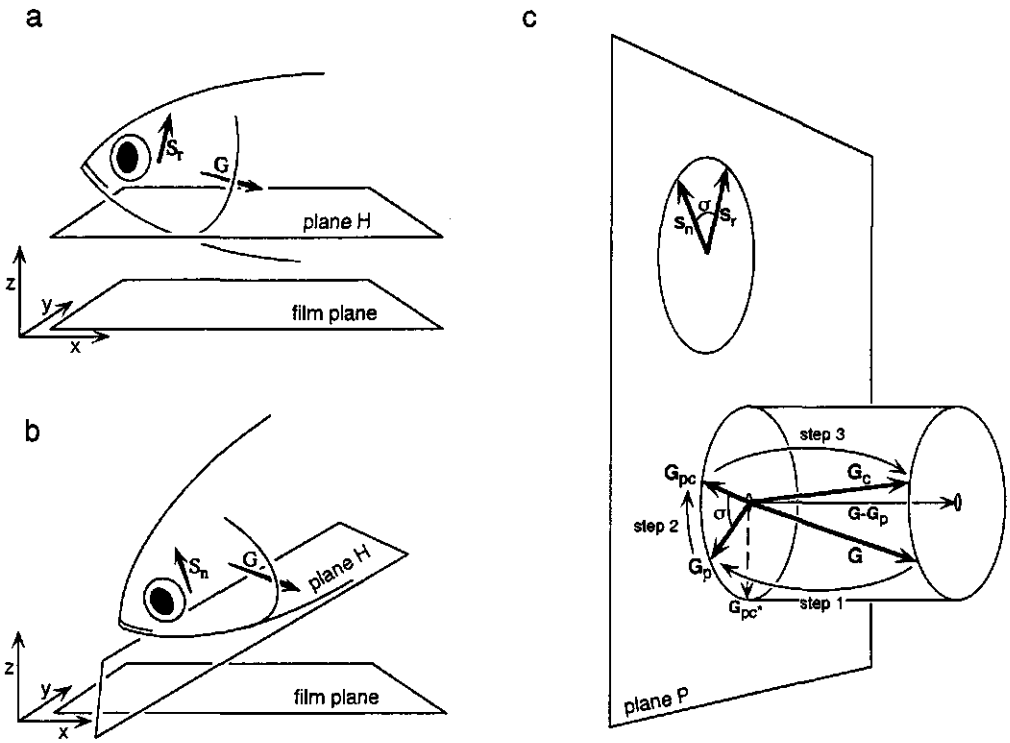

Figure 2

The depression angle of the gill arch vector G is calculated in a fish-bound frame by correcting G for rotation of the skull vector S.

a) Vector S in the reference frame is S_r. In the reference frame plane H (the horizontal plane in the fish-bound frame) is parallel to the xy-plane (by definition).

b) In film frame number n, the skull (vector S_n) has rotated with respect to S_r, over an angle σ. Plane H has also rotated over angle σ. The orientation of plane H with respect to vector S is unaltered. Vector G has to be transformed to the reference orientation given in (a).

c) Vector S_r and S_n define a plane P. This plane can have any orientation, depending on the way the skull has rotated (a combination of pitch, roll and yaw). G is projected on plane P (G_P; step 1), rotated over angle σ (G_{PC}; step 2) and restored to its original length (G_C; step 3), by adding G-G_P.

G_{PC}* = the wrong solution of G_{PC} (rotated over angle -σ instead of σ).

---

can then be calculated as the angle between the corrected vector **G** and the xy plane, since the xy plane is now always parallel to plane H. The correction method is based on the movement of the skull vector S_n with respect to its reference orientation S_r. The direction of S_r should preferably be perpendicular to the film frame (see appendix 1).

In each film frame S_r and S_n define a plane P (Fig. 2c). This plane can have any position in space, depending on the movement that the skull has made. Plane P is unrelated to the film-plane. σ is the angle between S_r and S_n. Angle σ is a combination of pitch, roll and yaw of the skull. Since $S_r = S_n$ (requirement 3), cos σ equals:

$$\cos \sigma = \frac{S_r \cdot S_n}{S_r^2} \qquad (3)$$

In each film frame, $\mathbf{G}$ is transformed from the $\mathbf{S}_n$ orientation to the $\mathbf{S}_r$ orientation in three steps (Fig. 2c):

Step 1. $\mathbf{G}$ is projected on plane P ($\mathbf{G}_P$)
Step 2. $\mathbf{G}_P$ is rotated over angle σ ($\mathbf{G}_{PC}$)
Step 3. with $\mathbf{G}_{PC}$ the corrected direction of $\mathbf{G}$ is calculated ($\mathbf{G}_C$); note that $\mathbf{G}_C = \mathbf{G}$.

When this is done, the depression angle of the gill arch is the angle between $\mathbf{G}_C$ and the xy-plane. Note that, in the calculations below, the coordinates are not transformed to a frame defined by plane P, but always remain defined in the original xyz-frame of the film-plane.

Step 1: projection of vector G on plane P

Just like any vector in plane P, vector $\mathbf{G}_P$ must be a linear combination of $\mathbf{S}_r$ and $\mathbf{S}_n$:

$$\mathbf{G}_P = \alpha_1 \mathbf{S}_r + \alpha_2 \mathbf{S}_n \tag{4a}$$

where α_1 and α_2 are scalar factors.
$\mathbf{G}_P$ is a perpendicular projection of $\mathbf{G}$, therefore:

$$\begin{aligned} (\mathbf{G}-\mathbf{G}_P)\cdot\mathbf{S}_r &= 0 \\ (\mathbf{G}-\mathbf{G}_P)\cdot\mathbf{S}_n &= 0 \end{aligned} \tag{4b}$$

Substituting 4a in 4b results in two equations with two unknowns (α_1, α_2):

$$\begin{aligned} \alpha_1(\mathbf{S}_r\cdot\mathbf{S}_r) + \alpha_2(\mathbf{S}_r\cdot\mathbf{S}_n) &= \mathbf{G}\cdot\mathbf{S}_r \\ \alpha_1(\mathbf{S}_r\cdot\mathbf{S}_n) + \alpha_2(\mathbf{S}_n\cdot\mathbf{S}_n) &= \mathbf{G}\cdot\mathbf{S}_n \end{aligned} \tag{4c}$$

With these equations α_1 and α_2 and hence $\mathbf{G}_P$ can be determined.

Step 2: rotation of vector G_P over angle σ

The coordinates of $\mathbf{G}_{PC}$ (three unknowns: x_{PC}, y_{PC}, z_{PC}) are calculated with three equations, which are based on three conditions for the rotation (compare Fig. 2c):

2.1 $\mathbf{G}_{PC}$ has the same length as $\mathbf{G}_P$
2.2 $\mathbf{G}_{PC}$ is rotated over angle σ
2.3 $\mathbf{G}_{PC}$ lies in plane P

2.1 $G_{PC} = G_P$, or:

$$x_{PC}^2 + y_{PC}^2 + z_{PC}^2 = x_P^2 + y_P^2 + z_P^2 \tag{5}$$

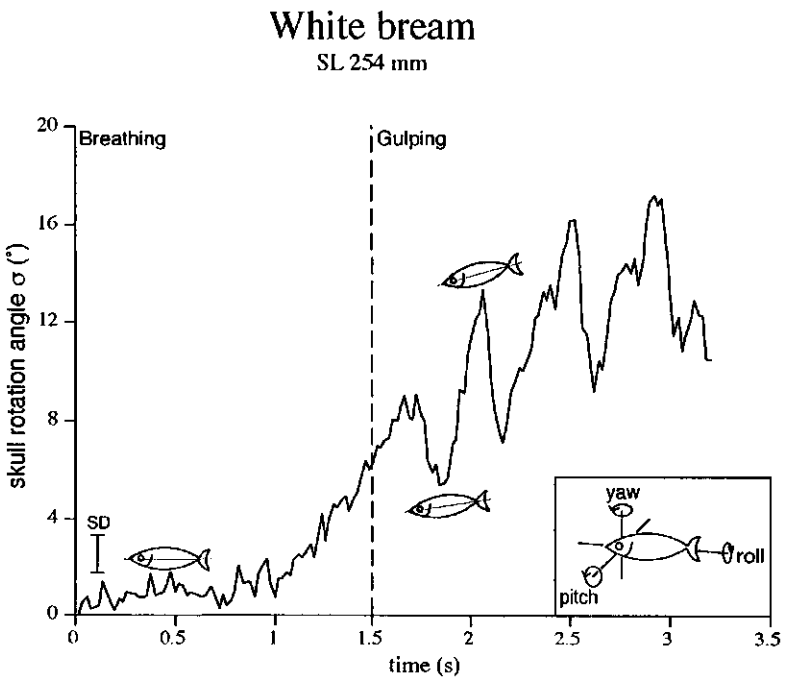

Figure 3

The angle σ (in degrees) between the skull position in the first (reference) film frame and its subsequent positions increases during this scene of white bream feeding on *Daphnia*. The first 1.5 s the white bream was breathing as it swam towards the zooplankton. In the following two seconds it was feeding (gulping). Prior to each gulp the fish turned down (pitch), resulting in peaks of angle σ. During each gulp the head turned up (valleys of angle σ). The figure in the right hand corner shows the definition of pitch, roll and yaw. The small fishes in the graph illustrate the position of the fish at three values of angle σ. The standard deviation (SD) is indicated on the left.

2.2 $\mathbf{G}_{PC}$ is rotated over angle σ; combined with $\mathbf{G}_{PC} = \mathbf{G}_P$ (step 2.1):

$$\cos\sigma = \frac{\mathbf{G}_P \cdot \mathbf{G}_{PC}}{G_P^2}$$

combined with equation 3:

$$\mathbf{G}_P \cdot \mathbf{G}_{PC} = \frac{G_P^2}{S_r^2}\mathbf{S}_r \cdot \mathbf{S}_n$$

or:

$$x_P x_{PC} + y_P y_{PC} + z_P z_{PC} = \frac{G_P^2}{S_r^2}(x_{Sr}x_{Sn} + y_{Sr}y_{Sn} + z_{Sr}z_{Sn}) \qquad (6)$$

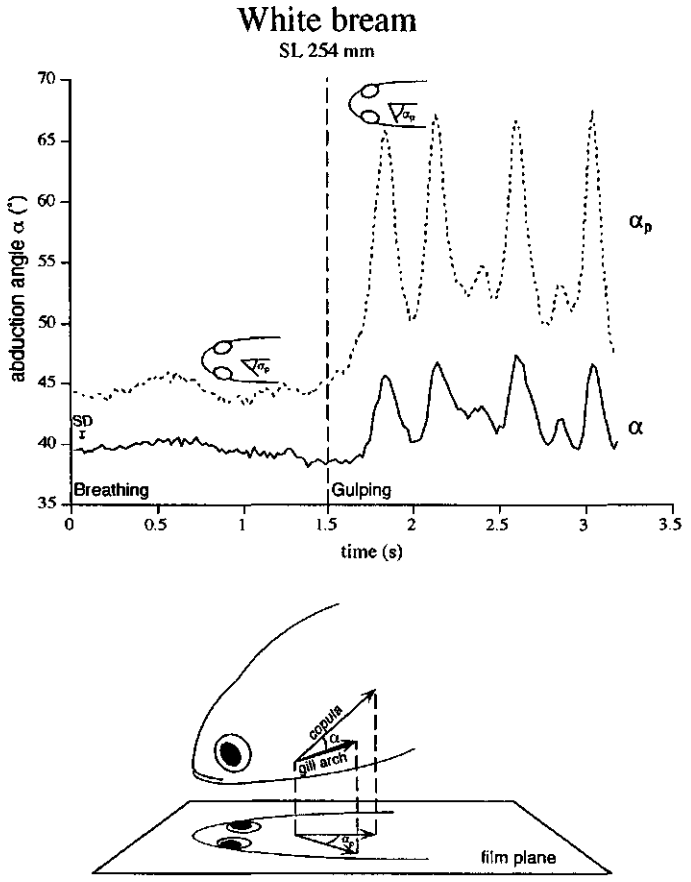

Figure 4

The abduction angle α (in degrees) between the left first gill arch and the *copula communis* of white bream during the same scene as in Fig. 3 (see legend to figure 3). There is a large difference between the projected angle α_p (2D method) and the real angle α (3D method), both in absolute value and in amplitude. The standard deviation (SD) is indicated on the left.
The figure below illustrates how α and α_p are measured.

2.3 $\mathbf{G}_{PC}$ lies in plane P; all vectors in plane P are perpendicular to $\mathbf{S}_r \times \mathbf{S}_n$, therefore:

$$\mathbf{G}_{PC} \cdot (\mathbf{S}_r \times \mathbf{S}_n) = 0$$

or:

$$x_{PC}x_{Sr\times Sn} + y_{PC}y_{Sr\times Sn} + z_{PC}z_{Sr\times Sn} = 0 \qquad (7)$$

Combination of equations 5, 6 and 7 yields a quadratic equation, with two solutions for $\mathbf{G}_{PC}$ (see appendix 2). These solutions represent rotation over angle σ in both directions in plane P (Fig. 2c). The right solution is found by considering that the

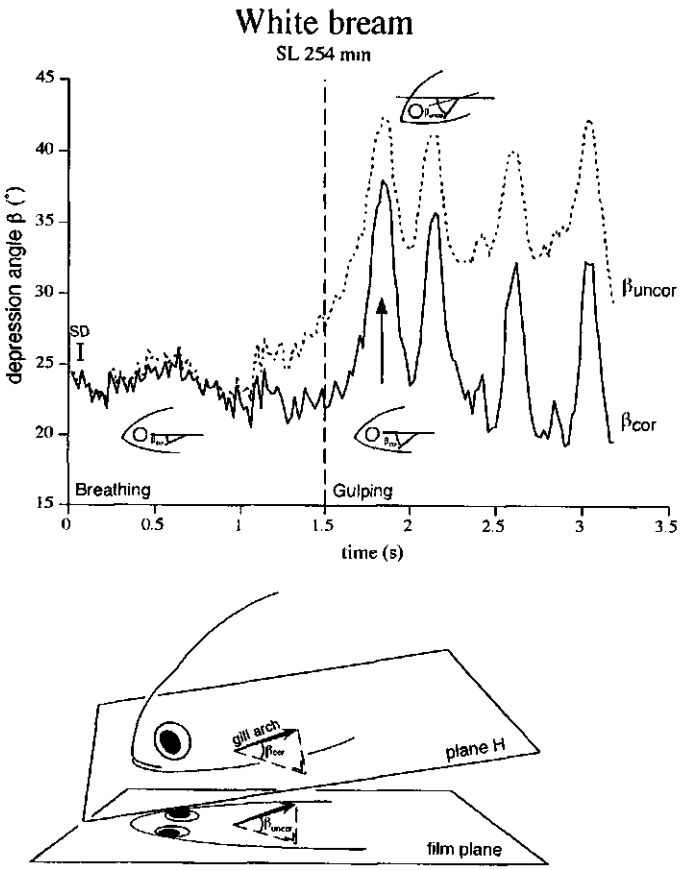

Figure 5

The depression angle β (in degrees) between the left first gill arch and a horizontal plane in the fish, during the same scene as in Fig. 3 (see legend to figure 3). In the uncorrected version β_{uncor} (measured relative to the xy-plane), the gill arch seems to be put in a 'special orientation' prior to gulping (t=1-1.5s). The corrected version β_{cor} shows that this is an artefact. This artefact is caused by the gradually increasing angle σ (Fig. 3). The standard deviation (SD) is indicated on the left.
The figure below illustrates how β_{cor} and β_{uncor} are measured.

---

angle between $\mathbf{S}_r$ and $\mathbf{G}_{PC}$ should equal the angle between $\mathbf{S}_n$ and $\mathbf{G}_P$ (see Fig. 2c). Combined with $S_r = S_n$ and $G_{PC} = G_P$ we find:

$$\mathbf{S}_r \cdot \mathbf{G}_{PC} = \mathbf{S}_n \cdot \mathbf{G}_P \qquad (8)$$

The solution of $\mathbf{G}_{PC}$ that fulfils this equation is the right one.

Step 3: restoring G_{PC} to its original length

To put $\mathbf{G}_{PC}$ 'back in space', we simply add the part of **G** that is perpendicular to plane P. This part, $\mathbf{G} - \mathbf{G}_P$, is not affected by the rotation in plane P (Fig. 2c):

$$\mathbf{G}_C = \mathbf{G}_{PC} + (\mathbf{G} - \mathbf{G}_P) \qquad (9)$$

Note that the effect on **G** of the above correction for skull rotation is dependent on the angle between **G** and plane P. When this angle is large, the effect of the correction is small. When the angle is 90°, its effect is even nil, since $\mathbf{G}_C$ equals **G**.

MPW FORTRAN subroutines (for Macintosh computers) with the present calculations are available on request.

Comparison of the 2D method and the 3D method

Example

The example of the gill arch movements of white bream will be used again to illustrate the difference between the 2D and 3D method of analysis. One scene in an X-ray film of white bream was worked out with both methods. In the first 1.5 seconds of this scene the fish was breathing and moving towards the zooplankton. In the next 2 seconds it was taking up zooplankton (gulping). The variation of angle σ (rotation of the skull) during this scene is shown in figure 3. The peaks of angle σ are caused largely by pitch of the fish as it rotates its head down to suck up food prior to each gulp (Fig. 3). During each gulp the fish head turns up again.

The abduction angle α between the left first gill arch and the *copula communis* was measured (Fig. 4). The projected angle α_p (2D method) is larger and has an amplitude two times larger (!) than the real angle α (3D method). This is not surprising. The angle between two lines, which point in the same direction from the plane of projection will always appear larger in the projected image, never smaller. The uncorrected depression angle β_{uncor} (Fig. 5) is the angle between the left first gill arch and the xy-plane in each film frame. The peaks of this angle correspond to those of abduction angle α, which explains the increased amplitude of the projected angle α_p.

The uncorrected angle β_{uncor} (Fig. 5) suggests that the branchial sieve is put in a special, depressed position prior to gulping (t=1-1.5 s). The corrected angle β_{cor} shows that this is an artefact. This artefact is caused by the gradual increase of angle σ during the scene (Fig. 3). The amplitude of β_{uncor} is about 1.5x smaller than that of β_{cor}, because the synchronous downward peaks of angle σ reduce the height of the upward peaks of angle β_{uncor}.

Conclusions

The movement components perpendicular to the film-plane can lead to large errors (up to 100% in the example!) in the 2D calculation of the rotation of structures. Therefore, the 3D method is essential for a quantitative analysis of animal movements.

Using the present 3D method the rotation of elements can be determined accurately from single view films. Furthermore, rotations can be measured in an object-bound frame. If axial rotation of vector **S** is measured (with a third skull marker), pitch, roll and yaw can even be calculated exactly in any orientation of the animal. This means that much

more scenes are suitable for analysis with this method because pitch, roll and yaw are no longer a problem.

The 3D method is essential when the movement of a structure is not in one plane. The gill arch movement in our example consisted of a combination of abduction (angle α) and depression (angle β). It is impossible to measure such a movement accurately with a 2D method. The 3D method is also essential when changes in the orientation of the animal are an integral part of its feeding behaviour. In our example pitch was an integral part of the feeding behaviour of white bream. Such changes in orientation lead to both quantitative and qualitative (e.g. so-called 'special position of the branchial sieve') errors. Therefore, the 3D approach should be strongly advised for both quantitative and qualitative studies of animal movement.

Acknowledgments

This research was supported by the Foundation for Fundamental Biological Research (BION), which is subsidized by the Dutch Organization for Scientific Research (NWO), project number 811-428-265. B. van den Berg is thanked for identifying the possibility of axial rotation around vector **S**. Mees Muller, Nand A. Sibbing, Jos G.M. van den Boogaart and Jan W.M. Osse are thanked for their critical comments on the manuscript.

List of Symbols

$\mathbf{G}$	= vector representing the gill arch
$\mathbf{G}_P$	= the projection of **G** on plane P
$\mathbf{G}_{PC}$	= $\mathbf{G}_P$ corrected for rotation of vector **S**
$\mathbf{G}_C$	= **G** corrected for rotation of vector **S**
plane H	= horizontal plane in the fish, which is parallel to the film plane when the fish is in the reference orientation
plane P	= plane defined by vector $\mathbf{S}_r$ and $\mathbf{S}_n$
film plane	= xy-plane
$\mathbf{S}$	= vector representing the skull
$\mathbf{S}_r$	= reference orientation of vector **S**
$\mathbf{S}_n$	= vector **S** in frame number n
x, y, z	= x, y and z coordinate of vector **G**
x_P, y_P, z_P	= x, y and z coordinate of vector $\mathbf{G}_P$
x_{PC}, y_{PC}, z_{PC}	= x, y and z coordinate of vector $\mathbf{G}_{PC}$
x_C, y_C, z_C	= x, y and z coordinate of vector $\mathbf{G}_C$
x_{Sr}, y_{Sr}, z_{Sr}	= x, y and z coordinate of vector $\mathbf{S}_r$
x_{Sn}, y_{Sn}, z_{Sn}	= x, y and z coordinate of vector $\mathbf{S}_n$
$x_{Sr\times Sn}, y_{Sr\times Sn}, z_{Sr\times Sn}$	= x, y and z coordinate of vector $\mathbf{S}_r \times \mathbf{S}_n$
α_1, α_2	= scalar factors to express $\mathbf{G}_P$ in terms of $\mathbf{S}_r$ and $\mathbf{S}_n$
angle α	= the angle between a gill arch and the *copula communis*
angle β	= the angle between a gill arch and plane H
angle σ	= the angle between vector $\mathbf{S}_r$ and $\mathbf{S}_n$
$\mathbf{G}\cdot\mathbf{G}$	= notation for the dot product
$\mathbf{G}\times\mathbf{G}$	= notation for the cross product
$\|\mathbf{G}\|$	= notation for the length of a vector (= |G|)

Literature cited

Batty, R.S. 1981. Locomotion of plaice larvae. Symp. Zool. Soc. Lond. 48: 53-69.

Claes, G. and F. de Vree. 1991. Kinematics of the pharyngeal jaws during feeding in *Oreochromis niloticus* (Pisces, Perciformes). J. Morph. 208: 227-245.

Drost, M.R. and J.G.M. van den Boogaart. 1986. A simple method for measuring the changing volume of small biological objects, illustrated by studies of suction feeding by fish larvae and of shrinkage due to histological fixation. J. Zool. Lond.(A) 209: 239-249.

Dudley, R. and C.P. Ellington. 1990. Mechanics of forward flight in bumblebees. I Kinematics and morphology. J. Exp. Biol. 148: 19-52.

Ellington, C.P. 1984. The aerodynamics of hovering insect flight. III. Kinematics. Phil. Trans. R. Soc. Lond. B 305: 41-78.

Gambaryan, P.P. 1974. How mammals run. John Wiley & Sons Inc., New York.

Hoogenboezem, W., F.A. Sibbing, J.W.M. Osse, J.G.M. van den Boogaart, E.H.R.R. Lammens and A. Terlouw. 1990. X-ray measurements of gill-arch movements in filter-feeding bream, *Abramis brama* (Cyprinidae). J.Fish Biol. 36: 47-58.

Jenkins, F.A. Jr. 1981. Wrist rotation in primates: a critical adaptation for brachiators. Symp. Zool. Soc. Lond. 48: 429-451.

Liem, K.F. 1979. Modulatory multiplicity in the feeding mechanism in cichlid fishes, as exemplified by the invertebrate pickers of lake Tanganyika. J. Zool., Lond. 189: 93-125.

Liem, K.F. and S.L. Sanderson. 1986. The pharyngeal jaw apparatus of labrid fishes: a functional morphological perspective. J. Morph. 187: 143-158.

Nachtigall, W. 1983. Biophysics of locomotion in air. In: Biophysics. Eds.: W.Hoppe, W. Lohmann, H. Markl and H. Ziegler. Springer-Verlag.

Sibbing, F.A. 1982. Pharyngeal mastication and food transport in the carp (*Cyprinus carpio* L.): a cineradiographic and electromyographic study. J. Morph. 172: 223-258.

Sibbing, F.A., J.W.M. Osse and A. Terlouw. 1986. Food handling in the carp (*Cyprinus carpio*): its movement patterns, mechanisms and limitations. J. Zool. Lond. (A) 210: 161-203.

Van den Berg, C., J.G.M. van den Boogaart, F.A. Sibbing and J.W.M. Osse. in prep. Gill arch movements of filter-feeding white bream (*Blicca bjoerkna*) and common bream (*Abramis brama*). J. Exp. Biol.

Van Leeuwen, J.L. 1984. A quantitative study of flow in prey capture of the rainbow trout, with general consideration of the actinopterygian feeding mechanism. Trans. Zool. Soc. Lond. 37: 171-227.

Videler, J.J. 1981. Swimming movements, body structure and propulsion in cod *Gadus morhua*. Symp. Zool. Soc. Lond. 48: 1-27.

Westneat, M.W. 1990. Feeding mechanics of teleost fishes (Labridae; Perciformes): a test of four-bar linkage models. J. Morph. 205: 269-296.

Zarnack, W. 1972. Flugbiophysik der Wanderheuschrecke (*Locusta migratoria* L.). I. Die Bewegungen der Vorderflügel. J. Comp. Physiol. 78: 356-395.

Appendix 1

Vector $\mathbf{S}_r$ should be perpendicular to the film-plane. There are two reasons for this:

1) The length of the projection of vector **S** on the film-plane is the length S multiplied by the cosine of the angle between vector **S** and the film-plane. The cosine is most sensitive to rotation when the angle is approximately 90°. This holds true for vector **G**, as well. One should preferably film in the direction of **G**, rather than perpendicular to it, because in the latter case the projection is very insensitive to rotation of **G** (see Ellington 1984, pg. 46-47). The perpendicular direction is common in the literature, probably because it disguises (!) projection errors.

2) Axial rotation around vector $\mathbf{S}_r$ is not measured (but see below). When $\mathbf{S}_r$ is perpendicular to the film-plane, this unmeasured rotation component is rotation in the film-plane (yaw, in the example). This rotation component can easily be corrected during analysis of film frames by always positioning the image of the animal in the same way. Even if there is still some rotation in the film-plane, it has no influence on depression angles.

When there are three markers in the skull (not on one line), axial rotation of $\mathbf{S}_r$ can be measured. This extra correction is omitted here, since, in the example, $\mathbf{S}_r$ was almost perpendicular to the film-plane. I will briefly describe how this axial rotation should be included in the correction. With the third skull marker a second skull vector can be defined, $\mathbf{S}_{n2}$, and a second reference vector $\mathbf{S}_{r2}$. During the first correction (see paper) $\mathbf{S}_{n2}$ is treated like vector **G** (it is transformed to the $\mathbf{S}_r$ orientation). Then $\mathbf{G}_C$ is corrected again (for axial rotation around $\mathbf{S}_r$), but now in plane P_2, which is defined by vector $\mathbf{S}_{r2C}$ and $\mathbf{S}_{n2C}$. This second correction follows the same formulae as the first one.

Appendix 2

The rotation of vector G_P in plane P was described with three equations (5, 6 and 7) and three unknowns (x_{PC}, y_{PC}, z_{PC}). These equations can be solved in various ways. In this appendix an expression is derived for z_{PC}. The calculations are not difficult, but they are complex. Therefore, it is very useful to introduce abbreviations. Equations 5, 6 and 7 can be rewritten as:

$$x_{PC}^2 + y_{PC}^2 + z_{PC}^2 = a \quad (10)$$

$$bx_{PC} + cy_{PC} + dz_{PC} = e \quad (11)$$

$$fx_{PC} + gy_{PC} + hz_{PC} = 0 \quad (12)$$

where

$$a = G_P^2 \qquad e = (G_P^2/S_r^2)\, S_r \cdot S_n$$

$$b = x_P \qquad f = x_{Sr \times Sn}$$

$$c = y_P \qquad g = y_{Sr \times Sn}$$

$$d = z_P \qquad h = z_{Sr \times Sn}$$

Using equation 10 and 11 x_{PC} can be eliminated:

$$x_{PC}^2 = a - y_{PC}^2 - z_{PC}^2$$

$$x_{PC}^2 = \frac{(e - cy_{PC} - dz_{PC})^2}{b^2}$$

$$b^2 (a - y_{PC}^2 - z_{PC}^2) = (e - cy_{PC} - dz_{PC})^2 \quad \Rightarrow$$

$$(b^2 + c^2)\, y_{PC}^2 + (b^2 + d^2)\, z_{PC}^2 - 2ec\, y_{PC} - 2ed\, z_{PC} + 2cd\, y_{PC} z_{PC} + e^2 - ab^2 = 0 \quad (13)$$

Using equation 11 and 12 y_{PC} can be expressed in terms of z_{PC}, by, again, eliminating x_{PC}:

$$x_{PC} + (c/b)\, y_{PC} + (d/b)\, z_{PC} = e/b$$

$$x_{PC} + (g/f)\, y_{PC} + (h/f)\, z_{PC} = 0$$

$$(c/b - g/f)\, y_{PC} + (d/b - h/f)\, z_{PC} = e/b \quad \Rightarrow$$

$$y_{PC} = \frac{e/b}{(c/b - g/f)} + \frac{(h/f - d/b)}{(c/b - g/f)} z_{PC} \quad (14)$$

For clarity, some further abbreviations are introduced:

$$A = b^2 + c^2 = x_P^2 + y_P^2$$

$$B = b^2 + d^2 = x_P^2 + z_P^2$$

$$C = e^2 - ab^2 = [(G_P^2/S_r^2)\,\mathbf{S}_r\cdot\mathbf{S}_n]^2 - G_P^2 x_P^2$$

$$D = \frac{e/b}{(c/b - g/f)} = \frac{[(G_P^2/S_r^2)\mathbf{S}_r\cdot\mathbf{S}_n]/x_P}{(y_P/x_P - y_{Sr\times Sn}/x_{Sr\times Sn})}$$

$$E = \frac{(h/f - d/b)}{(c/b - g/f)} = \frac{(z_{Sr\times Sn}/x_{Sr\times Sn} - z_P/x_P)}{(y_P/x_P - y_{Sr\times Sn}/x_{Sr\times Sn})}$$

With equations 13 and 14 z_{PC} can be expressed in terms of constants:

$$[AE^2 + B + 2cdE]\, z_{PC}^2 + [2ADE - 2ecE - 2ed + 2cdD]\, z_{PC} + [AD^2 - 2ecD + C] = 0$$

This quadratic equation can be solved routinely. In practice there will always be two solutions for z_{PC}. For each solution y_{PC} follows from equation 14 and x_{PC} from equation 11 (or 12).

Chapter 6

Implications of gill arch movements for filter-feeding. An X-ray cinematographical study of filter-feeding white bream (*Blicca bjoerkna*).

Coen van den Berg, Jos G.M. van den Boogaart, Ferdinand A. Sibbing and Jan W.M. Osse

To be submitted to the Journal of Experimental Biology

keywords: *common bream, retention ability, filtering rate, reducible-channel model*

Abstract

Gill arch movements during suction feeding may well disturb the particle retention mechanism of the branchial sieve. In the reducible-channel model zooplankton is retained in the channels between the medial gill rakers. The mesh size of the medial channels is reduced when the lateral rakers of the neighbouring gill arch are lowered into the centre of these channels. Due to gill arch movements depressed lateral gill rakers will move in and out of the opposite medial channels (ΔSW) and also shift out of the centre (ΔRP) of these channels. Branchial sieve movements were measured in dorsal X-ray films of filter-feeding white bream and common bream, using a high resolution 3D method of film analysis. In both species the lateral rakers are long enough to bridge the gill slits. ΔRP was 40-50% of the medial channel width in white bream and 75% in common bream. A dynamic description of the reducible-channel model was formulated. Once a particle is trapped in a reduced channel, the channel walls release mucus and the particle becomes sticky. Hence, particles need to be retained mechanically only during part of the gulping cycle. This mechanical retention can be achieved by sidewards rotation of the lateral rakers in combination with their tapering shape. Common bream has reached a compromise in the conflict between increasing the filtering rate and increasing the retention ability. Due to their limits on the retention ability, interdigitating retention mechanisms are expected in facultative filter-feeders only.

Introduction

Many fish species filter-feed on zooplankton by means of suction feeding (gulping) (see Sibbing 1991). During suction feeding water is forced through the branchial sieve by rhythmic contraction and expansion of the head. These pumping movements result in movements of the gill arches (see Hoogenboezem et al. 1990). In general, fishes retain zooplankton with the gill rakers on their branchial sieve. The retention mechanism of the branchial sieve often depends on relatively narrow gill slits and on the interaction between gill rakers on neighbouring gill arches. Therefore, gill arch movements may well disturb the retention mechanism of the branchial sieve. We studied the movements of the branchial sieve during filter-feeding of white bream (*Blicca bjoerkna*) and common

bream (*Abramis brama*). The data of their gill arch movements were combined with morphological data of their branchial sieves. In this way the disturbing effect of the gill arch movements on the reducible-channel model of filter-feeding (Hoogenboezem et al. 1991) could be studied. The effect on the saw-tooth model of zooplankton retention (Sibbing 1991) will briefly be discussed, as well.

According to the saw-tooth model particles are retained on the gill slits between the gill arches; the mesh size of the branchial sieve is directly related to the width of the gill slits. According to the reducible-channel model (Fig. 1) zooplankton is retained in the medial channels on the gill arches. The lateral rakers from one side of each gill slit can be lowered into the centre of these medial channels on the other side of the gill slit, reducing their mesh size by at least 50%. Zooplankton feeding experiments and micro-anatomical studies corroborate the reducible-channel model for common bream (Hoogenboezem et al. 1991 in press), whereas white bream can probably not reduce its medial channels (Van den Berg et al. subm. a, b). The zooplankton that is trapped in the medial channels is encapsulated in a mucus layer and remains in the channels during a number of gulps, prior to being transported to a large mucus bolus in the back of the pharyngeal cavity (Hoogenboezem and Van den Boogaart in press).

The major objective of this study was to quantify the effect of the gill arch movements during gulping on the retention of zooplankton in reduced channels. Furthermore, the differences in movement pattern of the branchial sieves of white bream and common bream were studied to try to identify adaptations of common bream for the reducible-channel model. Two aspects of the gill arch movements need to be studied. Hoogenboezem et al. (1990) pointed out that the maximal gill slit width during gulping may not exceed the length of the lateral rakers. A second restriction is that the lateral rakers should remain centred in the medial channels (see Fig. 3a). Possibly, these restrictions should hold during several gulps, since the trapped particles remain in the channels during several gulps. However, once a particle is encapsulated in mucus it will become sticky. Therefore, the restrictions possibly only hold during a limited part of each gulp.

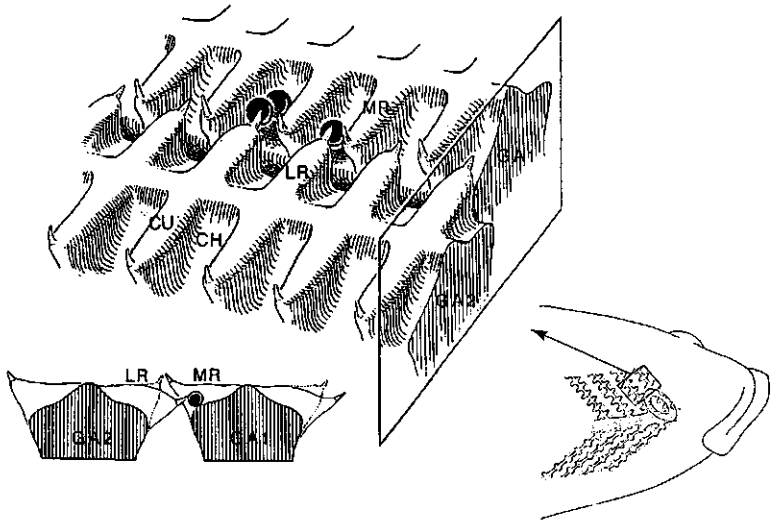

Figure 1

The reducible-channel model of filter-feeding. Adapted from Hoogenboezem et al. (1991). CH, channel; CU, raker cushion; GA1,2, gill arch 1,2; LR, lateral gill raker; MR, medial gill raker.

Measurement of the head movements of suction feeding fish is complicated by technical and computational problems (Van den Berg in prep.). Such movements have been measured with X-ray cinematography (e.g. Sibbing 1982, Sibbing et al. 1986, Hoogenboezem et al. 1990, Westneat 1990, Claes and de Vree 1991), but the data of these experiments are not quantitatively reliable, since a 2D method of film analysis was used for the analysis of 3D movements. For the present study we used a 3D method of analysis (Van den Berg in prep.). This accurate method was required for two reasons. Firstly, the movement of the gill arches is expected to have both abduction and depression components; the 2D method of analysis is inappropriate for such movements. Secondly, we are interested in small movements on the scale of individual gill rakers, hence an accuracy of at least 50 μm is required. A similar experimental design as that of Hoogenboezem et al. (1990) was used: dorsoventral X-ray films of trained fishes with platinum markers inserted at crucial points. New scenes of a filter-feeding white bream and an existing scene of common bream were analyzed with the 3D method of film analysis.

Materials and methods

The experimental set-up and procedures

The experimental white bream (*Blicca bjoerkna*) of 254 mm SL was caught in the dutch lake IJsselmeer. It was kept in tanks of well aerated water at 18°C and fed with commercial food pellets and *Daphnia*, which was stored deep-frozen. During half a year the white bream was trained to feed freely on *Daphnia*, while living in a 14x25x100 cm cuvette (width x height x length). Prior to each X-ray experiment, the water level was reduced to about 11 cm, to reduce X-ray absorption by the water.

Our filming set-up consisted of a Philips Super 100 X-ray apparatus and a 9/5 inch image intensifier in combination with an Arriflex cine camera, using 35 mm Agfa-Gevaert Scopix RP-1C film. We made dorsal X-ray films of the filter-feeding fish. The focus/image intensifier distance was 85 cm. The films were made at 60 kV, 50 frames s^{-1} and an exposure time of 5 ms, using a 1.5 mm^2 focus. During the X-ray experiments lateral video recordings of the fish were made. The correlation between video and X-ray films was obtained using a LED that lit up, when an X-ray film scene was being shot.

The frames of the selected film scenes were projected on sheets of paper (magnification 6.4x). The centre of each marker was indicated on the sheets. The marker positions were digitized with a Calcomp 9100 data tablet. The kinematic parameters of the movements under study were calculated using a Macintosh IIfx computer (the MPW FORTRAN program is available on request).

An X-ray film scene of a common bream (*Abramis brama*) (SL 354 mm) made by Hoogenboezem et al. (1990) was re-analyzed with the 3D method. The fish was trained and filmed under comparable circumstances as the present white bream. However, since some important markers were lacking, some parameters had to be estimated and the analysis is less accurate than that of white bream.

Platinum markers

The individual bones in the head of a feeding fish cannot be identified clearly (if at all) in X-ray films at 50 frames per second. Therefore, it is essential to mark important positions in the fish with pieces of platinum wire (Ø 0.35 mm, length 1-2 mm), which serve as identifiable points in the films. These markers were implanted surgically in the white bream, while it was anaesthetized using 100 mg l^{-1} TMS. For details of the surgical techniques, see Hoogenboezem et al. (1990). As required by the 3D method of analysis

(Van den Berg in prep.), each structure under study was marked with at least two platinum markers (Fig. 2). Several X-ray photographs were made of the marked fish to determine the real (unprojected) distances between the two markers on each structure. Using these distances and the coordinates of the projected markers on each film frame, each structure can be represented as a 3D vector and the kinematic parameters (see below) can be calculated accurately (Van den Berg in prep.).

Position of the markers; the kinematic parameters

2D (qualitative) parameters

The measurements in this paragraph can only be used as a rough indication of the real movement, because they are calculated with a 2D method of analysis. The **mouth opening** was calculated as the distance between the projections of markers in the upper and lower lip. The **opercular expansion** was calculated as the distance between the projections of markers in each operculum. The mouth **protrusion** was calculated as the projected distance between the upper lip marker and a marker on top of the skull. The phase of these 2D parameters was used as reference for the phase of the other movements. Since opercular expansion consists primarily of abduction and adduction, it

Figure 2

Lateral and dorsal X-ray picture of the white bream, showing the position of the platinum markers. The skull vector **S** is indicated in the lateral view. This vector is used to calculate depression angles in a fish-bound frame.

is largely restricted to the film-plane. Therefore, the opercular expansion measurement is almost as good as a 3D calculation. This does not apply to the mouth opening and protrusion. A large vertical movement component is expected when the mouth is protruded (Fig. 2). Furthermore, these measurements are influenced by pitch of the fish.

The slit width between the first gill arch and the *hyomandibula* (**gill slit 1**) could not be calculated quantitatively, because these structures are not connected by a single joint. One marker was placed on the lateral side (outside) of the left *hyomandibula*, approximately opposite the first gill arch (the marker on the right side was rejected by the tissue of the fish prior to the experiment, a common problem in fish X-ray cinematography). The width of the first gill slit was calculated as the perpendicular distance between the projection of the *hyomandibula* marker and the projection of the left first gill arch vector. This calculation is 2D and can hence only be used as a rough indication of the real width of the first gill slit.

3D (quantitative) parameters

One marker was inserted on top of the skull and one at the bottom of the skull (inside the mouth, just in front of the palatal organ). These markers define the skull vector **S**. The first frame of the film scenes was defined as the reference frame, because the position of the white bream in this frame was always nearly horizontal. Skull rotation is defined as the **angle** σ between vector **S** in the reference frame and vector **S** the subsequent film frames (Van den Berg in prep.). Angle σ shows the movement of the fish skull in an earth-bound frame. It is a combination of pitch, roll and yaw. Calculation of movements in a fish-bound frame can be performed with the aid of angle σ. First, all vectors in each frame are rotated to the reference frame (using angle σ). After this transformation movements can be calculated in a fish-bound frame (Van den Berg in prep.). In the analyzed scenes the reference vector **S** was almost perpendicular to the film-plane (Fig. 2a), which is optimal for calculating parameters in a fish-bound frame (Van den Berg in prep.).

The central kinematic parameter in this study is the abduction **angle** α between each gill arch and the *copula communis* (the fused *basibranchialia* which connect the gill arches mid-ventrally). Both a posterior and an anterior marker were implanted in the gill arches 1 to 4, the pharyngeal jaws and the *copula communis*. These markers define the gill arch vectors and the *copula* vector. The angles α can only be calculated if each gill arch vector and the *copula* vector can be connected at the joint between the gill arch and the *copula*. It was not possible to insert platinum markers exactly above these joints; their position had to be determined from a detailed X-ray photograph of the *copula* and the proximal part of the gill arches. In a normal X-ray photograph the anatomical details of the *copula* and the gill arches are obscured by the heavy bones of the skull. Therefore, a strip of an unexposed X-ray photograph was pushed into the mouth of the anaesthetized white bream (in a darkened room), placed on the *copula* and exposed through the ventral part of the head. In this way the skull bones were not recorded on the X-ray photo strip and the position of the joints relative to the implanted markers could be determined accurately. With this information the abduction angles α could be calculated. With angle α two more kinematic parameters were calculated, the **slit width** (SW) and the **relative raker position** (RP) (Fig. 3b,c,d). A detailed description of these parameters is given in the next section.

The depression angle of the gill arches (**angle** β) and of the *copula* (**angle** γ) were calculated as well. Unlike abduction angle α, the depression angles describe the position of the branchial sieve with respect to the fish. Hence these must be calculated in a fish-bound frame. They are defined as the angle between the gill arch / *copula* vector and a

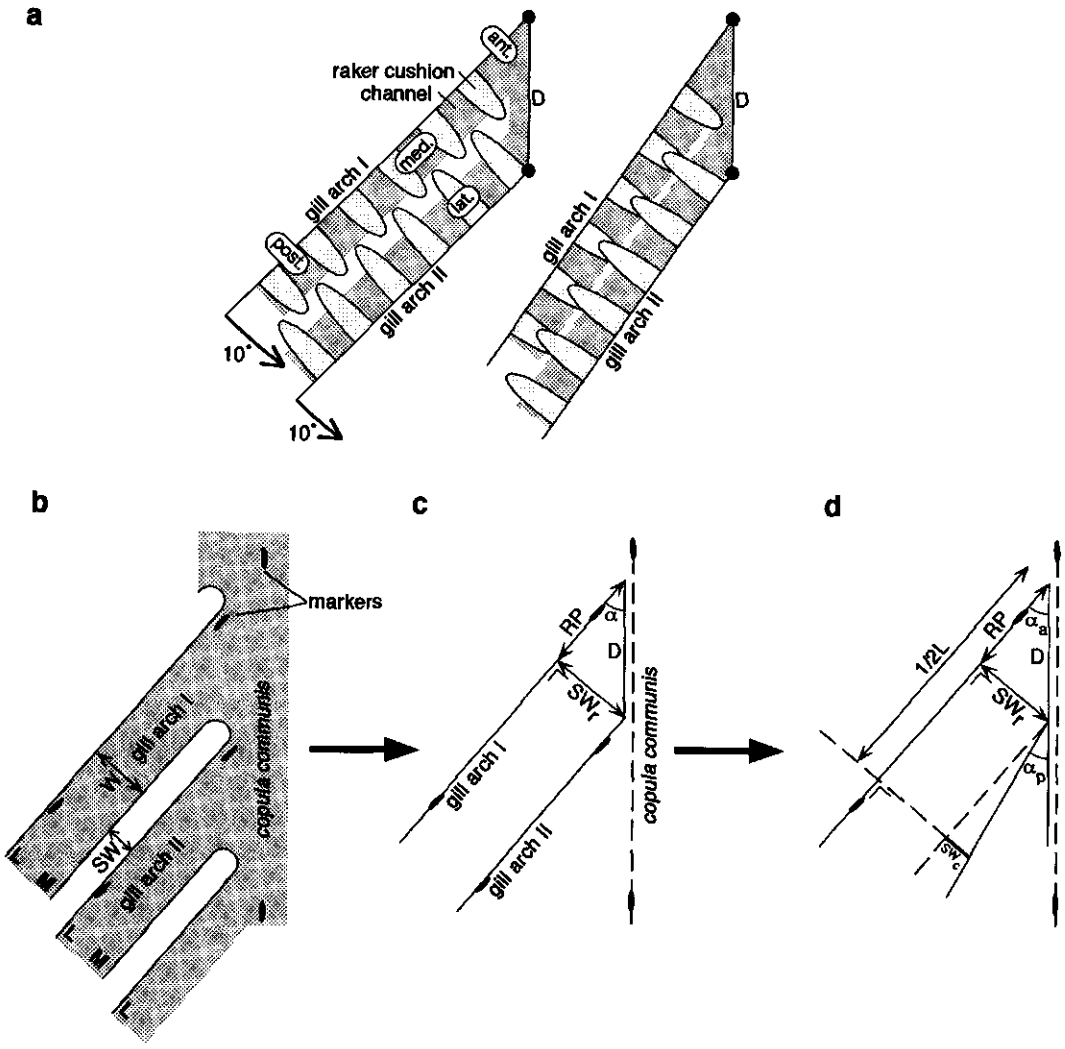

Figure 3

a) This scheme shows that 10° rotation of the gill arches strongly affects the position of the lateral rakers with respect to the medial channels on the other side of a gill slit.

D = the distance between neighbouring gill arch/*copula communis* joints

med., lat. = medial and lateral side of the gill arch

post., ant. = posterior and anterior side of the gill arch

b) The position of the markers in the gill arches and the *copula communis*. The markers in the gill arches are positioned at the lateral side (= L; M = medial side). SW is the slit width between gill arch I and II. W = the width of gill arch I.

c) The marker positions are used to calculate the angle α between each gill arch and the *copula*. Angle α is used to calculate the movement of the lateral rakers with respect to the medial channels on the neighbouring gill arch. The relative slit width (SW_r) is the sine of angle α multiplied by the distance between the gill arch joints (D). The cosine of angle α multiplied by D indicates the shift, or relative raker position (RP).

d) The calculation of the slit width is more complicated when angle α_a of the anterior gill arch differs from angle α_p of the posterior gill arch. The slit width has to be corrected with a factor SW_c. The effect on RP is negligible. L = the length of gill arch I.

horizontal plane H in a fish-bound frame (see Fig. 5). By definition, plane H is parallel to the film plane in the reference frame. The angles β and γ must be calculated with the aid of the skull rotation angle σ (Van den Berg in prep.).

One marker was implanted superficially in the **post lingual organ** (the muscular tissue on top of the *copula communis*). The movement of this marker relative to the anterior and posterior *copula* markers provides information about peristaltic movements of the post lingual organ (cf. Sibbing 1991).

Slit width and relative raker position

Due to the gill arch movements the gill rakers on either side of a gill slit move with respect to each other. This movement has two components, perpendicular to and along the gill arches. It can be fully described with abduction angle α. Movements of the branchial sieve as a whole (angles β and γ) play no role. When the angles α of two neighbouring gill arches decrease, the depressed lateral rakers move deeper into the opposite medial channels and at the same time shift anteriorly, i.e. they cannot stay centred in the medial channels (Fig. 3a).

For the present detailed study of the effect of gill arch movements on filter-feeding, the relative movement of the gill rakers on either side of a gill slit must be analyzed in more detail. It is assumed that neighbouring gill arches lie in one plane. The platinum markers (Fig. 2, 3b) are used to define the gill arches and the *copula communis*. Each gill arch position can be described with two parameters: the relative slit width (SW_r, not corrected for the width of the gill arch) and the relative raker position (RP) (Fig. 3b,c):

$$SW_r = D \sin \alpha \quad (1)$$

$$RP = D \cos \alpha \quad (2)$$

where D = the distance between neighbouring gill arch/*copula* joints

SW_r is a measure of the width of the gill slit. Furthermore, it indicates how far each depressed lateral raker is moved into the opposite medial channel. RP is a measure of the centring (shift) of the lateral rakers in the medial channels. RP is a relative measure, the exact position of the lateral rakers with respect to the medial channels is unknown.

The calculation of the real slit width is more complicated when the abduction angles α of neighbouring gill arches are unequal. When these angles are unequal SW_r changes along the gill slit; RP however, is hardly influenced (Fig. 3d). The slit width was measured at half the length (L) of the anterior gill arch. Therefore, SW_r has to be corrected by adding SW_c (Fig. 3d):

$$SW_c = \tan (\alpha_a - \alpha_p) \cdot (0.5\ L - D \cos \alpha_a) \quad (3)$$

where α_a, α_p = angle α of the anterior and posterior gill arch respectively

To obtain the real slit width (SW, Fig. 3b), the width of the gill arch has to be subtracted from the sum of SW_r and SW_c. In the experimental white bream, all gill arch markers were situated on the lateral side of the gill arches (Fig. 3b). Therefore, the width of the anterior gill arch (W, measured at the middle of the gill arch) was subtracted to obtain the slit width (SW) at the middle of the gill arch:

$$SW = SW_r + SW_c - W \quad (4)$$

In the present X-ray films of white bream α_a was usually slightly larger than α_p; at half the length of the gill arch SW_c was in the order of 5% of SW_r. The sum of SW_r and SW_c increases along the gill arch. However, it was observed in preparations of the branchial sieves of white bream and common bream that SW is actually quite regular along the gill slits. The explanation is that W increases along the gill arch, as well. The increase of $SW_r + SW_c$ is compensated by the increase of W.

Results

First, the movement of mouth, operculars, skull and postlingual organ during breathing and gulping of the white bream are treated as a general context of the movements of its branchial sieve, followed by the movements of the sieve itself. Next, the available data of common bream are presented with some comments on their accuracy. Finally, the implications of the gill arch movements for the reducible-channel model of filter-feeding are shown.

White bream

Two scenes were analyzed of white bream filter-feeding on *Daphnia*. Both scenes consisted of two breathing strokes followed by four gulps (checked with the synchronous video recordings).

General kinematic parameters of head movement

The general kinematic parameters are shown in figure 4. The peaks of the opercular expansion are indicated with vertical lines. For comparison, these lines are also drawn in figure 5.

In both scenes, the frequency of the breathing strokes was roughly half that of the gulps (Table 1). Furthermore, the amplitude of the mouth opening and opercular expansion was much higher during gulping than during breathing (Fig. 4). The phase difference between the mouth opening and opercular expansion during gulping was approximately 40 ms (Fig. 4). The second and third gulp of scene 2 are followed by a second expansion of the operculars, but not by a clear mouth opening or protrusion.

Angle σ (skull rotation) increased up to 9° in scene 1 and up to 16° in scene 2 (Fig. 4). In the synchronous video recordings we observed that the skull rotation consisted mainly of pitch. When angle σ increased the snout of the fish turned down (pitch). A peak of angle σ preceded each mouth opening. In other words, prior to each gulp the white bream turned down towards the zooplankton on the floor of the cuvette.

The marker in the post lingual organ moved over approximately 1.1 mm. Its forward movements were roughly synchronous with the gulps.

Although the data of the width of the first gill slit (SW_1) result from a 2D analysis, they can be compared roughly with the other gill slits. ΔSW_1 was 2-2.5 mm in the white bream and 4-4.5 mm in the common bream, which is almost 3x larger than ΔSW_2. The peaks of SW_1 generally just preceded the peaks of opercular expansion.

Movement of the branchial sieve

The amplitude of the angles α, β and γ was always much higher during gulping then during breathing, just like the amplitude of the opercular expansion and mouth opening (Fig. 4, 5). The peaks of angle α, β and γ slightly preceded or coincided with those of the opercular expansion (Fig. 5). However, during the two secondary opercular

Table 1

The frequency of the breathing strokes and the gulps and the approximate range of the movements of the branchial sieve (±0.5°) during breathing and during gulping on *Daphnia*.

white bream	scene 1		scene 2		
	breathing	gulping	breathing	first gulp	last gulp
frequency	1.7 Hz	3.5 Hz	1.7 Hz	2.5 Hz	
range of angle α	40-42°	41-46°	38-41°	40-47°	
range of angle β	24-27°	32-42°	22-24°	24-38°	21-32°
range of angle γ	29-33°	33-43°	29-31°	30-41°	28-37°

expansions in scene 2 (Fig. 4) the peaks of these angles followed those of the opercular expansion. This reversed phase of the opercular and branchial sieve movements suggests that the secondary peaks represent back-washing (Sibbing et al. 1986) (see discussion).

The variation of abduction angle α of the left first gill arch of the white bream was almost the same in both scenes (Fig. 5, Table 1). The depression angles β and γ (in a fish-bound frame) were different in each scene. In scene 1 these angles shifted to an increased level during gulping, whereas in scene 2 they decreased slowly during gulping (Fig. 5, Table 1). In other words, during gulping the branchial sieve was slightly depressed in scene 1, whereas it was slightly levated, towards the palatal organ, in scene 2.

Common bream

A scene of a filter-feeding common bream (Hoogenboezem et al. 1990) was re-analyzed with the 3D method of analysis. Figure 6 shows the mouth opening, opercular expansion and gill arch abduction angle α. The skull rotation and the depression angles could not be measured accurately. The scene consists of three gulps. The gulping frequency was approximately 1.2 Hz and the phase difference between mouth opening and opercular expansion was approximately 90 ms. The variation of angle α was larger than in the white bream: 37-46°. The peaks of angle α coincided with or came slightly after the peaks of opercular expansion. The systematic error of angle α might be quite large, because some structural parameters were estimated instead of measured. These parameters are the position of the gill arch joints with respect to the markers and the distance between the gill arch joints (distance D in formula 1 and 2).

Table 2

A comparison of the measurements by Hoogenboezem et al. (1990) with the present measurements of the variation of the slit width (ΔSW) in a scene of common bream feeding on *Daphnia*. The maximum variation (between the tips of the standard deviations) is indicated. All values are in mm.

	old results	new results
ΔSW 2	1.58	1.40
ΔSW 3	0.92	1.51
ΔSW 4	0.43	1.62

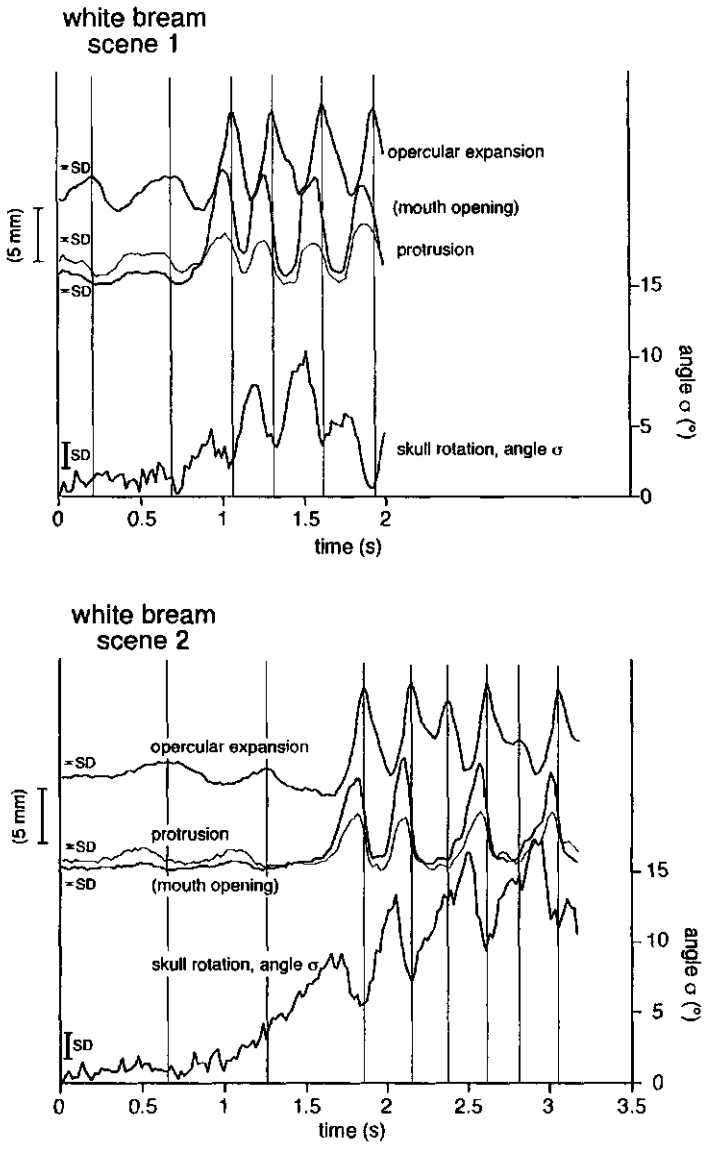

Figure 4

General kinematic parameters of the head of two scenes of white bream filter-feeding on *Daphnia*. Both scenes start with two breathing strokes followed by four gulps. The thin vertical lines show the peaks of the opercular expansion. Angle σ indicates the rotation of the skull in an earth-bound frame. Note the transition from slow, low-amplitude breathing movements to fast, high-amplitude gulping movements. The strong head movements during gulping will lead to increased movements of the branchial sieve. Note that in scene 2 the second and third gulp are followed by a secondary opercular expansion. N.B.: the 2D calculation of the other parameters contain projection errors. The indication in mm (left y-axis) refers to these 2D measurements.

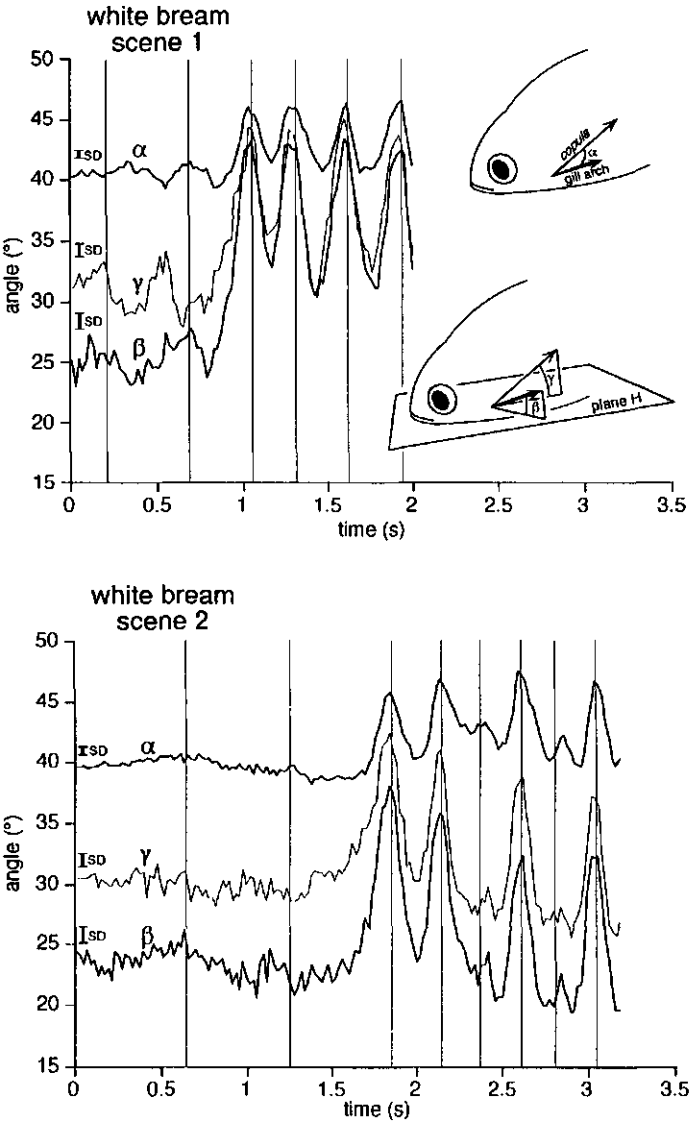

Figure 5

The movement of the branchial sieve of white bream during the same scenes as in figure 4. The data of the left first gill arch and the *copula communis* are shown. The amplitude of the branchial sieve movements is increased during gulping, just like the general head movements (Fig. 4). The thin vertical lines show the peaks of the opercular expansion; note that the peaks of the branchial sieve movements come after the peaks of opercular expansion during the two secondary opercular expansions in scene 2 (see Fig. 4).

Angle α = the angle between the left first gill arch and the *copula communis*

Angle β = the angle between the left first gill arch and a horizontal plane H in a fish-bound frame

Angle γ = the angle between the *copula communis* and plane H.

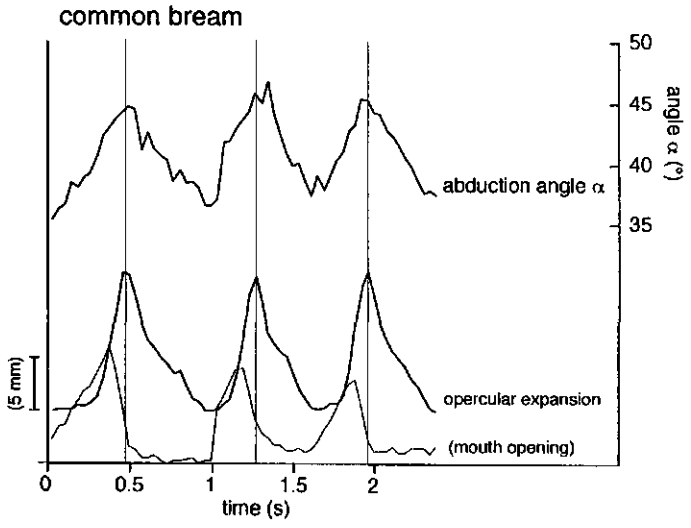

Figure 6
A scene of common bream gulping on *Daphnia* from Hoogenboezem et al. (1991). The angle α was calculated with the present 3D method of analysis. The thin vertical lines show the peaks of the opercular expansion. N.B.: the 2D calculation of mouth opening and opercular expansion contains projection errors. The indication in mm (left y-axis) refers to these 2D measurements.
Angle α = the angle between the left first gill arch and the *copula communis*

Table 2 (page 127) shows the difference between the present data of the gill slit width (ΔSW) and the data of Hoogenboezem et al. (1990). Hoogenboezem et al. found an unexpected decline in ΔSW from gill slit 2 to 4, which we did not find. The differences between the old and new data (Table 2) are partly caused by Hoogenboezems 2D method of analysis and partly by our inaccurate estimation of the position of the gill arch joints. ΔSW of the second gill slit is approximately the largest (and almost the same) in both approaches. Obviously, the largest ΔSW and ΔRP will cause the largest problems with the reducible-channel model. Hence, the 3D data of this gill slit were examined in detail in white bream and common bream.

Slit width (SW) and relative raker position (RP)

During breathing the gill slits of white bream are narrow, varying between 0 and 0.3 mm. During gulping the amplitude of the movements is increased. As shown before, the gill arch movements can be split in the slit width (SW) and the relative raker position (RP). SW represents the movement of the lateral rakers in and out of the medial channels and RP represents the shift of the lateral rakers with respect to the medial channels (Fig. 3a). The consequences for the reducible-channel model are best demonstrated by expressing SW as a fraction of the lateral raker length (LR) and RP as a fraction of the medial channel width (CW) (Fig. 7). CW equals 0.88 and 1.56 mm and LR equals 1.23 and 2.67 mm for the white and common bream respectively (Van den Berg et al. 1992). In both species the maximum SW was approximately 60% of LR. ΔRP equalled 40-50% of CW for the white bream and 75% of CW for the common bream (Fig. 7); the movement of the lateral rakers is considerably eccentric in both species.

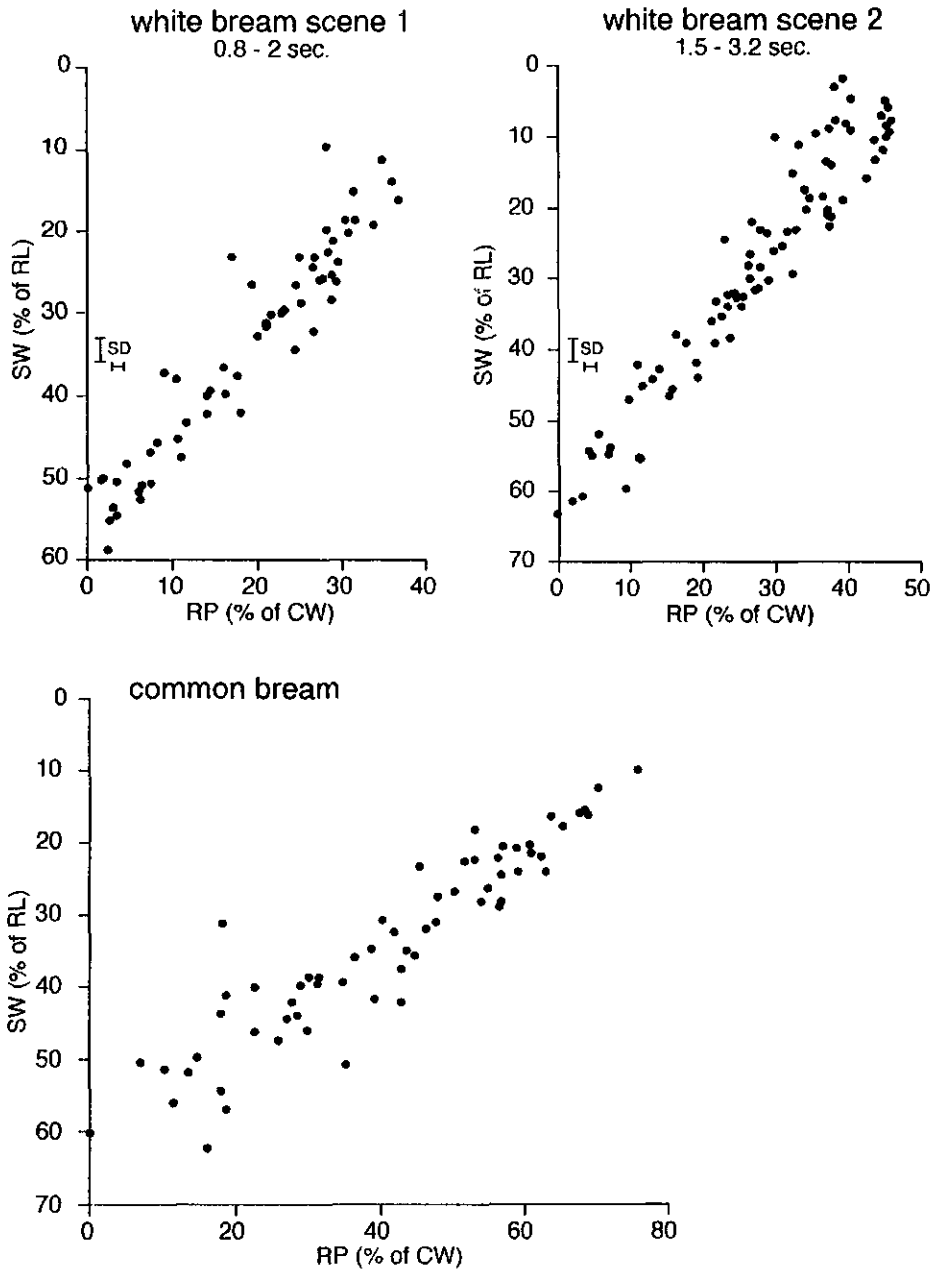

Figure 7

Using the data of angle α (Fig. 5 and 6) the gill slit width (SW) and the relative raker position (RP) in white bream and common bream were calculated. SW represents the movement of the depressed lateral rakers in and out of the medial channels and RP represents their shift with respect to the medial channels (Fig. 3a). Together, they show the total movement of the depressed lateral rakers with respect to the medial channels. The consequences for the reducible-channel model are clearly visible in this figure, since SW is expressed as a fraction of the lateral raker length (LR) and RP as a fraction of the medial channel width (CW). In these plots the data of angle α during breathing are omitted.

Discussion

This discussion starts with an estimation of the filtering rate. Next it is argued whether the increased gill arch movements during gulping are compatible with the reducible-channel model of filter-feeding. First, the variation of the slit width is discussed, followed by the shift of the lateral rakers in the medial channels. This leads to a description of the dynamics of the reducible-channel model. The secondary movements in scene 2 are explained as back-washing, which serves to collect mucus-covered particles from the medial channels. Next, the movement pattern of the branchial sieves of white bream and common bream are compared. Finally, the conflict between retention ability and filtering rate in the reducible-channel model is treated and the reducible-channel model is linked to an opportunistic lifestyle.

Filtering rate

The product of the frequency and amplitude of the opercular expansion can be used for a rough comparison of the flow rate of the water during breathing and gulping. It was argued that the opercular expansion data are nearly quantitative, even though they were calculated with a 2D method. It was estimated (Fig. 4) that the amplitude of the opercular expansion was three times larger during gulping than during breathing. In scene 1 the frequency was 1.7 Hz during breathing and 3.5 Hz during gulping. Hence, the flow rate was roughly (3.5/1.7)*3 $\approx$ 6 times larger during gulping than during breathing. During gulping a high flow rate (=filtering rate) is advantageous, because more prey are ingested per unit time. However, during gulping the gill arch movements are larger than during breathing. What price is paid for increasing the filtering rate, is the retention ability reduced?

Retention ability versus gill arch movements

Variation of the gill slit width (ΔSW)

When the lateral rakers are depressed into the medial channels they are not horizontal. From the realistic drawing of a cross section of a reduced channel (Fig. 1) it was estimated that their maximum depression angle is approximately 45°. Hence, the lateral rakers can bridge a gap of cos 45° times the raker length $\approx$ 71% of the raker length. The maximal slit width (SW) equalled approximately 60% of the lateral raker length in both species (Fig. 7). Therefore, in both species the depressed lateral rakers can quite easily reach across the maximal gill slit width during gulping.

Shift of the depressed lateral rakers in the medial channels (ΔRP)

The shift (ΔRP) was 40-50% of the medial channel width in the white bream and even 75% in the common bream (Fig. 7). Hence, depressed lateral gill rakers will not remain centred in the medial channels during gulping (Fig. 3a). Clearly, our previous static description of the reducible-channel model has to be replaced by a dynamic one.

Particles are retained in a reduced channel when they get stuck between the depressed lateral raker and the walls of the medial channel. Upon contact, each mucus cell in these channel walls immediately releases its store of mucus. The released mucus encapsulates the retained particles, which, as a result, become sticky (Hoogenboezem and Van den Boogaart in press). Therefore, mechanical retention by the lateral raker is not required during the entire gulping cycle (Fig. 8a). During a gulp the particles will reach the branchial sieve in the second half of the expansion phase of the head (between $^1/_2SW_{max}$ and SW_{max}). It is assumed that the trapped particles become sticky

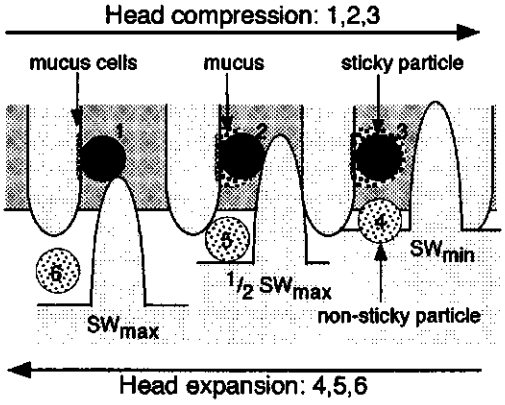

Figure 8
Scheme of the influence of mucus on retention. Once particles are trapped in a reduced channel, they stimulate the mucus cells in the channel wall and become encapsulated in a mucus layer (phase 1, 2 and 3). From then on they stick to the channel wall and retention by the lateral rakers is no longer necessary. Hence, retention of particles by the lateral rakers is only required during approximately half the gulping cycle. Particles which are not properly encapsulated in mucus during the compression phase are lost during the expansion phase (phase 4, 5 and 6).

during the first half of the compression phase of the head (between SW_{max} and $^1/_2SW_{max}$). Hence, the particles only need to be retained by the lateral raker during one half of the gulping cycle, from $^1/_2SW_{max}$ to SW_{max} and back to $^1/_2SW_{max}$, i.e. when $SW > {}^1/_2SW_{max}$. Two mechanisms may help to keep the lateral rakers centred during this part of the gulping cycle. These mechanisms will first be described separately. Next, a new, dynamic description of the reducible-channel model will be given, which combines the mucus encapsulation and both these mechanisms.

Due to their tapering shape, the lateral gill rakers can still block the centre of the medial channels when they are not exactly centred. Hence, prey particles of half the size of the medial channel width can still be retained. In Figure 9 the raker positions at SW_{max} and at $^1/_2SW_{max}$ are drawn. The lateral rakers can almost block the centres of the medial channels during this half of the gulping cycle. However, during the other half of the cycle the depressed lateral rakers will be pressed forcefully in the medial channel walls (Fig. 9).

The lateral rakers are lowered into the medial channels with their abductor muscles, *m. abductor branchiospinalis* (Hoogenboezem et al. 1991). The fibres of this muscle fan out from their insertion on the foot of the lateral gill raker to their origo on the forked feet of the *radii branchiales* (Van den Berg et al. subm. b). By one-sided contraction of this muscle the lateral rakers can rotate sidewards and thus remain centred. In figure 10 it is shown that the angle ϕ of sidewards rotation should equal 'asin(0.5ΔRP/RL)' to keep the lateral raker tips centred during the entire gulping cycle. Angle ϕ should equal approximately 8° in white bream and 12° in common bream. This rotation should be in phase with the gulps. Such rhythmically coordinated rotations might be neurally regulated with a common pattern generator for the gulping movements. De Graaf (1990) showed that each gill arch (in particular its lateral side) of carp (*Cyprinus carpio*) is innervated by the internal pretrematic branch of the vagal ganglion. The external musculature of the branchial arches (and the palatal organ) are innervated from branches of the same ganglion. Hence, a synchronous activation of the *m. abductores branchiospinales* and the branchial arch muscles is not unlikely.

A dynamic particle retention mechanism of the reducible-channel model can now be formulated. From $^1/_2SW_{max}$ to SW_{max} and back to $^1/_2SW_{max}$ the particles are trapped in the reduced medial channels of the branchial sieve. During this period they are retained mechanically by a combination of the tapering shape of the lateral rakers and by sidewards rotation of the lateral rakers (Fig. 9, 10). The effective mesh size of the

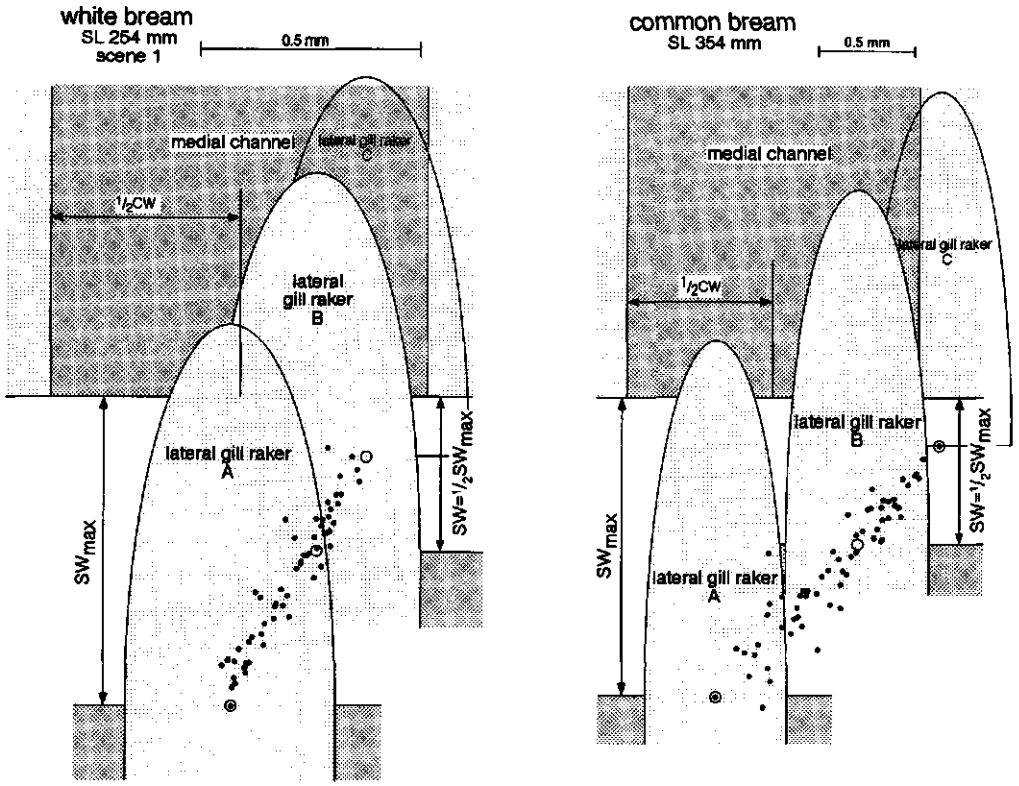

Figure 9

These schemes combine morphological data and the RP/SW plots (Fig. 7) of white bream and common bream. The schemes illustrate the dynamic description of the reducible-channel model.

The lateral gill rakers have a tapering shape. As each lateral raker moves into the opposite medial channel, their movement out of the centre of the channel (ΔRP) is partly compensated by their increasing cross-section at the entrance of the channel. Hence, the centre of the channel remains almost blocked. At position A the slit width is maximal (SW_{max}). At position B the slit width is half of SW_{max}. At position C the slit width is minimal, the depressed lateral rakers are pushed into the medial channel wall (but see fig. 10). The lateral rakers are depressed over 45°, hence their length in this top view is reduced to 71% of their real length.

branchial sieve remains $^1/_2$CW. Meanwhile, the particles stimulate the mucus cells in the channel walls, become encapsulated in mucus and become sticky (Fig. 8). From then on they stick to the channel wall until they are collected by back-washing, mechanical retention is no longer required. During maximal compression of the branchial sieve crushing of the depressed lateral rakers and the medial channel walls is prevented by active rotation of the lateral gill rakers.

When a particle is not properly encapsulated in mucus during the first half of the gulping cycle (e.g. because the mucus cells in the channel walls are exhausted) it will be

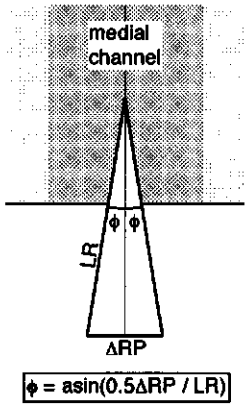

Figure 10

Sidewards rotation of the lateral gill rakers by local contraction of the lateral raker abductor muscle (*m. abductor branchiospinalis*) can keep the tip of the lateral raker in the centre of the medial channel. By compensating for half of the shift (ΔRP) on either side by rotation over angle ϕ, the lateral raker tip will remain exactly centred in the medial channel (see formula). Due to this sidewards rotation the depressed lateral rakers need not be pushed into the medial channel wall.

lost, unless it is larger than the unreduced medial channel width. This might explain the finding in Van den Berg et al. (subm. a) that common bream did not retain all large particles for 100% when its medial channels were reduced.

In the description of the dynamics of the reducible-channel model some new structural requirements for the branchial sieve emerge:

1) During growth of the branchial sieve, all rakers and channels on either side of each gill slit should remain neatly interdigitated, because it is improbable that the centring of each individual lateral raker in the corresponding medial channel can be regulated separately.
2) The position of the lateral rakers with respect to the medial channels should be as in figure 9. As a result, during breathing the lateral rakers are expected to be directly opposite the medial rakers rather than alternating with them.
3) The maximal slit width (and hence the gulping amplitude) may not exceed a fixed value (SW_{max} in Fig. 9), which is predetermined by the structure of the branchial sieve.

Transport and collection of particles captured with the branchial sieve

In scene 2 two gulps were followed by a second expansion of the operculars, but no appreciable mouth opening or protrusion (Fig. 4). The phases of the angles α, β and γ were reversed (Fig. 5), which suggests that the direction of the water flow was inverted and that this movement pattern is back-washing (Sibbing et al. 1986). The inverted flow during back-washing probably serves to collect mucus-covered particles from the medial channels in the branchial sieve (Hoogenboezem and Van den Boogaart in press). During back-washing closed protrusion is expected following opercular expansion and branchial sieve movements. The closed protrusion might be hidden in the flanks of the next gulps (Fig. 4), i.e. after closed protrusion the mouth might be not retracted, but opened for the next gulp. The X-ray films showed that the post lingual organ and the pharyngeal jaws had a reduced activity during the secondary movements, which indicates that food transport and mastication (Sibbing et al. 1986) did not occur.

Differences between white bream and common bream

It was shown above that gill arch movements interfere with the functioning of the reducible-channel model. Four mechanisms are described which can help to reduce the amplitude of the gill arch movements without reducing the filtering rate. The data of white bream and common bream are compared to investigate whether the movement

pattern of common bream is especially adapted for these mechanism. Next, the prey retention mechanism of white bream is discussed, with some remarks on roach (*Rutilus rutilus*).

A fish minimizes the variation of the slit width, ΔSW (Δsin α) when angle α is in the range of 90°, it minimizes the shift, ΔRP (Δcos α) when angle α is in the range of 0° (see formula 1 and 2). A large ΔRP is far more serious than a large ΔSW, since ΔSW can easily be overcome by increasing the length of the lateral rakers. Therefore, it was expected that angle α varies around a value of much less than 45° when the reducible-channel model can be applied. However, in both common bream and white bream angle α is on average only slightly less than 45°.

Depression of the branchial sieve (angles β and γ) has no influence on the reducible-channel mechanism, but branchial sieve abduction (angle α) does. Therefore, comparatively little expansion was expected during gulping. In the white bream, the amplitude of the depression angle γ was approximately 9°, whereas that of the abduction angle α was approximately 6°. A rough estimation of angle γ in common bream (using the re-analyzed scene) indicated that common bream is not better adapted than white bream in this respect; the amplitude of angle γ was roughly 12°, whereas that of angle α was roughly 9°.

The branchial sieve of the white bream was depressed during gulping in scene 1, but not in scene 2. In the reducible-channel model, the palatal organ is supposed to help to guide the water flow and possibly to form the roof of the medial channels (Hoogenboezem et al. 1990). If the branchial sieve is depressed, this becomes highly unlikely. Data of lateral X-ray films by Hoogenboezem et al. (1990) indicate that depression of the branchial sieve during gulping does not occur in the common bream. Hence, common bream seems to be better adapted to the reducible-channel model in this respect.

The degree of expansion of the head differs drastically between breathing and gulping. Possibly, the large first gill slit width during gulping (3x larger than during breathing) serves to prevent a too large abduction of the gill arches. But how is loss of water and food particles through this slit prevented? Van den Berg et al. (subm. b) suggested that the lateral rakers of the first gill arch form a sieve across the wide first gill slit during gulping. The length of these rakers is approximately 1.3 mm in the white bream (SL 254 mm) and 4.4 mm in the common bream (SL 354 mm) (Van den Berg et al. 1992). In common bream these rakers are much longer than all its other rakers. The width of the first gill slit varied by 2-2.5 mm in the white bream and by 4-4.5 mm in the common bream (2D data). Therefore, the lateral rakers of the white bream cannot completely close off the first gill slit during the entire gulp, but those of common bream can. Alternatively, the first gill slit may be closed off with the palatal organ (in the roof of the pharyngeal cavity).

From the point of view of the reducible-channel model the head movements of common bream can be optimized. Common bream has not adapted the functioning of its 'pumping mechanism' during gulping by reducing abduction in favour of depression/ levation, nor has it adapted the construction of its branchial sieve by reducing angle α. Possibly, such adaptations were overruled by other demands (like the necessity of a good contact between the palatal organ and the branchial sieve). Alternatively, there may have been no environmental pressure on common bream to further reduce the mesh size of its branchial sieve. On the other hand, in contrast to white bream, common bream does not seem to depress its branchial sieve during gulping and it has extra long lateral gill rakers of the first gill arch, which may serve to keep the first gill slit closed during gulping.

The shift (ΔRP) of white bream was smaller than that of common bream. Therefore, in white bream the centring of reduced channels would be less disturbed than in common bream. Nevertheless, both zooplankton feeding experiments and micro anatomical study clearly indicate that common bream can reduce its channels and white bream cannot (Van den Berg et al. subm. a,b). It is unclear why white bream has no *m. abductor branchiospinalis*. The movement pattern of its gill arches is well suited for the reducible-channel model. If white bream would be able to reduce its channels it would be a better filter-feeder than common bream. The only investment would be to have a set of tiny raker abductor muscles.

Which retention model might apply to white bream? The maximum slit width of the white bream is almost equal to its medial channel width. Therefore, white bream might catch zooplankton on its gill slits, according to the saw-tooth model (Sibbing 1991). However, a prediction of the saw-tooth model is that *Daphnias* are not retained as well as copepods, due to their flatness (Van den Berg et al. in press). Such a difference was not found (Van den Berg et al. subm. a). It was concluded that the unreducible-channel model (retention in the medial channels, but no possibility to reduce their mesh size) can be applied to white bream. In the same paper we concluded that the saw-tooth model can probably be applied to roach (*Rutilus rutilus*). Although we did not succeed in making X-ray films of filter-feeding roach, the gill arch movements of roach that are expected if the saw-tooth model applies, in view of the zooplankton retention data (see Van den Berg et al. subm. a), are comparable to those of white and common bream. In freshly killed roach, angle α is approximately 45°, just like in common and white bream. Considering the expected gill arch movements, the saw-tooth model is not unreasonable for roach.

The conflict between filtering rate and retention ability

The reducible-channel model induces a conflict between increasing the amplitude of the head movements (to increase the filtering rate) and reducing the medial channel width (to increase the retention ability), in other words, a conflict between number of prey taken up per unit time and minimum size of prey that can be retained.

Common bream has pushed its gill arch movements on the one hand and the size of its medial channels on the other hand to the limits allowed by the reducible-channel model. If ΔRP would be more than 75% of CW, rotation of the depressed lateral rakers could no longer prevent them from being pushed into the medial channel walls when SW is minimal. The gulping movements therefore set severe limits to the use of the reducible-channel mechanism of filter-feeding.

A fine sieve with a mesh size of 10-70 μm as found in the silver carp (*Hypophthalmichthys molitrix*), a cyprinid obligate filter-feeder, cannot be achieved with the reducible-channel mechanism; indeed, silver carp does not use an interdigitating sieve (Smith 1989). The reducible-channel model is typically a retention mechanism for *facultative* filter-feeders, like common bream. The major advantage of the reducible-channel model over the mechanism of e.g. silver carp is the adjustability of the mesh size. Zooplankton is not the only food source of common bream, chironomid larvae are an important food source, as well. If the branchial sieve is too fine, separating food from substrate becomes difficult (Janssen 1978). The coarse sieve of common bream (unreduced channels) will therefore be better suited to filter chironomid larvae from substrate than the fine sieve (reduced channels) (see Van den Berg et al. subm. a).

In general, a retention mechanism depending on the interaction of gill rakers across a gill slit has the advantage of adjustability (e.g. reducible-channel model, saw-tooth model), but the disadvantage of a limited retention ability due to the gill arch movements,

which are coupled to head expansion. Retention mechanisms with a fixed mesh-size (e.g. unreducible-channel model, comb model) can reach a much higher retention ability, but they do have a fixed mesh size. Interdigitating mechanisms are expected in opportunistic filter-feeders, non-interdigitating mechanisms in obligate filter-feeders and 'non'-filter-feeders.

Acknowledgments

This research was supported by the Foundation for Fundamental Biological Research (BION), which is subsidized by the Netherlands Organization for Scientific Research (NWO), project number 811-428-265. The OVB (Organization for Improvement of Inland Fisheries) provided fishes for this research. Kareltje and Geert van Snik are thanked for their help in making the X-ray films.

List of symbols

plane H	= horizontal plane in a fish-bound frame. By definition plane H is parallel to the film-plane in the reference frame of each film scene
CW	= medial channel width
D	= the distance between neighbouring gill arch/*copula communis* joints
L	= gill arch length (ceratobranchial)
LR	= lateral gill raker length
RP	= relative position of the lateral gill rakers with respect to the medial channels;centring of the lateral gill rakers
ΔRP	= shift; variation of RP
SW	= real gill slit width
ΔSW	= variation of SW
SW_1, SW_2	= slit width of the first and second gill slit respectively
$SW_{max, min}$	= maximal, minimal value of SW during gulping
SW_c	= slit width factor, which corrects for the effect of $\alpha_a \neq \alpha_p$
SW_r	= relative slit width (not corrected)
W	= gill arch width (measured at the middle of the ceratobranchial)
angle α	= abduction angle between a gill arch and the *copula communis*
angle α_a, α_p	= angle α of the gill arch on the anterior and the posterior side of a gill slit
angle β	= the depression angle of a gill arch; the angle between a gill arch and plane H
angle γ	= the depression angle of the *copula communis*
angle σ	= rotation angle of the skull; angle between the skull vector in a particular frame and the skull vector in the reference frame

Literature cited

Claes, G. and F. de Vree. 1991. Kinematics of the pharyngeal jaws during feeding in *Oreochromis niloticus* (Pisces, Perciformes). J. Morph. 208: 227-245.

De Graaf, P.J.F. 1990. Innervation pattern of the gill arches and gills of the carp (*Cyprinus carpio*). J. Morph. 206: 71-78.

Hoogenboezem, W., F.A. Sibbing, J.W.M. Osse, J.G.M. van den Boogaart, E.H.R.R. Lammens and A. Terlouw. 1990. X-ray measurements of gill-arch movements in filter-feeding bream, *Abramis brama* (Cyprinidae). J.Fish Biol. 36: 47-58.

Hoogenboezem, W., J.G.M. van den Boogaart, F.A. Sibbing, E.H.R.R. Lammens, A. Terlouw and J.W.M. Osse. 1991. A new model of particle retention and branchial sieve adjustment in filter-feeding bream (Abramis brama (L.), Cyprinidae). Can. J. Fisheries Aquat. Sci. 48: 7-18.

Hoogenboezem, W. and J.G.M. van den Boogaart. in press. The importance of oro-pharyngeal mucus in filter-feeding of bream (*Abramis brama*). Can. J. Fish. Aquat. Sci.

Hoogenboezem, W., E.H.R.R. Lammens, P.J. MacGillavry and F.A. Sibbing. in press. Size selectivity and sieve adjustment in filter-feeding bream *Abramis brama* (L.), Cyprinidae. Can. J. Fish. Aquat. Sci.

Sibbing, F.A. 1982. Pharyngeal mastication and food transport in the carp (*Cyprinus carpio* L.): a cineradiographic and electromyographic study. J. Morph. 172: 223-258.

Sibbing, F.A., J.W.M. Osse and A. Terlouw. 1986. Food handling in the carp (*Cyprinus carpio*): its movement patterns, mechanisms and limitations. J. Zool. Lond. (A) 210: 161-203.

Sibbing, F.A. (1991) Food capture and oral processing. *In* I.J. Winfield and J. Nelson (eds): Cyprinid Fishes; Systematics, Biology and Exploitation. London: Chapman and Hall, pp. 377-412.

Smith, D.W. 1989. The feeding selectivity of silver carp, *Hypophthalmichthys molitrix* Val.. J. Fish Biol. 34: 819-828.

Van den Berg, C., F.A. Sibbing, J.W.M. Osse and W. Hoogenboezem. 1992. Structure, development and function of the branchial sieve of common bream, *Abramis brama*, white bream, *Blicca bjoerkna*, and roach, *Rutilus rutilus*. Env. Biol. Fish. 33: 105-124.

Van den Berg, C., J.G.M. van den Boogaart, F.A. Sibbing, E.H.R.R. Lammens and J.W.M. Osse. in press. Shape of zooplankton and retention in filter-feeding. A quantitative comparison between industrial sieves and the branchial sieves of common bream (*Abramis brama*) and white bream (*Blicca bjoerkna*). Can. J. Fish. Aquat. Sci.

Van den Berg, C., J.G.M. van den Boogaart, E.H.R.R. Lammens, F.A. Sibbing and J.W.M. Osse. subm. a The retention ability of filter-feeding common bream (*Abramis brama*), white bream (*Blicca bjoerkna*) and roach (*Rutilus rutilus*), in relation to filter-feeding models, with implications for energy intake. Can. J. Fish. Aquat. Sci.

Van den Berg, C., G. van Snik, J.G.M. van den Boogaart, F.A. Sibbing and J.W.M. Osse. subm. b Comparative micro anatomy of the branchial sieve of three sympatric cyprinid species in relation to filter-feeding mechanisms. J. Morph.

Van den Berg, C. in prep. A vector approach to determine 3D distances and rotations from 2D films of movements. J. Exp. Biol.

Westneat, M.W. 1990. Feeding mechanics of teleost fishes (Labridae; Perciformes): a test of four-bar linkage models. J. Morph. 205: 269-296.

Error analysis

For this detailed quantitative study a detailed error analysis is indispensable. In the analysis of X-ray films several errors can occur, mainly due to projection effects. Five errors are discussed here: four systematic errors and the measuring error.

1) Errors due to divergence of the X-ray beams

a) The distance to the X-ray source

The distance between the X-ray source and the image intensifier was 85 cm. The magnification (M) of a structure is dependent on its distance x (in cm) from the X-ray source, because the X-ray beam diverges: $M = 85 / x$. The white bream was always feeding from the floor of the cuvette. During a film scene the distance between each gill arch and the image intensifier varied between approximately 2 and 3 cm. Therefore the magnification of each gill arch varied from approximately 1.024 to 1.037 (i.e. by 1.2%).

b) The orientation with respect to the X-ray beams

The projected length of a structure is dependent on its orientation relative to the X-ray beam (Fig. 11). In the white bream the vertical distance between the markers on the top and on the base of the skull was approximately 2 cm (Fig. 2). The distance between the lower marker and the image intensifier was approximately 3 cm. For realistic sideward movement of the fish in the cuvette the magnification of the projection of the skull vector varies by some 3%. The vertical distance between the markers in the gill arches and the *copula* does not exceed 1 cm, hence this error will be less than 1% for the gill arch and *copula* vectors.

2) Deformation by the image intensifier

Deformation by the image intensifier was determined by Hoogenboezem et al. (1990) by filming a steel grid with square meshes. They found that the error increases rapidly from the centre to the edges; in a central circle of 10 cm diameter it was less than 1.6%. During filming, the head of the white bream was always well within this area.

3) The lens error of the film projector

Deformation due to projection of the film frames on paper was measured by projecting paper with 1 mm squares. The error increases rapidly from the centre to the edges. It was 2-3% at the edges and less than 1% in the central area, where the image of the fish was always projected.

4) Errors in the measurement of the anatomical constants

a) The unprojected distance between the markers

An error in the measurement of the real distance between the two markers in each structure causes a systematic error in the calculations. This source of errors was tested by altering the value of these distances in the computer calculations. An error of 1 mm caused a systematic error in angle α of the first gill arch of approximately 0.7-0.8°. Such an error would occur if the angle between the gill arch vector of 20 mm and the plane of the X-ray photograph in which the distance is measured is 18° instead of 0°; in fact, the X-ray photographs were much better than that.

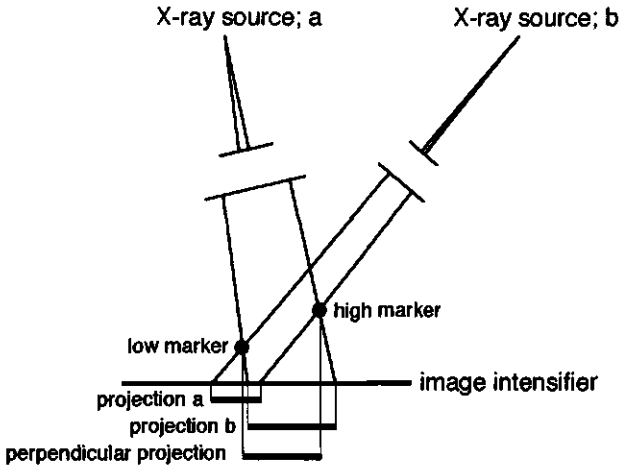

Figure 11

This figure shows two very different positions of the X-ray source (a, b) with respect to two markers with a different vertical distance from the image intensifier. Clearly, the projected distance between these markers depends on the position of the X-ray source.

4b) The position of the gill arch / copula joint

If the real position of the gill arch/*copula* joint is 1 mm more caudal than measured in the X-ray photo strips the error in angle α is approximately 0.7° (determined by altering parameters in the computer calculations). The calculation of angle α is clearly not very sensitive for this type of systematic error. The real error in the position of the joint is probably much less than 1 mm.

5) The measuring error

The measuring errors of the kinematic parameters were determined empirically. They are somewhat dependent on the depression angles of the structures. We projected one representative frame ten times and digitized the ten sets of marker positions. The resulting standard deviations (SD) are indicated in figure 4, 5 and 7; the 95% reliability interval is ±1.96SD. For the angles SD was always (much) less than 1°. The SD of the distances RP and SW was always less than 50 μm.

Summary

Filter-feeding in common bream (*Abramis brama*), white bream (*Blicca bjoerkna*) and roach (*Rutilus rutilus*); structures, functions and ecological significance.

In this thesis the retention mechanism of the branchial sieve of three sympatric cyprinid fish species, the common bream (*Abramis brama*), the white bream (*Blicca bjoerkna*) and the roach (*Rutilus rutilus*), is studied. In eutrophic lakes zooplankton is an important food resource and common bream is dominant. Previous research indicated that common bream retains zooplankters in the medial channels on its gill arches. The mesh size of its branchial sieve can be reduced by rotating the lateral rakers into these channels. In this thesis it is shown that of the three species under study the channels of common bream are comparatively the widest. Because of its extra long and pointed lateral gill rakers common bream is most suited to reduce its channels, in the way described above. The retention ability of the fishes was calculated from the decline in density of zooplankton as a function of its size in experimental tanks with filter-feeding fish. These data were compared with the predictions from three retention models. In these predictions the influence of the shape of the zooplankton on retention was taken into account. This aspect was studied in a separate experiment with industrial sieves (with square meshes). The ratio of body width and depth of the zooplankton proved to be a crucial size parameter for retention. It was concluded from the filter-feeding experiments that the channel model with adjustable mesh size can be applied to common bream. The same model can be applied to white bream, but without the possibility to adjust the mesh size. Roach probably retains zooplankton on its gill slits, according to the saw-tooth model. The presence of abductor muscles for the lateral rakers, which allows them to rotate, is a prerequisite for the application of the reducible-channel model. A detailed micro anatomical study showed that all lateral gill rakers of each gill arch of common bream have such muscles. In white bream and roach, however, these muscles are only present on the lateral gill rakers of the first gill arch. Therefore, the reducible-channel model cannot be applied to these species. During the uptake of zooplankton by suction feeding, the gill arches move along with the expanding head. These gill arch movements affect the relative position of the gill rakers on either side of each gill slit. The gill arch movements were studied in X-ray films of white bream and common bream. A novel, 3D method of analysis was developed to analyze these films quantitatively. The lateral gill rakers of both species proved to be long enough to reach across the gill slit (i.e. into the medial channels), even when the width of the gill slits was maximal. The sideward movement of the lateral gill rakers out of the centre of the medial channels was considerable. The adjustable branchial sieve is not rigid. Due to the mucus

encapsulement of trapped particles, the conical shape of the lateral gill rakers and the possibility to rotate them sidewards, the reducible-channel mechanism still functions well. The filter-feeding effectiveness of the three species was quantified in terms of energy. Common bream proved to have a higher energy gain from filter-feeding than its relatives white bream and roach. This difference is probably a crucial factor explaining the dominance of common bream in eutrophic lakes. The present research corroborates the fundamental idea that there is a strong relation between the functional morphology and the ecological niche of a species. Furthermore, small morphological differences between related species (the presence of abductor muscles of the lateral gill rakers) can be used to explain and predict interspecific differences in the exploitation of food sources and the performance in the ecosystem.

Samenvatting

Voedselopname door filter-feeding bij de brasem (*Abramis brama*), de kolblei (*Blicca bjoerkna*) en de blankvoorn (*Rutilus rutilus*); structuren, functies en ecologisch belang.

In dit proefschrift wordt de werking van de kieuwzeef bestudeerd in drie sympatrische karperachtige vissen: de brasem (*Abramis brama*), de kolblei (*Blicca bjoerkna*) en de blankvoorn (*Rutilus rutilus*). In eutrofe meren, waar zoöplankton een belangrijke voedselbron is, is de brasem dominant. Eerder onderzoek gaf aanwijzingen voor de hypothese dat de brasem planktondeeltjes vasthoudt in de mediale kanaaltjes op de kieuwbogen en dat de maaswijdte van de kieuwzeef gereduceerd kan worden door de laterale kieuwdoorns in deze kanaaltjes te draaien. Dit proefschrift laat zien dat de breedte van de kanaaltjes bij brasem relatief het grootst is van de drie bestudeerde soorten. De extra lange en puntige kieuwdoorns van brasem maken deze soort het meest geschikt om de diameter van haar kanaaltjes op bovenstaande wijze te reduceren. In aquaria met 'filter-feedende' vissen werd het retentievermogen gemeten aan de hand van de afname van de dichtheid van het zoöplankton als funktie van de grootte van het zoöplankton. Deze gegevens werden vergeleken met de verwachtingen vanuit drie retentie modellen. In deze verwachtingen werd rekening gehouden met de invloed van de vorm van het zoöplankton op de retentie. Dit aspect was vooraf bestudeerd in een apart experiment met industriële zeven (met vierkante mazen). De ratio van lichaamsbreedte en -diepte van het zoöplankton bleek een essentiële parameter te zijn voor de retentie. Uit de filter-feeding experimenten werd geconcludeerd dat het kanaaltjesmodel met instelbare maaswijdte op brasem kan worden toegepast. Op kolblei kan het kanaaltjesmodel worden toegepast, maar dan zonder de mogelijkheid de maaswijdte in te stellen. De blankvoorn vangt zoöplankton

waarschijnlijk op de kieuwspleten (tussen de kieuwbogen), volgens het zaagtand-model. Een vereiste voor het toepassen van het instelbare kanaaltjesmodel is dat de laterale kieuwdoorns abductorspieren bezitten, zodat ze kunnen roteren. Een gedetailleerde microanatomische studie liet zien dat bij de brasem alle laterale kieuwdoorns van elke kieuwboog deze spiertjes bezitten. Bij kolblei en blankvoorn hebben echter alleen de laterale kieuwdoorns van de eerste kieuwboog deze spiertjes. Het instelbare kanaaltjesmodel kan daarom niet op deze soorten toegepast worden. Tijdens de zuigende planktonopname bewegen de kieuwbogen mee met de expanderende kop. De kieuwboogbewegingen beïnvloeden de onderlinge positie van de kieuwdoorns aan weerszijden van elke kieuwspleet. De kieuwboogbewegingen werden bestudeerd met röntgenfilms van de kolblei en de brasem. Voor de kwantitatieve uitwerking van deze films werd een 3D-analyse-methode ontwikkeld. De laterale kieuwdoorns van beide soorten bleken lang genoeg te zijn om de overkant van de kieuwspleet (d.w.z. de mediale kanaaltjes) ook bij de maximale spleetbreedte te bereiken. De zijwaartse beweging van de kieuwdoorns uit het centrum van de mediale kanaaltjes is aanzienlijk. De instelbare kieuwzeef is niet star. Dankzij het inslijmen van gevangen voedsel-deeltjes, de conische vorm van de laterale kieuwdoorns en de mogelijkheid ze zijdelings te roteren, werkt het instelbare kanaaltjesmodel toch goed. De filter-feeding effectiviteit van de bestudeerde soorten werd in termen van energie gekwantificeerd. Het bleek dat brasem een hogere energiewinst behaalt met filter-feeding dan zijn verwanten kolblei en blankvoorn. Dit verschil speelt waarschijn-lijk een belangrijke rol in de dominantie van brasem in eutrofe meren. Het onderzoek in dit proefschrift bevestigt het fundamentele idee dat er een sterk verband is tussen de functionele morfologie en de ecologische niche van een soort. Tevens blijkt dat kleine morfologische verschillen tussen verwante soorten (de aanwezigheid van abductor spiertjes van de laterale kieuwdoorns) gebruikt kunnen worden om interspecifieke verschillen in het exploiteren van voedsel-bronnen en het functioneren in het oecosysteem te verklaren en te voorspellen.

Dankwoord

Een dankwoord schrijven is een hachelijke zaak. Vele mensen spelen op velerlei wijzen een rol bij het totstandkomen van een proefschrift zoals dit. De afgelopen vier en een half jaar zijn voor mij een proces van niet alleen wetenschappelijke groei geweest. Het feit dat ik mijn emoties en de irrationele zijde van mijn geest meer serieus ben gaan nemen heeft mij hopelijk behoed voor het gevaar van een door rationele oogkleppen vernauwde blik. Goede wetenschap is een dialoog tussen het irrationele en het rationele. Vandaar ook, dat niet alleen collega's, maar ook vrienden en familie een rol spelen. Als het goed is, is een dankwoord slechts een formalisering van gevoelens die je toch al laat blijken. Daarom zal ik me hier beperken tot het noemen van degenen die direct bij het onderzoek betrokken zijn geweest.

In de eerste plaats Jan Osse en Nand Sibbing, die het project geïnitieerd hebben en het wordingsproces uitstekend begeleid hebben door vele diepgravende en openhartige discussies, elk op zijn eigen wijze. Jan heeft veel aandacht voor de nieuwe perspectieven en de terugkoppeling met de Grote Vragen en zet vraagtekens bij elke 'vanzelfsprekendheid'. Bij Nand ligt de nadruk meer op de zorgvuldigheid en de opbouw en logica van de verhalen. Naast deze twee primaire begeleiders is vooral Jos van den Boogaart van onschatbare waarde geweest. In de eerste plaats was hij een gezellige kamergenoot, die altijd bereid is te helpen bij allerlei problemen. Hij is zelf buitengewoon handig en heeft mij vele technische vaardigheden geleerd en ook om met beperkte middelen een probleem creatief op te lossen. Bovendien was hij mijn intellectuele partner op de eerste linie. Vele (waan-)ideeën hebben we over en weer aan elkaar voorgelegd en bediscussieerd. Het was vaak moeilijk om te bepalen van wie de op deze manier gerijpte ideeën uiteindelijk afkomstig waren. Het bovengenoemde trio heeft ervoor gezorgd dat de onderzoeksgegevens en -ideeën telkens op een hoger plan getrokken werden.

Arie Terlouw was niet alleen degene die zorgde dat de sectie 's middags gezellig samen koffie kon drinken, maar heeft mij ook met veel kennis van zaken geholpen bij de röntgenfilm experimenten, het trainen van de vissen en ook bij de technisch veeleisende NMR stromingsvisualisatie experimenten. Ondanks zijn twijfels over zijn studie heeft Peter Klinkhamer geduldig gegevens verzameld voor het 'saaie artikel', bovendien is hij een goede vriend geworden. Dat laatste geldt ook voor Geert van Snik, die het exacte verloop van de kieuwdoornspiertjes heeft ontdekt, röntgenfilms heeft gemaakt van Kareltje de Kolblei en die met zijn kritische, onafhankelijke geest een uitstekende discussie partner was.

Naast deze mensen hebben nog vele anderen op Zodiac op enigerlei wijze een bijdrage geleverd en bovendien hebben zij en vele andere medewerkers voor een prima werksfeer gezorgd. Ik zal geen namen noemen, omdat ik bang ben er één (paar) te missen, maar je weet wel dat ik jou ook bedoel, bedankt! Ik heb ook nog vier maanden in het kale Oosterzee gewerkt. De goede sfeer die ook daar op het instituut heerste voorkwam dat ik (nog) gek(ker) werd. Bedankt allemaal! Verder heb ik samengewerkt met prof. Schaafsma, Henk van As en Dagmar van Dusschoten van de vakgroep Moleculaire Fysica aan het NMR stromingsvisualisatie onderzoek. Hoewel er geen publiceerbare resultaten zijn behaald geloof ik dat beide partijen plezier hebben gehad van de samenwerking tussen deze twee ver uiteenlopende vakgebieden. Tenslotte bedank ik iedereen die ik nog niet genoemd heb en die toch een rol heeft gespeeld bij de totstandkoming van dit werkje (sorry dat ik je gemist heb!).

Beste lezer, ik hoop dat je iets aan dit boekje hebt en meer leest dan alleen de stellingen en het dankwoord. Bekijk op z'n minst de plaatjes, er zitten hele leuke tussen!

Als uitsmijter een persoonlijke noot. Op 2 januari 1992 had ik de volgende droom, die mogelijk iets te maken heeft met de problemen van de experimenteel bioloog die dieren bestudeerd in een niet-natuurlijke omgeving:
"Ik was in een dierenwinkel. Aan de linkerzijde van het gangpad waarin ik me bevond stond een rij terraria waarin kleine mensjes rondliepen over het zand en tussen de weinige planten. Aan mijn rechterzijde bevond zich een groot aquarium, prachtig ingericht met vele waterplanten, waarin een vingergroot mensje vrolijk rondzwom. Het mannetje was goudvis-oranje van kleur en met zijn lange benen, eindigend in flippers, stuwde hij zich met elegante golven voort. Ik probeerde een praatje met hem te maken en haalde hem uit het water. Meteen begon hij zich veel visachtiger te gedragen, kronkelde in mijn hand en glibberde op de grond, waar hij met felle knipmes-bewegingen op en neer sprong, als een vis op het droge. Woedend kwam de baas van de dierenwinkel van achter uit de zaak. Het schaamrood steeg naar mijn kaken. Met enige moeite wisten we het oranje mannetje te pakken te krijgen en in zijn bak terug te zetten. Hij was onbeschadigd en zwom weer vrolijk door, alsof er niets gebeurd was".

Levensloop

Coen van den Berg is geboren op 5 augustus 1965 te Amsterdam. Vanaf 1967 woonde hij in Badhoevedorp. In 1978 verhuisde hij naar Nunspeet. In 1983 begon zijn studie biologie aan de Landbouwhogeschool Wageningen (later omgedoopt tot Landbouwuniversiteit). Tijdens deze studie deed hij een doctoraalvak bij Mees Muller, vakgroep E.D.C., sectie Functionele Morfologie, met als onderwerp het 4-stangenstelsel als mechanisch model voor de razendsnelle koplevatie bij de grote zeenaald (*Syngnathus acus*). Dit onderzoek bestond voornamelijk uit theoretisch werk. In Bristol deed hij een stage bij Jeremy Rayner, met als onderwerp het traagheidmoment van vogelvleugels. Dit onderzoek had vooral een praktisch karakter. In 1988 studeerde hij cum laude af en begon direct aansluitend als OIO aan een promotieonderzoek bij de vakgroep E.D.C. Dit onderzoek werd gefinancierd door de stichting BION, projectnummer 811-428-265 en resulteerde tot nu toe in twee verschenen publicaties en een geaccepteerde publicatie (elk in internationale vakbladen) en in dit proefschrift. Nog drie andere publicaties zijn opgestuurd naar internationale vakbladen.

Daphnia's Nightmare